# DIALOGUES IN THE MIDST

*Workshop in the MIDST* of

## Simulating soft matter with dissipative particle dynamics

**Gökhan Kaçar**
**Trakya University**

EURO

Sabancı Üniversitesi

# Outline

- Soft matter
  - Definition and examples
- Molecular dynamics
  - Definitions and some basic theory
- Part 1
  - Coarse-graining and coarse-grained simulations: General concepts
- Part 2
  - Dissipative Particle Dynamics method
    - Definition
    - Some examples: Applications on soft matter
- Cases/properties to be studied in the hands-on session

# Soft matter

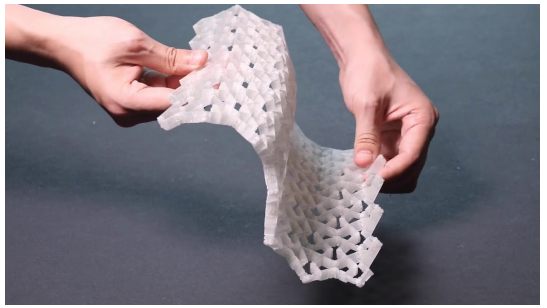

- Materials that can deform?
- Things that do not hurt your hand when you hit them?

- Water and cornstarch mixture?

- Fluid or solid?

# Soft matter

**Definition**

Materials that are easily deformed by thermal fluctuations and external forces

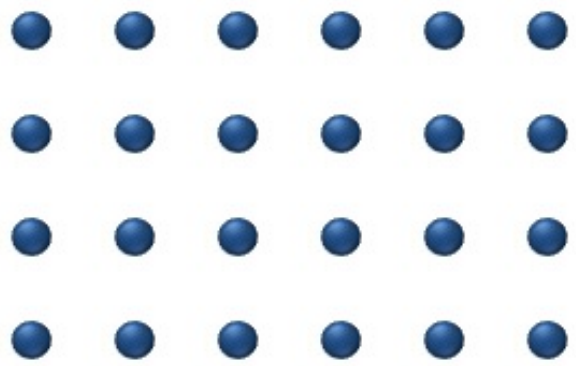

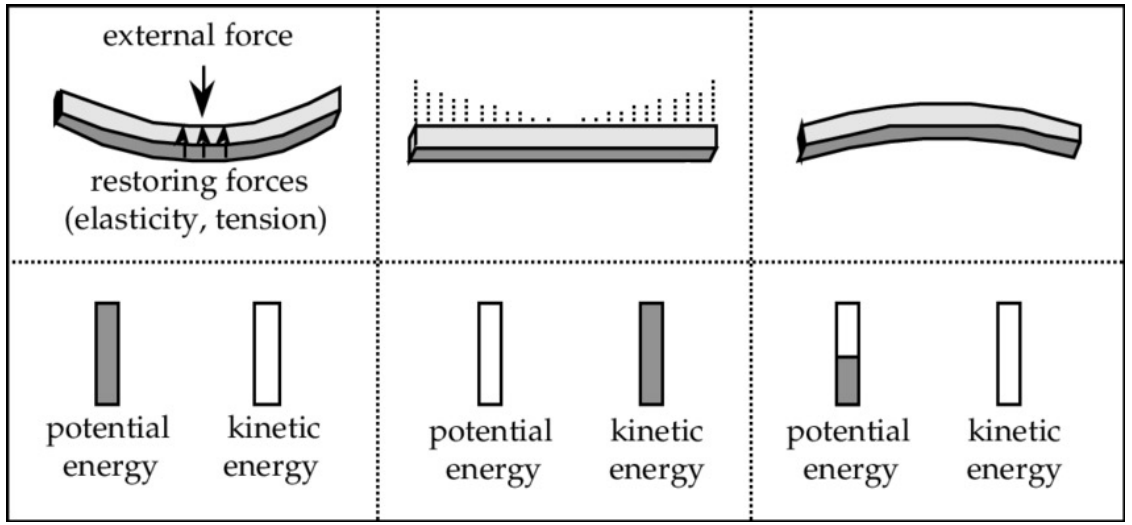


Sources: wikipedia.org
DOI: 10.1207/s15326969eco0501_1

# Soft matter

- hair gel, mayonnaise, shaving cream, colloidal crystals, polymer solutions and blends

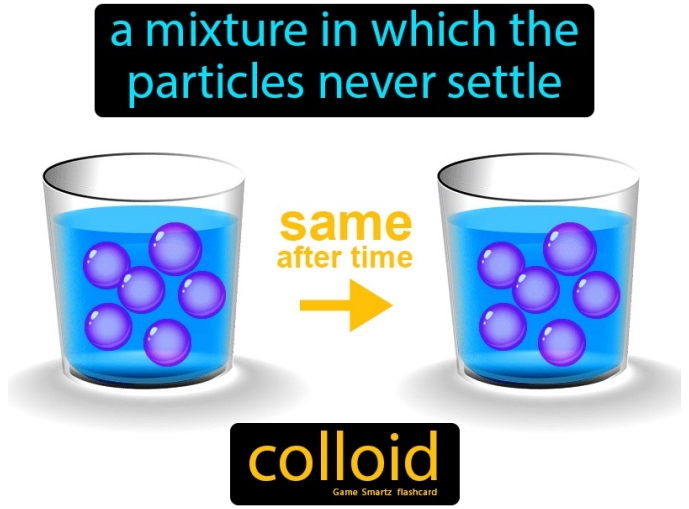


Sources: wikipedia.org
barbasol.com
recipeclinic
pinterest

# Soft matter

Similar to ordinary solids and liquids?

NO!

Individual molecules seem random and disordered ‘like a liquid’

Zoom in

Source: Flaticon.com

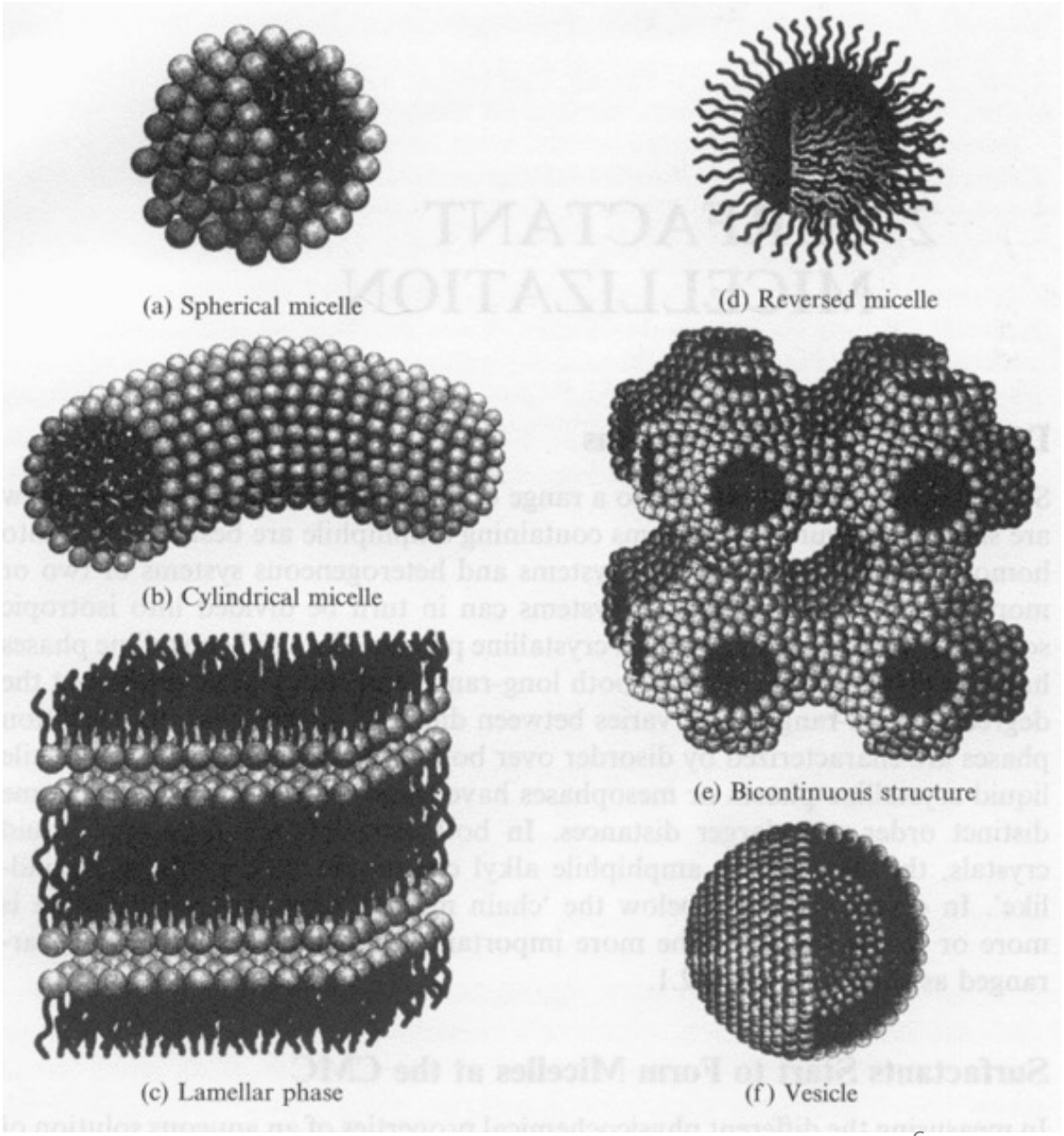

# Soft matter

Properties

Large response function

- Small change can dramatically change the properties
- Environmental changes (temperature, light, magnetic or electric field)

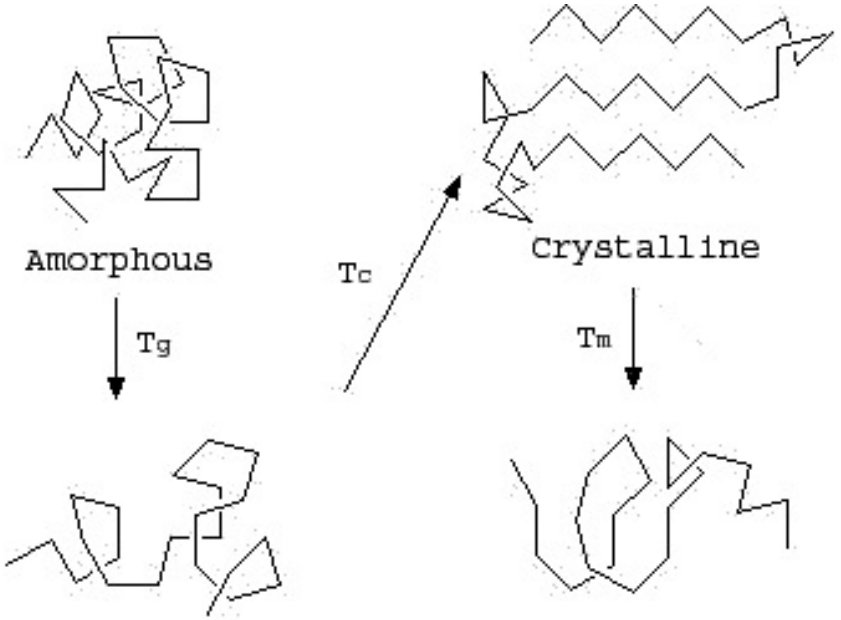


“Self-assembly”

$T_g$ marks the temperature at which an amorphous polymer changes from rigid solid to a more flexible rubber

$T_m > T_c > T_g$

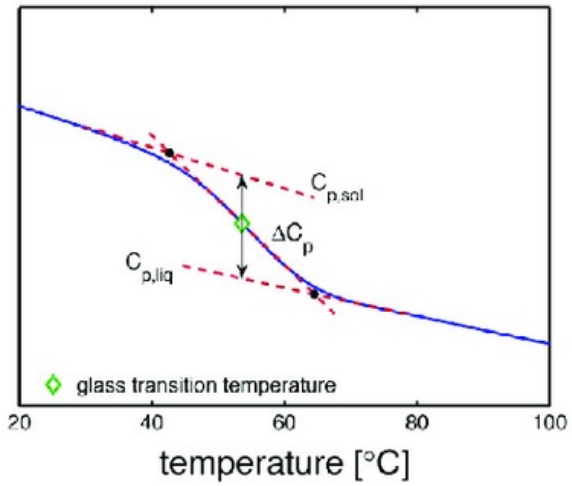


DOI: 10.1016/j.tca.2017.09.021

# Soft matter

Length-scales

Soft matter length scales fall in between atomistic and macroscopic scales

Mesoscopic length scale

However, fluctuations from Brownian motion are still important!!!

# Brownian Motion

Botanist Robert Brown (1773 - 1858)

Noticed the irregular motion of pollen granules in water

(Roman philosopher Lucretius' famous poem already gives some notice to the motion of dust particles in air)

Albert Einstein and Polish physicist Marian Smoluchowski explained the Brownian motion

Statistical mechanics-based explanation of the movement of pollen by the force exerted from individual water molecules

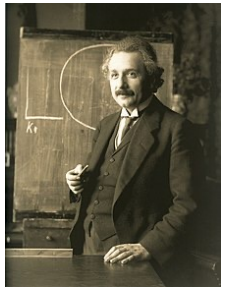

# Soft matter

Definition (again) – Complex matter or complex fluids

Molecular building blocks

Pierre-Gilles de Gennes

# Soft matter

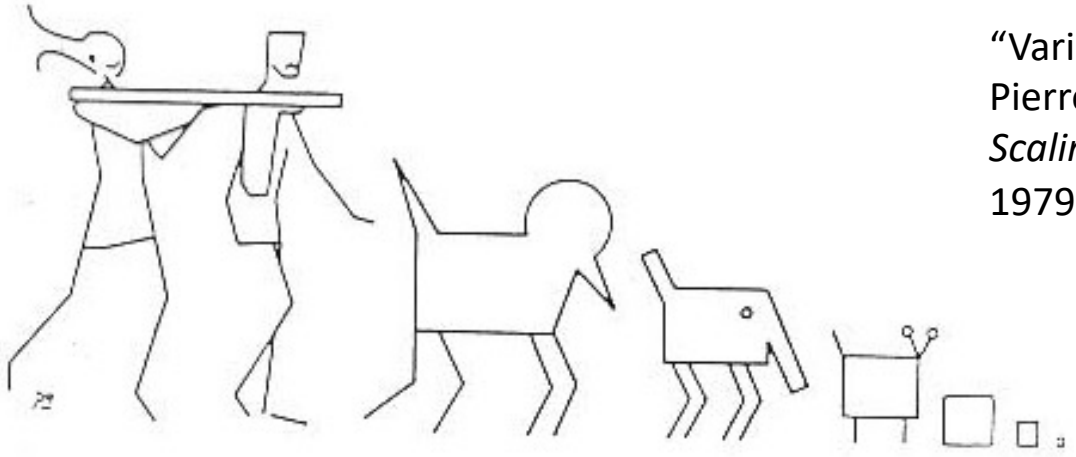

"Various animals attempting to follow a scaling law" by Pierre-Gilles de Gennes (Nobel prize in physics 1991) *Scaling Concepts in Polymer Physics*, Cornell University Press 1979.

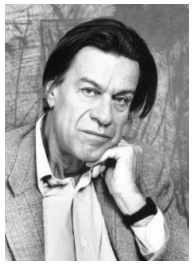

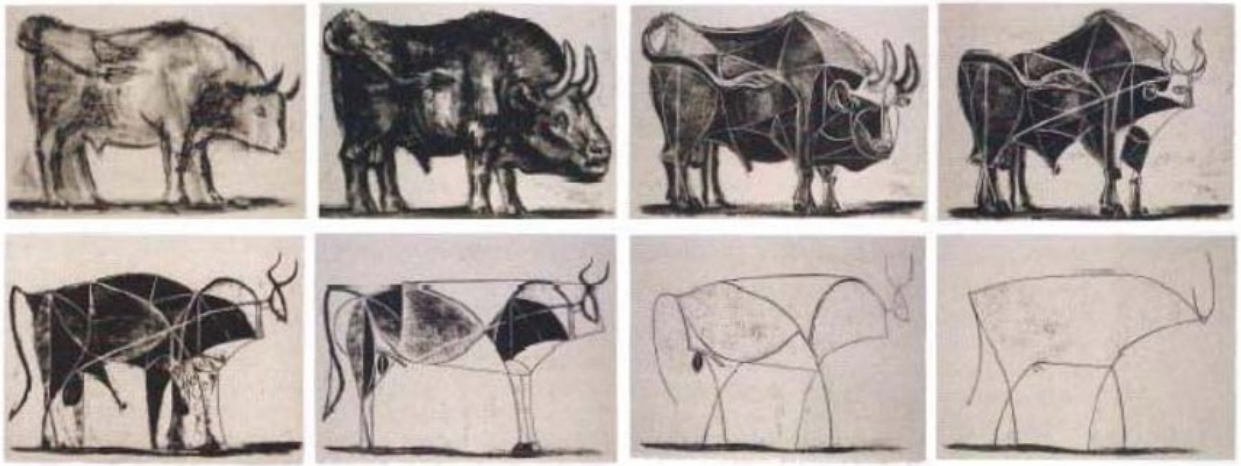

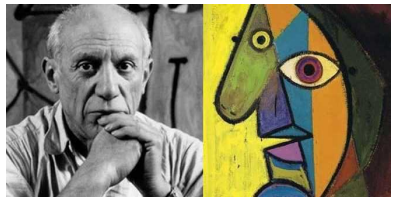

Picasso, *The Bull*, 1945.

*"According to Locke* (*John Locke*, 1632-1704)*, the complex idea of a substance is a collection of simple ideas that is believed capable of existing independently. Observing in experience that several features recur together frequently, we suppose that there must be some common subject that has all of them."*, The Philosophy Pages by Garth Kemerling.

# Complex *soft matter*

Why are we interested in soft matter?

*Complexity* is the hallmark of living systems/natural and synthetic soft materials

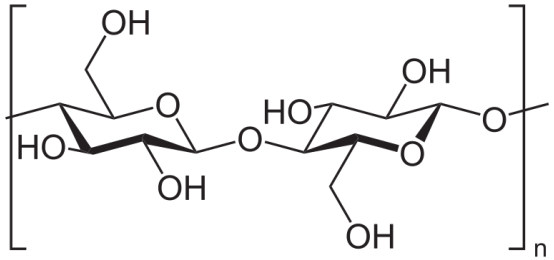


Cellulose

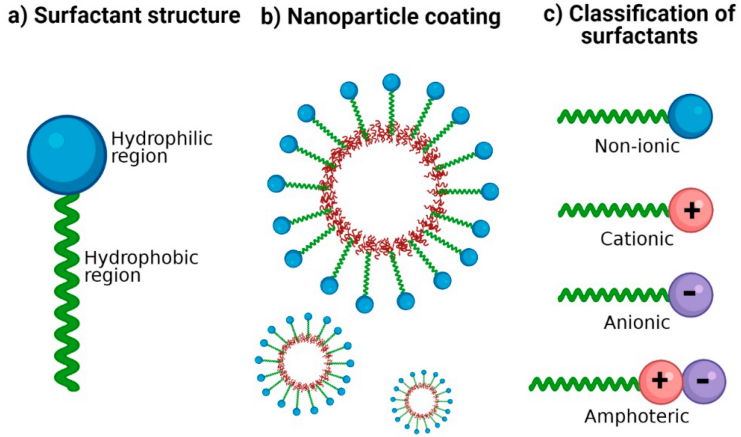


Surfactants

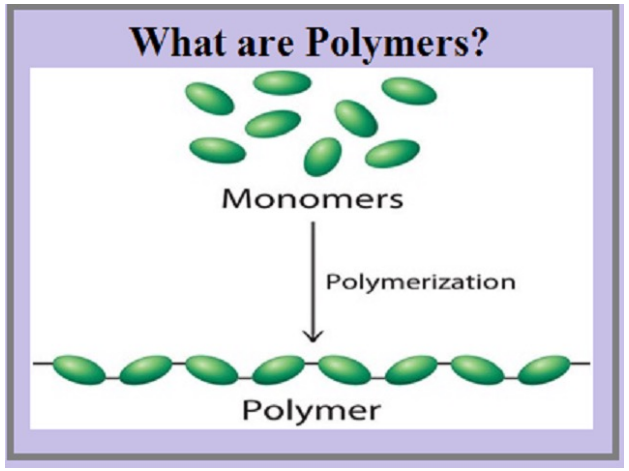


Polymers

wikipedia.org

# Complex *soft matter*

## Biological macromolecules

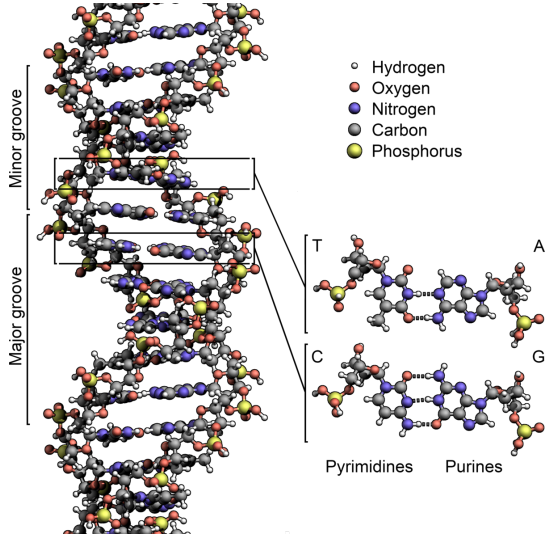


DNA

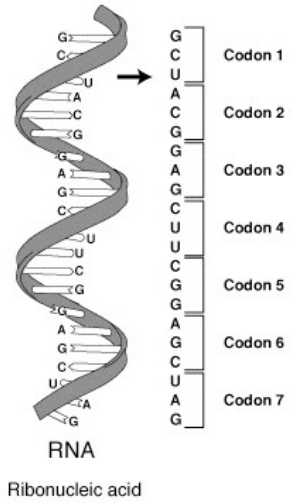


RNA

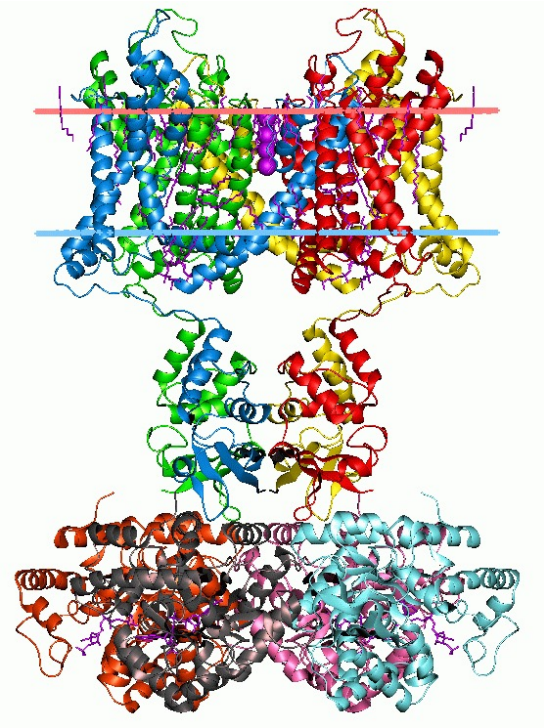

V-gated K channel

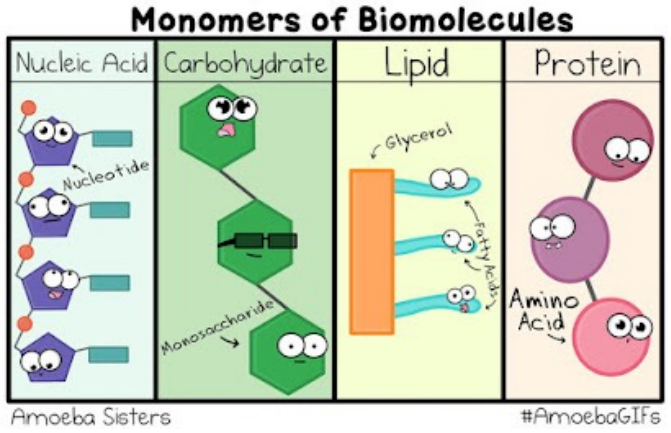


wikipedia.org

# Complex *soft matter*

Typically composed of nano-/meso- building blocks

Easily deformable when exposed to weak external fields

flow fields (microfluids), mechanical forces, electric/magnetic field, thermal agitation

*e.g.* paint, blood, milk, spreads and ice cream, …

Often formed as a result of self-assembly

Lacking quantitative description of heterogeneous, hierarchical, non-equilibrium soft materials in living systems/synthetic materials

Building blocks → determination of proper ‘scaling laws’

Time and length scale (= static and dynamic properties)

# Molecular Self-Assembly

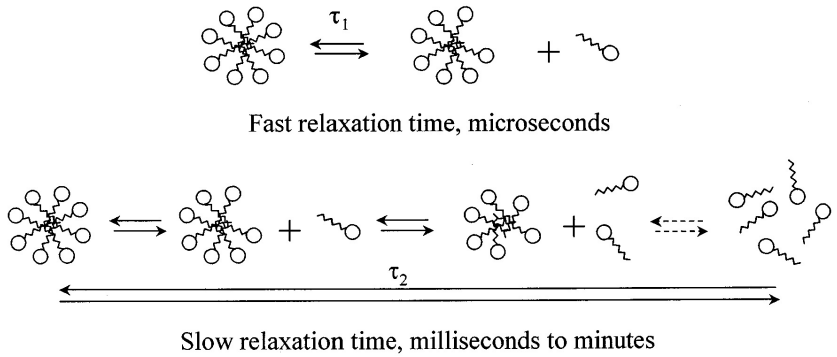


A. Patist et al. / Colloids and Surfaces A: Physicochem. Eng. Aspects 176 (2001) 3–16

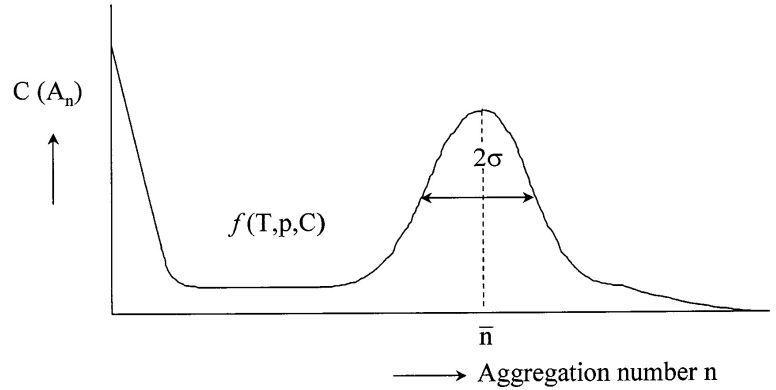


Typical size distribution curve of aggregates in a micellar solution.

$$A_1 + A_{n-1} \rightleftarrows^{k_n^+}_{k_n^-} A_n$$

*A*: aggregate

Fast relaxation process

$$\frac{1}{\tau_1} = \frac{k^-}{\sigma^2}\left(1 + \frac{\sigma^2}{n}a\right), \qquad a = \frac{C - CMC}{CMC}$$

Slow relaxation process

$$\frac{1}{\tau^2} = \frac{n^2}{CMC * R}\left(1 + \frac{\sigma^2}{n}a\right)^{-1}$$

Average micellar lifetime

$$T_m = \tau_2 \frac{na}{1 + \frac{\sigma^2}{n}a} \approx n\tau_2$$

# Colloidal Phase Behavior

Many sizes and shapes

surface charge, pH-salt concentration, polymeric additives, etc.

Self-organization into variety of structures/phases

Slower dynamics (even monitored by optical microscope)

Designer building blocks

**Molecular-level information to rationalize the experimental design**

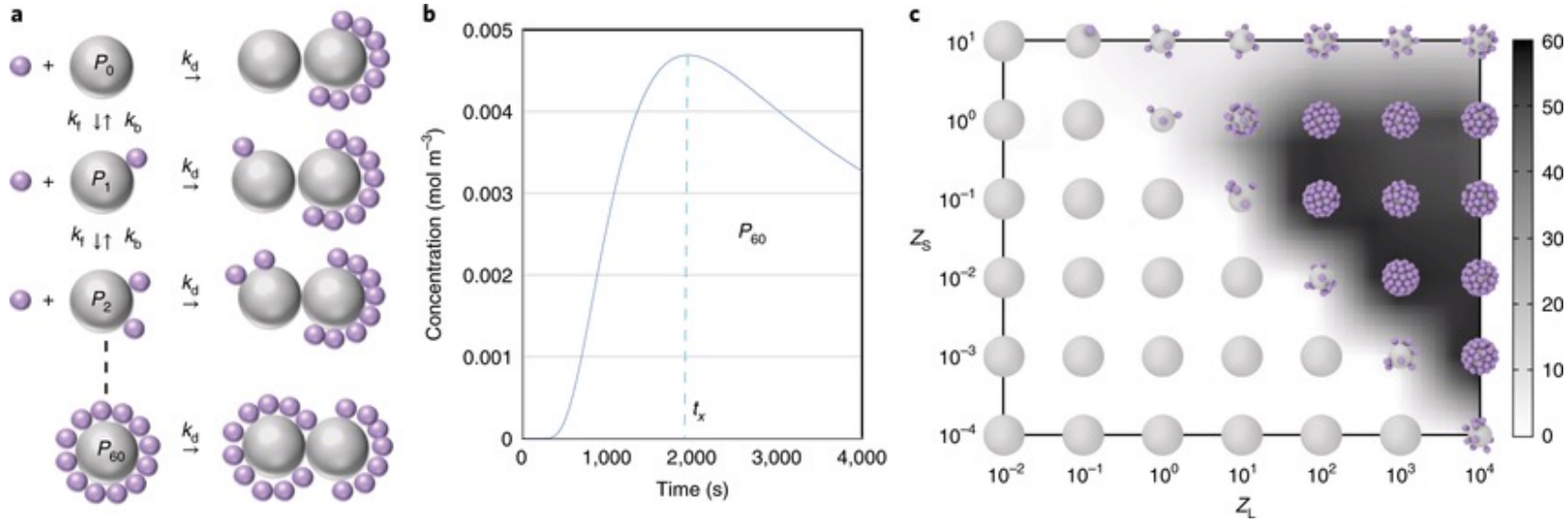


Nature Materials 20(4):1-7

# Molecular-level insight from *molecular simulations*

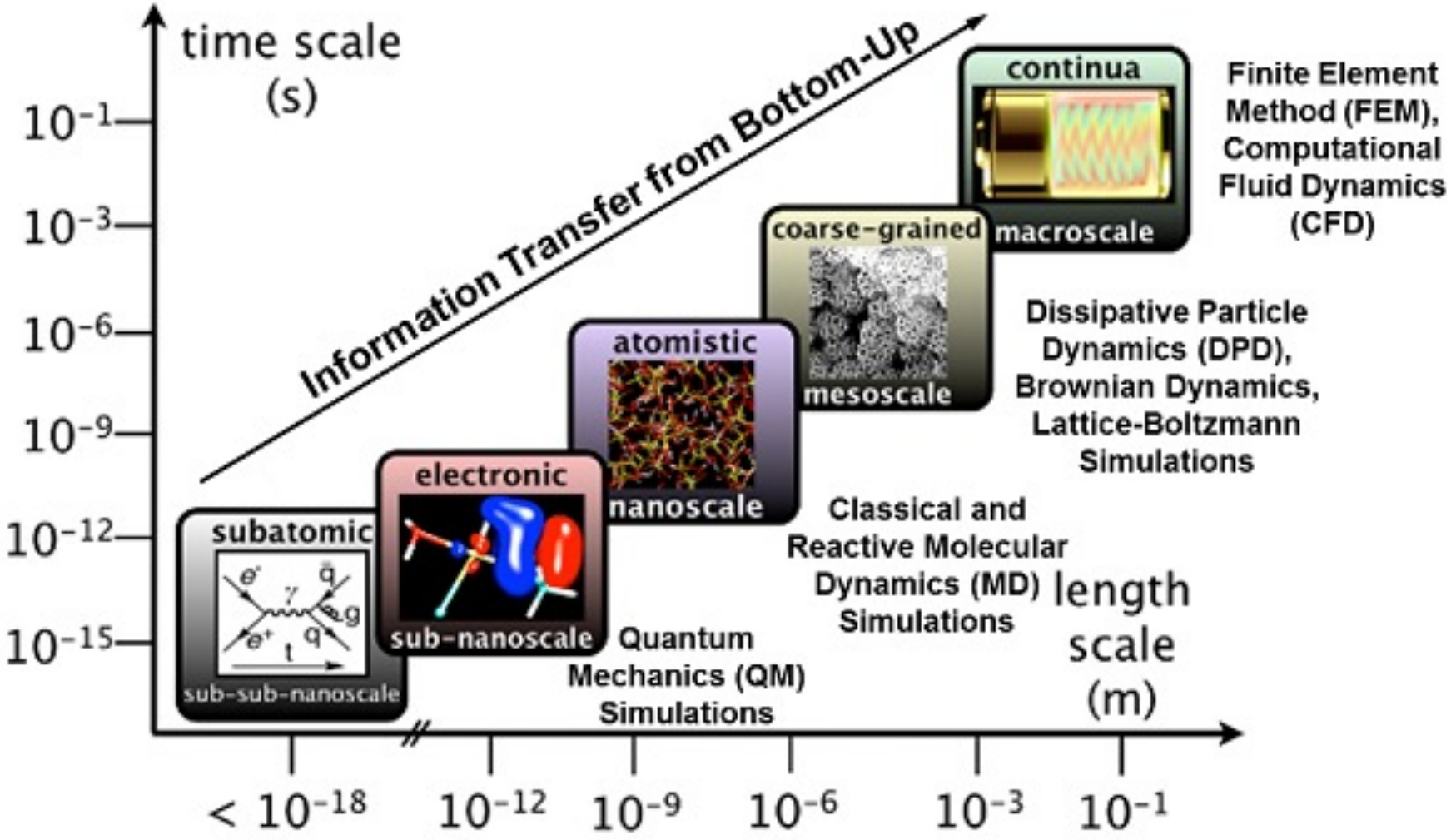


https://sites.google.com/site/lingroupfsu/

# Molecular dynamics

The solution of the classical equations of motion (Newton's equations) for a set of molecules.

$$\mathbf{F}_i = -\nabla_i V_B \qquad \vec{F} = m\vec{a}$$

First examples
Hard-sphere system

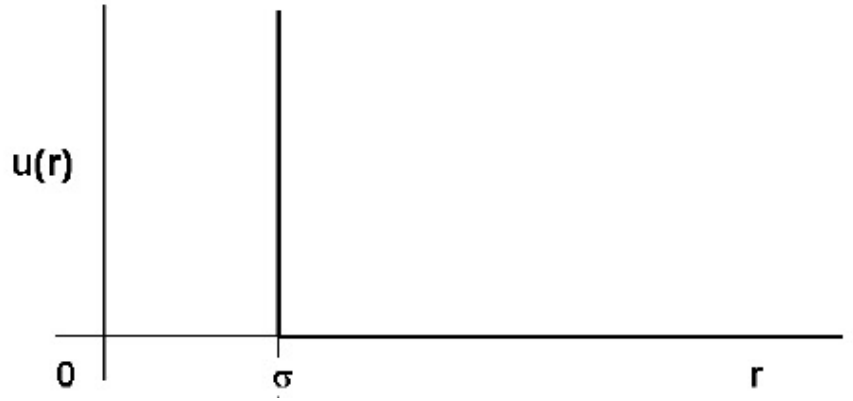


Berni Alder (1925–2020)
Thomas Wainwright (1927–2007)

IBM 704 at University of California Radiation Laboratory at Livermore.

# Molec

The solut ons) for a set of r

First exam
Hard-sphe

Berni Alde
Thomas W

IBM 704 a
Laboratory

Berni Alder (standing) with Mary Ann Mansigh (coder) and Tom E. Wainwright (physicist) in his office, 1962, "looking at oscillograph traces from the computer generated motion of particles. The pictures show the coexistence of cristallites and melt for two dimensional system of elastic disks". Courtesy AIP, Emilio Segré's visual Archives

# Molecular dynamics

Method is greatly extended by Aneesur Rahman (1927-1987)

- Particles characterized by continuous potentials
- Simulations of realistic atomic models

Frank Stillinger (born 1934)

- First MD simulation of liquid water

Macuglia, Roux and Ciccotti, Eur. Phys. 2022

Molecu

Method is gre

Particl

Simula

Frank Stillinge

First M

Eur. Phys. J. H (2022)47:13
https://doi.org/10.1140/epjh/s13129-022-00043-y

THE EUROPEAN PHYSICAL JOURNAL H

Regular Article

# The emergence of protein dynamics simulations: how computational statistical mechanics met biochemistry

Daniele Macuglia[1], Benoît Roux[2,a], and Giovanni Ciccotti[3,4,5]

[1] Department of History of Science, Technology and Medicine, Academy for Advanced Interdisciplinary Studies, Peking University, Beijing 100871, China
[2] Department of Biochemistry and Molecular Biology, University of Chicago, Chicago, IL 60637, USA
[3] Department of Physics, University of Rome "La Sapienza", 00185 Rome, Italy
[4] IAC-CNR, Institute for the Application of Computing "M. Picone", National Research Council, 00185 Rome, Italy
[5] School of Physics, University College Dublin, Belfield, Dublin 4, Ireland

Received 22 April 2022 / Accepted 22 August 2022


**Abstract** In this essay, we aim to illustrate how Martin Karplus and his research group effectively set in motion the engine of molecular dynamics (MD) simulations of biomolecules. This process saw its prodromes between 1969 and the early 1970s with Karplus' landing in biology, a transition that came to fruition with the treatment of 11-*cis*-retinal photoisomerization and the development of an allosteric model to account for the mechanism of cooperativity in hemoglobin. In 1977, J. Andrew McCammon, Bruce Gelin, and Martin Karplus published an article in *Nature* reporting the MD simulation of bovine pancreatic trypsin inhibitor (BPTI). This publication helped initiate the merger of computational statistical mechanics and biochemistry, a process that Karplus undertook at a later stage and whose beginnings we propose to reconstruct in this article through unpublished accounts of the key people who participated in this endeavor.

Macuglia, Roux and Ciccotti, Eur. Phys. 2022

# System definition

## Cartesian coordinates

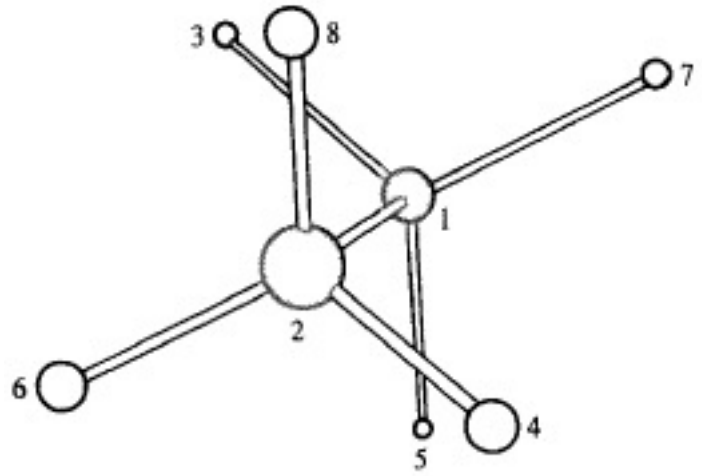


| | | | |
|---|---|---|---|
| C | 0.000000 | 0.000000 | 0.762209 |
| C | 0.000000 | 0.000000 | -0.762209 |
| H | 0.000000 | 1.018957 | 1.157229 |
| H | -0.882443 | -0.509479 | 1.157229 |
| H | 0.882443 | -0.509479 | 1.157229 |
| H | 0.000000 | -1.018957 | -1.157229 |
| H | -0.882443 | 0.509479 | -1.157229 |
| H | 0.882443 | 0.509479 | -1.157229 |

Leach, Mol. Mod. Princ. Appl., 2nd Ed.

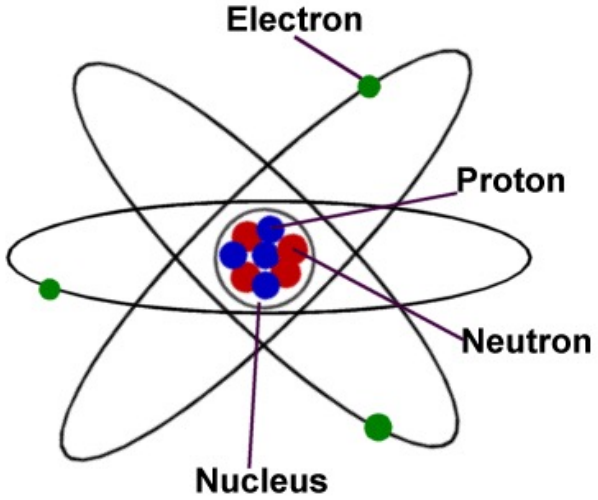


Underlying assumption: Born-Oppenheimer approximation

The wave functions of atomic nuclei and electrons in a molecule can be separated.

The nuclei are much heavier than the electrons.

The coordinates of the nuclei in a system are somewhat fixed, while the coordinates of the electrons are dynamic.

# Molecular dynamics

Compute the forces on the particles

Solve the equations of motion

Sample after some timesteps

Simulate collusions

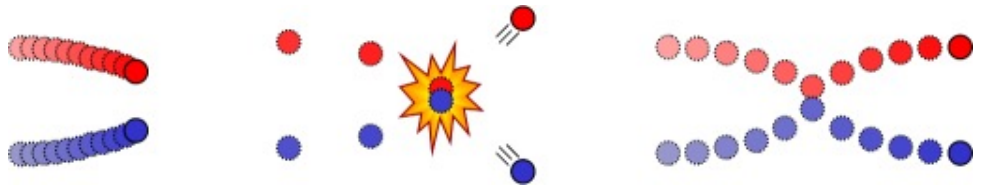

# Molecular dynamics

## A simple molecular dynamics program

```
program md                          simple MD program

call init                           initialization
t=0
do while (t.lt.tmax)                MD loop
   call force(f,en)                 determine the forces
   call integrate(f,en)             integrate equations of motion
   t=t+delt
   call sample                      sample averages
enddo
stop
end
```

Frenkel and Smit, 2001.

# Verlet and v-Verlet algorithms

Equations of motion

$$\mathbf{r}(t+\Delta t)=\mathbf{r}(t)+\mathbf{v}(t)\Delta t+\frac{\Delta t^2}{2m}\mathbf{f}(t)+\frac{\Delta t^3}{3!}\dddot{\mathbf{r}}(t)+\mathrm{O}\left(\Delta t^4\right)$$

$$\mathbf{r}(t-\Delta t)=\mathbf{r}(t)-\mathbf{v}(t)\Delta t+\frac{\Delta t^2}{2m}\mathbf{f}(t)-\frac{\Delta t^3}{3!}\dddot{\mathbf{r}}(t)+\mathrm{O}\left(\Delta t^4\right)$$

$$\mathbf{r}(t+\Delta t)+\mathbf{r}(t-\Delta t)=2\mathbf{r}(t)+\frac{\Delta t^2}{m}\mathbf{f}(t)+\mathrm{O}\left(\Delta t^4\right)$$

Verlet algorithm

$$\mathbf{r}(t+\Delta t)\approx 2\mathbf{r}(t)-\mathbf{r}(t-\Delta t)+\frac{\Delta t^2}{m}\mathbf{f}(t)$$

Velocity Verlet algorithm

$$\mathbf{r}(t+\Delta t)\approx \mathbf{r}(t)+\mathbf{v}(t)\Delta t+\frac{\Delta t^2}{2m}\mathbf{f}(t)$$

$$\mathbf{v}(t+\Delta t)\approx \mathbf{v}(t)+\frac{\Delta t}{2m}\left[\mathbf{f}(t+\Delta t)+\mathbf{f}(t)\right]$$

B. Smit, Molsim notes, 2019.

# Modeling molecular-level interactions

**Bonded potential**

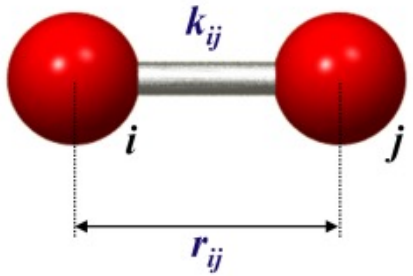


**Angle potential**

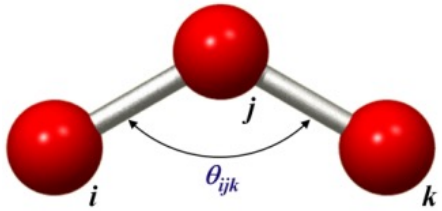


**Non-bonded potential**

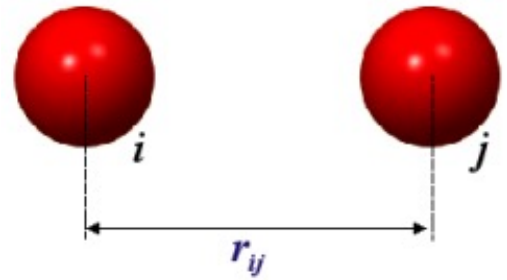


www.pumma.nl

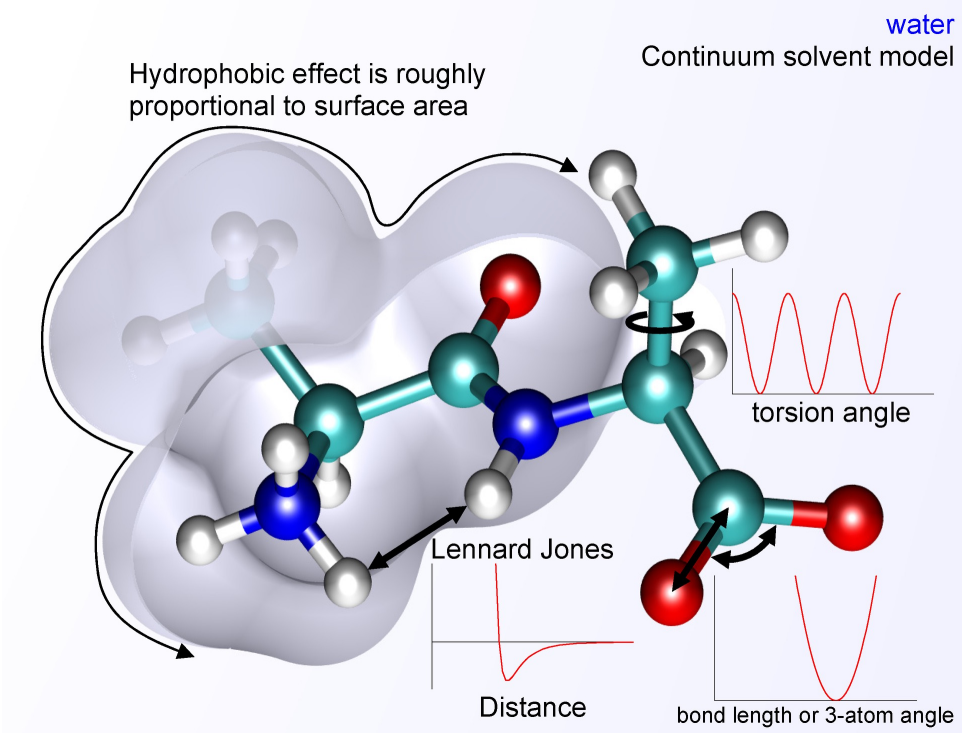


wikipedia.org

$$V_{vdW} = 4\,\epsilon_{ij}\left(\left(\frac{\sigma_{ij}}{r_{ij}}\right)^{12} - \left(\frac{\sigma_{ij}}{r_{ij}}\right)^{6}\right)$$

# Molecular dynamics

Proper sampling of system's potential energy

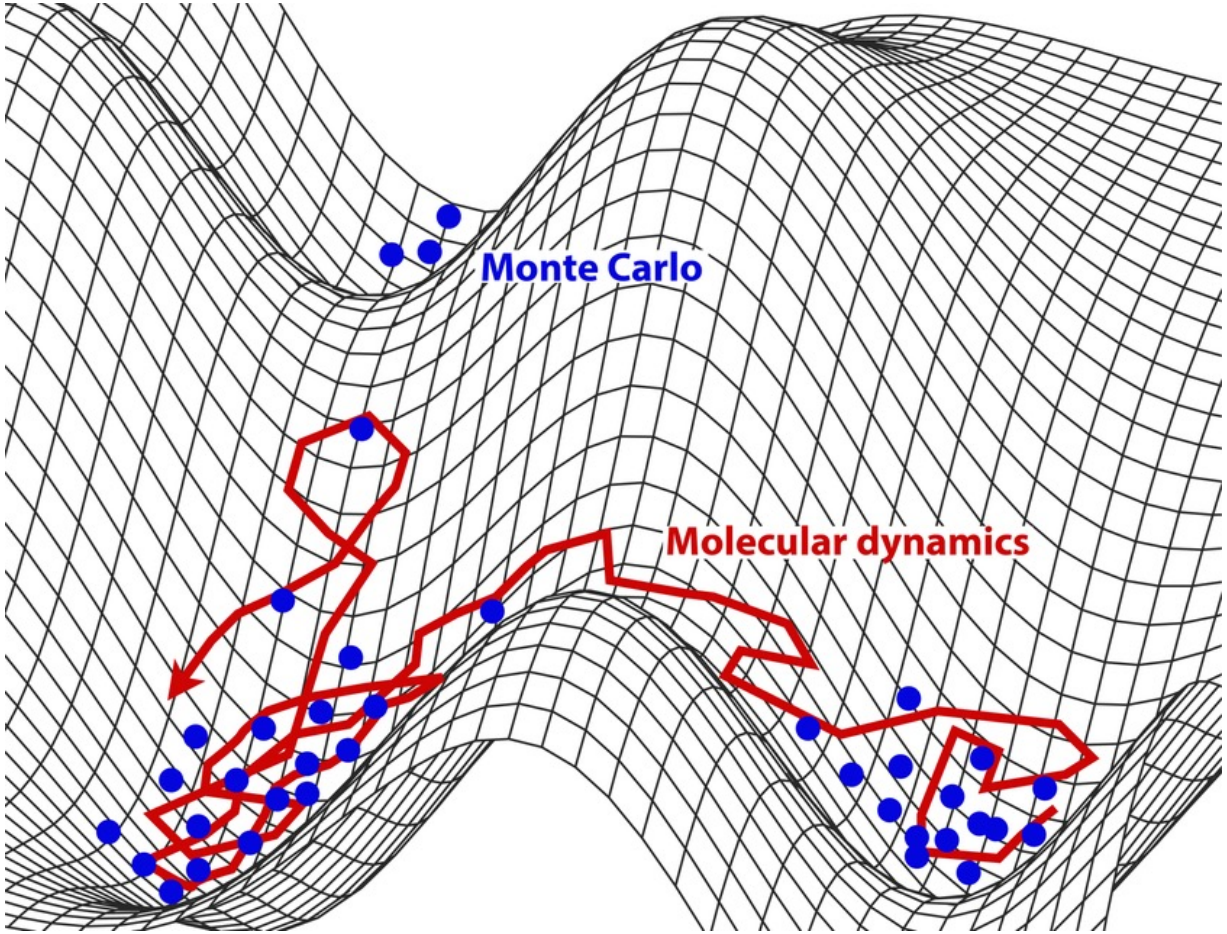

# Periodic Boundary Conditions

Taking care of close neighbors

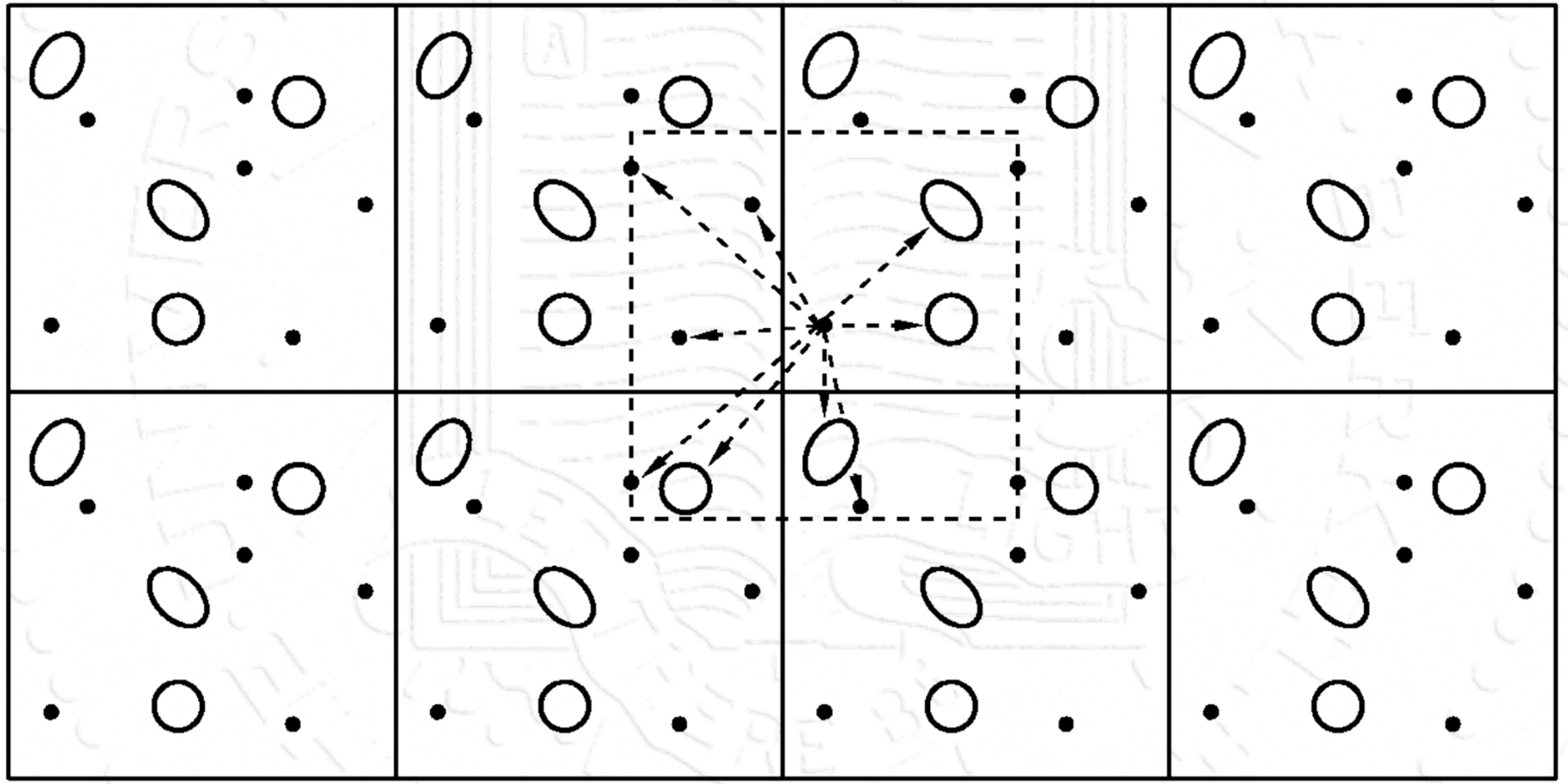

B. Smit, Molsim notes, 2019.

# Computational efficiency

- The Lennard-Jones potential

$$u^{LJ}(r) = 4\varepsilon\left[\left(\frac{\sigma}{r}\right)^{12} - \left(\frac{\sigma}{r}\right)^{6}\right]$$

- The truncated Lennard-Jones potential

$$u(r) = \begin{cases} u^{LJ}(r) & r \le r_c \\ 0 & r > r_c \end{cases}$$

- The truncated and shifted Lennard-Jones potential

$$u(r) = \begin{cases} u^{LJ}(r) - u^{LJ}(r_c) & r \le r_c \\ 0 & r > r_c \end{cases}$$

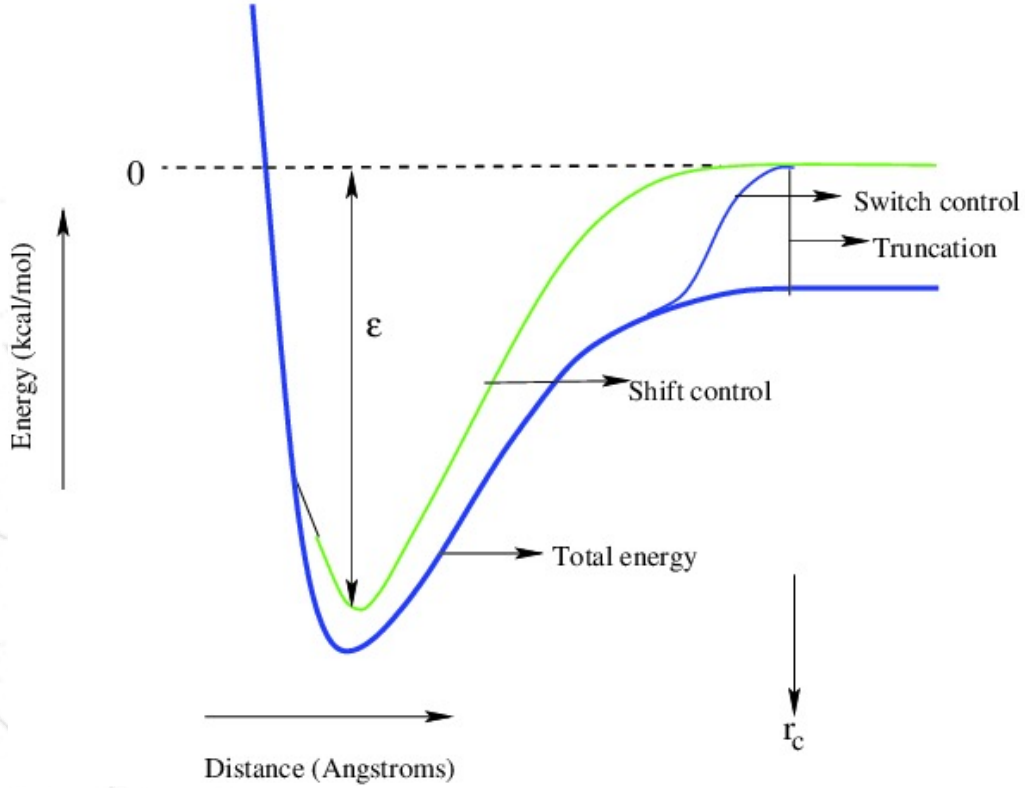


Zoe Cournia, Ph.D. Thesis, 2006.

B. Smit, Molsim notes, 2019.

# Minimizing energy

Algorithms to minimize the potential energy of the system

- Steepest Descent
- Conjugate Gradients
- Newton-Raphson

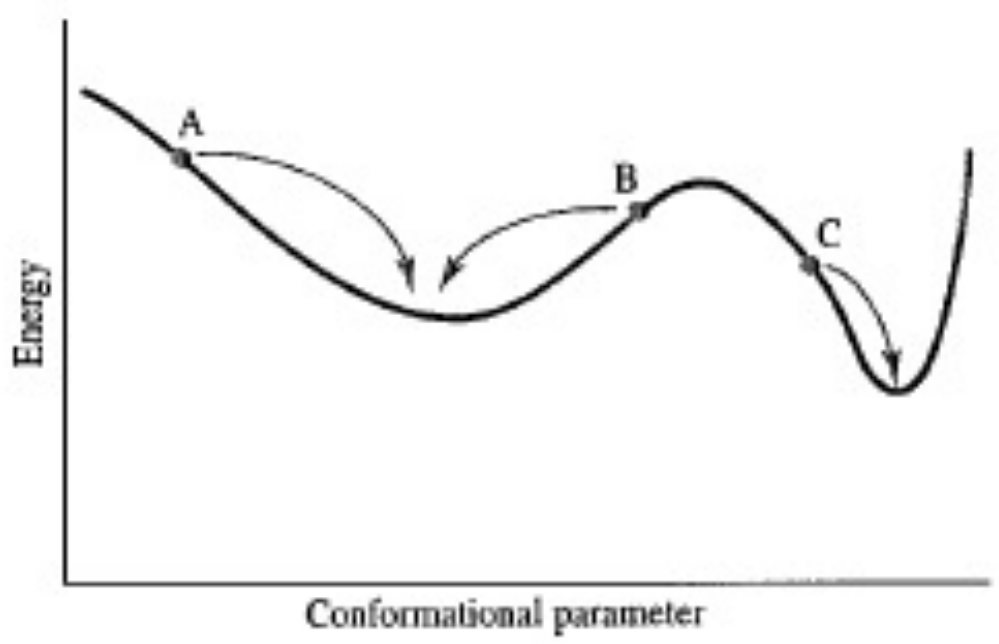


Leach, Mol. Mod. Princ. Appl., 2nd Ed.

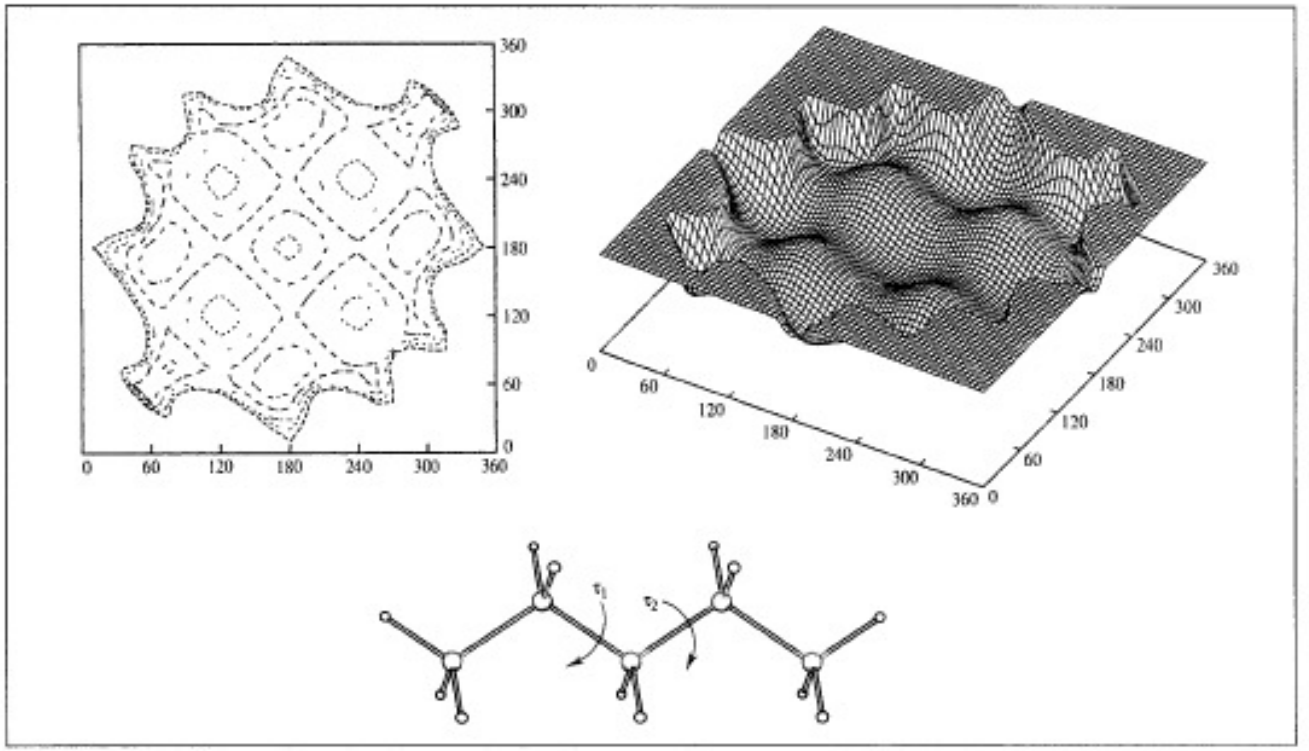


*Fig. 5.1 Variation in the energy of pentane with the two torsion angles indicated and represented as a contour diagram and isometric plot. Only the lowest-energy regions are shown.*

# Which one to use?

| | Initial refinement (Av. gradient <1 kcal Å$^{-2}$) | | Stringent minimisation (Av. gradient <0.1 kcal Å$^{-2}$) | |
|---|---|---|---|---|
| Method | CPU time (s) | Number of iterations | CPU time (s) | Number of iterations |
| Steepest descents | 67 | 98 | 1405 | 1893 |
| Conjugate gradients | 149 | 213 | 257 | 367 |

Leach, Mol. Mod. Princ. Appl., 2nd Ed.

# Concept of force-field

$$\vec{F} = m\vec{a} \qquad \mathbf{F}_i = -\nabla_i V_B \qquad \vec{a} = \frac{d\vec{v}}{dt} = \frac{d^2\vec{\boldsymbol{r}}}{dt^2}$$

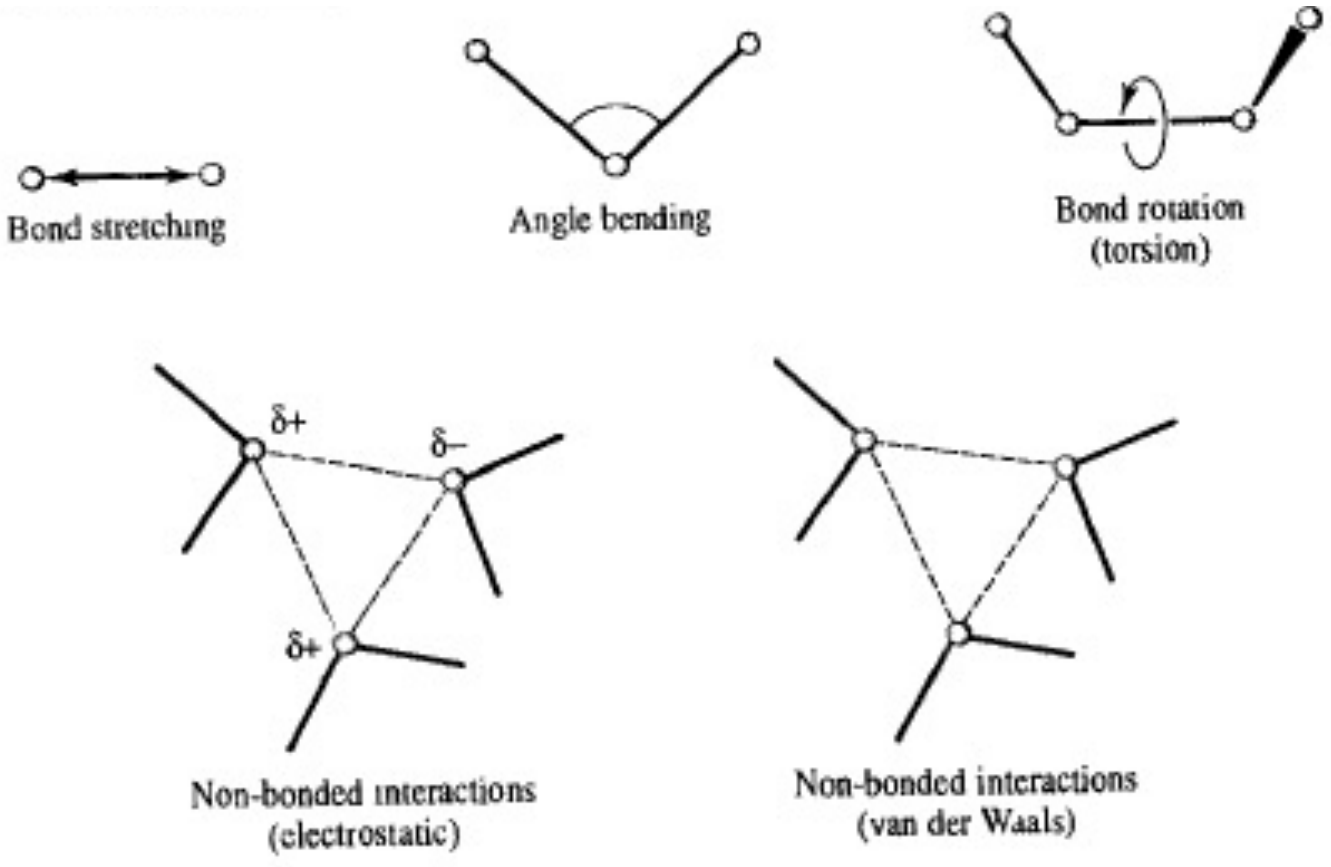


Leach, Mol. Mod. Princ. Appl., 2nd Ed.

# Concept of force-field

$$\mathcal{V}(\mathbf{r}^N) = \sum_{\text{bonds}} \frac{k_i}{2}(l_i - l_{i,0})^2 + \sum_{\text{angles}} \frac{k_i}{2}(\theta_i - \theta_{i,0})^2 + \sum_{\text{torsions}} \frac{V_n}{2}(1 + \cos(n\omega - \gamma))$$

$$+ \sum_{i=1}^{N} \sum_{j=i+1}^{N} \left( 4\varepsilon_{ij} \left[ \left( \frac{\sigma_{ij}}{r_{ij}} \right)^{12} - \left( \frac{\sigma_{ij}}{r_{ij}} \right)^{6} \right] + \frac{q_i q_j}{4\pi\varepsilon_0 r_{ij}} \right)$$

Leach, Mol. Mod. Princ. Appl., 2nd Ed.

# Force-field examples

## OPLS: 12-6 LJ potential

*J. Am. Chem. Soc.* **1996,** *118,* 11225−11236



### Development and Testing of the OPLS All-Atom Force Field on Conformational Energetics and Properties of Organic Liquids

**William L. Jorgensen,* David S. Maxwell, and Julian Tirado-Rives**

*Contribution from the Department of Chemistry, Yale University, New Haven, Connecticut 06520-8107*

*Received June 27, 1996. Revised Manuscript Received September 5, 1996*[⊗]

**Abstract:** The parametrization and testing of the OPLS all-atom force field for organic molecules and peptides are described. Parameters for both torsional and nonbonded energetics have been derived, while the bond stretching and angle bending parameters have been adopted mostly from the AMBER all-atom force field. The torsional parameters were determined by fitting to rotational energy profiles obtained from ab initio molecular orbital calculations at the RHF/6-31G*//RHF/6-31G* level for more than 50 organic molecules and ions. The quality of the fits was high with average errors for conformational energies of less than 0.2 kcal/mol. The force-field results for molecular structures are also demonstrated to closely match the ab initio predictions. The nonbonded parameters were developed in conjunction with Monte Carlo statistical mechanics simulations by computing thermodynamic and structural properties for 34 pure organic liquids including alkanes, alkenes, alcohols, ethers, acetals, thiols, sulfides, disulfides, aldehydes, ketones, and amides. Average errors in comparison with experimental data are 2% for heats of vaporization and densities. The Monte Carlo simulations included sampling all internal and intermolecular degrees of freedom. It is found that such non-polar and monofunctional systems do not show significant condensed-phase effects on internal energies in going from the gas phase to the pure liquids.

## COMPASS: 9-6 LJ potential



*J. Phys. Chem. B* **1998,** *102,* 7338−7364

### COMPASS: An ab Initio Force-Field Optimized for Condensed-Phase Applications—Overview with Details on Alkane and Benzene Compounds

**H. Sun**

*Molecular Simulations Inc., 9685 Scranton Road, San Diego, California 92121-3752*

*Received: January 29, 1998; In Final Form: May 22, 1998*

A general all-atom force field for atomistic simulation of common organic molecules, inorganic small molecules, and polymers was developed using state-of-the-art ab initio and empirical parametrization techniques. The valence parameters and atomic partial charges were derived by fitting to ab initio data, and the van der Waals (vdW) parameters were derived by conducting MD simulations of molecular liquids and fitting the simulated cohesive energies and equilibrium densities to experimental data. The combined parametrization procedure significantly improves the quality of a general force field. Validation studies based on large number of isolated molecules, molecular liquids and molecular crystals, representing 28 molecular classes, show that the present force field enables accurate and simultaneous prediction of structural, conformational, vibrational, and thermophysical properties for a broad range of molecules in isolation and in condensed phases. Detailed results of the parametrization and validation for alkane and benzene compounds are presented.

# Force-field examples

## DREIDING: 12-10 LJ potential

*J. Phys. Chem.* **1990**, *94*, 8897–8909



**DREIDING: A Generic Force Field for Molecular Simulations**

**Stephen L. Mayo, Barry D. Olafson, and William A. Goddard III*,[1]**

*BioDesign, Inc., 199 South Los Robles (Suite 540), Pasadena, California 91101* *(Received: October 2, 1989; In Final Form: February 2, 1990)*

We report the parameters for a new generic force field, DREIDING, that we find useful for predicting structures and dynamics of organic, biological, and main-group inorganic molecules. The philosophy in DREIDING is to use general force constants and geometry parameters based on simple hybridization considerations rather than individual force constants and geometric parameters that depend on the particular combination of atoms involved in the bond, angle, or torsion terms. Thus all bond distances are derived from atomic radii, and there is only one force constant each for bonds, angles, and inversions and only six different values for torsional barriers. Parameters are defined for all possible combinations of atoms and new atoms can be added to the force field rather simply. This paper reports the parameters for the "nonmetallic" main-group elements (B, C, N, O, F columns for the C, Si, Ge, and Sn rows) plus H and a few metals (Na, Ca, Zn, Fe). The accuracy of the DREIDING force field is tested by comparing with (i) 76 accurately determined crystal structures of organic compounds involving H, C, N, O, F, P, S, Cl, and Br, (ii) rotational barriers of a number of molecules, and (iii) relative conformational energies and barriers of a number of molecules. We find excellent results for these systems.

## CFF: 9-6 LJ potential

*J. Am. Chem. Soc.* **1994**, *116*, 2978–2987

**An ab Initio CFF93 All-Atom Force Field for Polycarbonates**

**Huai Sun, Stephen J. Mumby, Jon R. Maple, and Arnold T. Hagler***

*Contribution from the Biosym Technologies, Inc., 9685 Scranton Road, San Diego, California 92121*

*Received March 29, 1993. Revised Manuscript Received November 29, 1993**

**Abstract:** An all-atom CFF93 force field for polycarbonates based on *ab initio* calculations is reported. Force field parameters are derived by fitting to quantum mechanical total energies, first and second derivatives of total energies, and electrostatic potentials, all generated from *ab initio* quantum mechanical calculations on model compounds at HF/6-31G* level of theory. Valence parameters and *ab initio* charges are then scaled to correct for differences between experiment and the Hartree–Fock approximation. The van der Waals parameters and the scaling factors for atomic partial charges are determined from crystal structures. Based on the force field, molecular mechanics calculations are performed for several model compounds, and the results are compared with experimental values and with the results of the *ab initio* calculations.

# Coarse-graining and coarse-grained simulations

Smoothing out of the atomistic detail

Loss of degree of freedom

1) United atom representation

Combine small atoms such as H's with heavy atoms

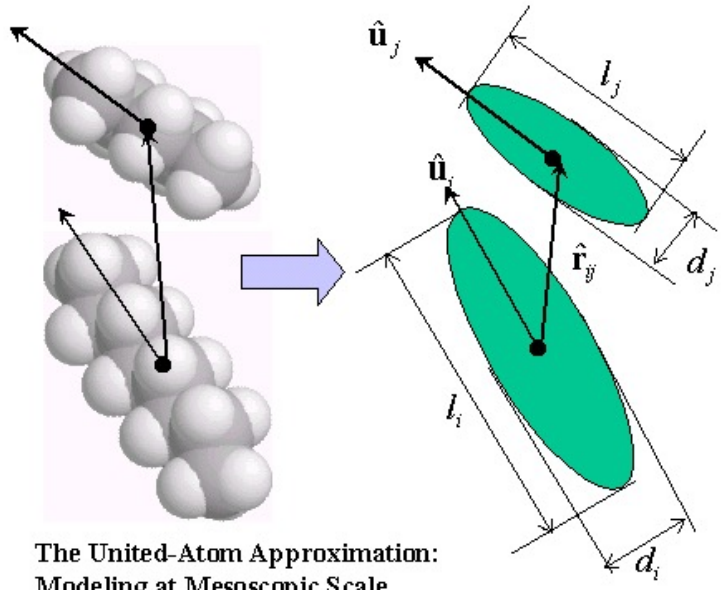


The United-Atom Approximation: Modeling at Mesoscopic Scale

Leach, Mol. Mod. Princ. Appl., 2nd Ed.

# Coarse-graining and coarse-grained simulations

Coarse-graining based on grouping of atoms

2) Grouping atoms together (order of 10:1)

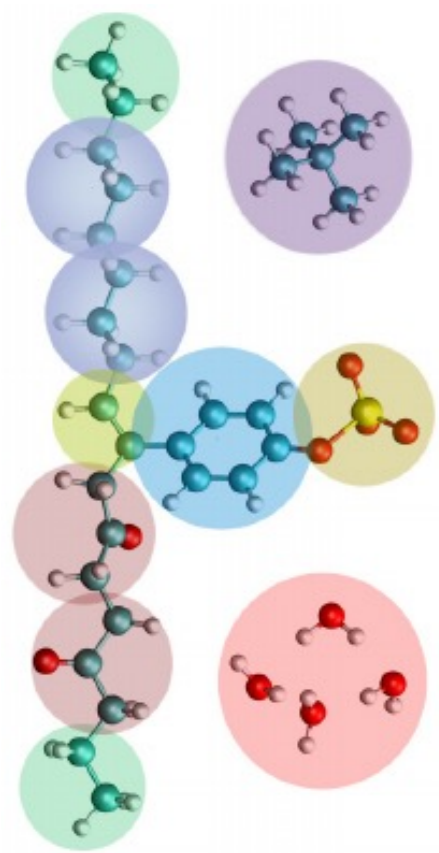

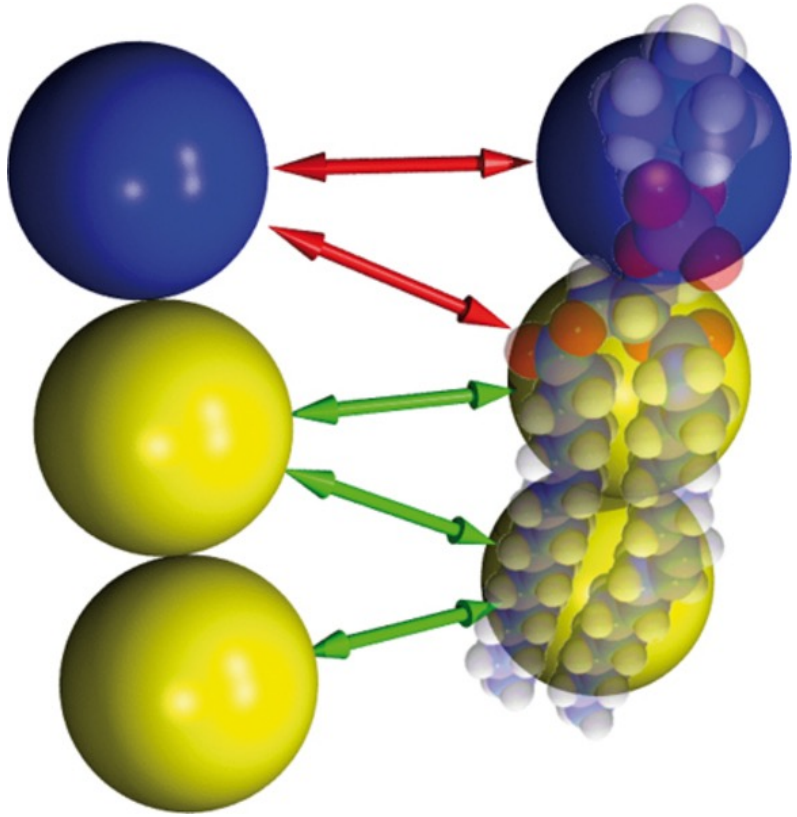

# Coarse-graining and coarse-grained simulations

## Different levels of coarse-graining

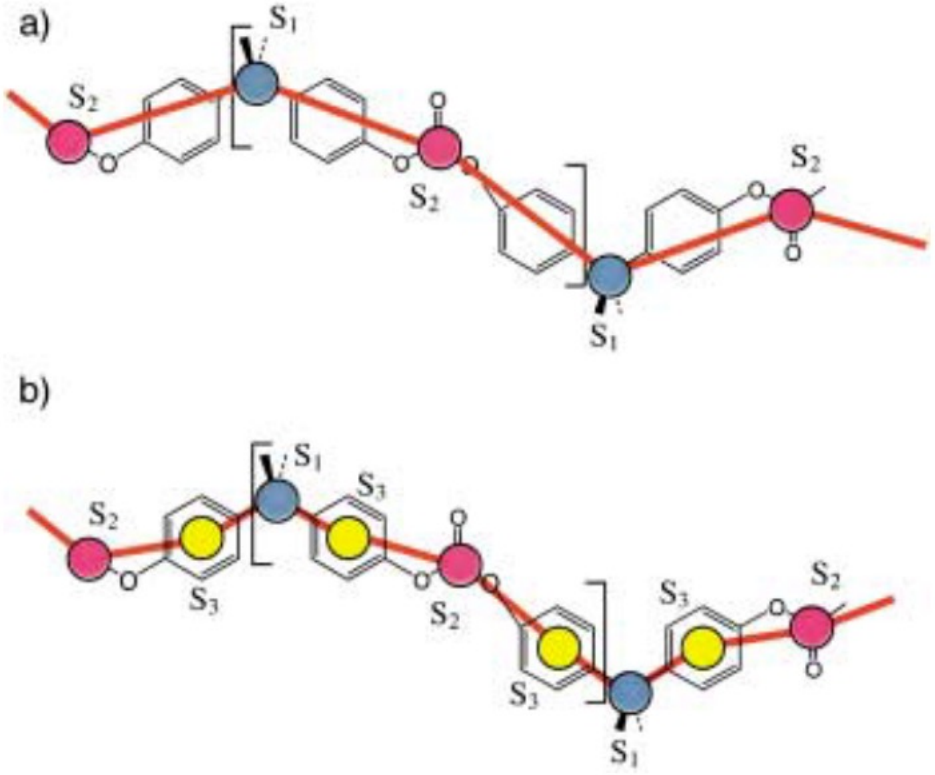


Coarse-graining of bisphenol-A polycarbonate

a) 2:1 scheme (two super-atoms per chemical repeat unit)

b) 4:1 scheme

ChemPhysChem, 2002, 3, 754 -769

# Coarse-grained potential

Integrated out atomistic detail yields smoothed potential energy surface

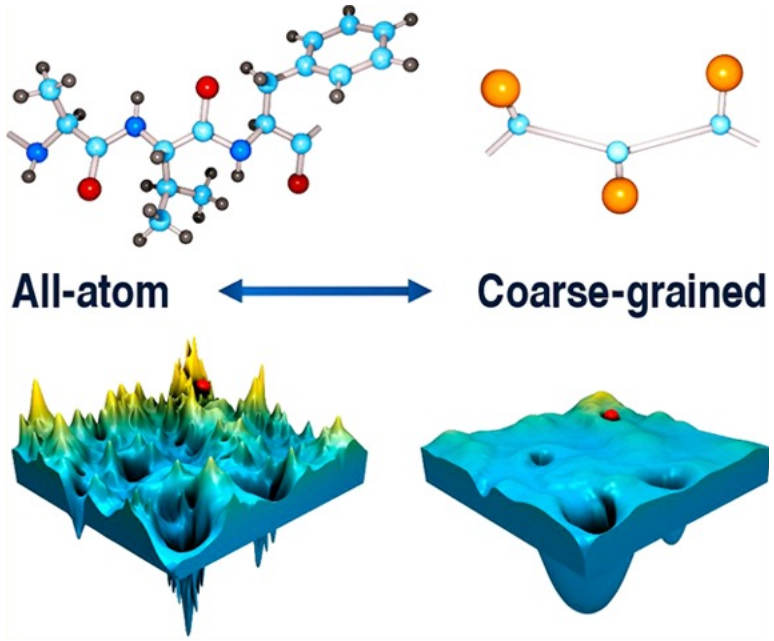


## Advantages

- Less rugged potential energy surface
- Simulating longer time and length scales
- Faster equilibration of polymeric (or complex soft matter) systems

## Disadvantages

- Poor performance in sampling local minima
- Less ability to compute energetic properties
- Loss of ability to perform unequilibrium dynamics
- Fail to predict some (e.g. mechanical) properties

Chem. Rev. 2016, 116, 7898−7936

# Coarse-grained potential

Smoothed out atomistic detail leads to ‘effective pair-wise’ interactions

- Interaction parameters are not differentiated based on different systems for atomistic simulations
- A generic all-atom (AA) model describes features common to all polymers

However,

- A coarse-grained model is different from a generic AA model
- Example: A CG model of polystyrene is different than polyisobutylene melt

# Coarse-grained potential

## How does the ‘effective pair-wise potential’ differ?

**Accelerated equilibration of polymer melts by time-coarse-graining**

Bruce M. Forrest and Ulrich W. Suter
*Institut für Polymere, Eidgenössische Technische Hochschule (ETH), CH-8092, Zürich, Switzerland*

(Received 8 November 1994; accepted 31 January 1995)

An effective-potential approach is presented for improving sampling efficiency in simulations of atomistically detailed models of dense long-chain liquids. The motion of atoms on short-time scales is described as rapid fluctuations about the slowly moving mean conformations of the chain molecules. The distribution of these fluctuations is approximated by that of isotropic elastic motion. The interactions between nonbonded pairs of atoms are preaveraged over this distribution and a much softer, effective interaction is obtained, allowing a correspondingly faster exploration of configuration space. The approximate sampling scheme is then tested on two model systems of united-atom liquid hydrocarbons—a melt of twenty $C_{24}$ chains and one of ten $C_{71}$ chains. In the $C_{24}$ melt, where a comparison with fully equilibrated samples from rigorous algorithms is possible, the preaveraging is shown to produce an improvement in sampling efficiency of up to an order of magnitude at the expense of only a moderate loss in accuracy. The method is then applied to the $C_{71}$ melt, where currently available, rigorous sampling algorithms fail to produce thorough equilibration. Also in this case, the preaveraging method proves to significantly enhance the sampling speed while producing satisfactory distributions of observables. 

# Coarse-grained potential

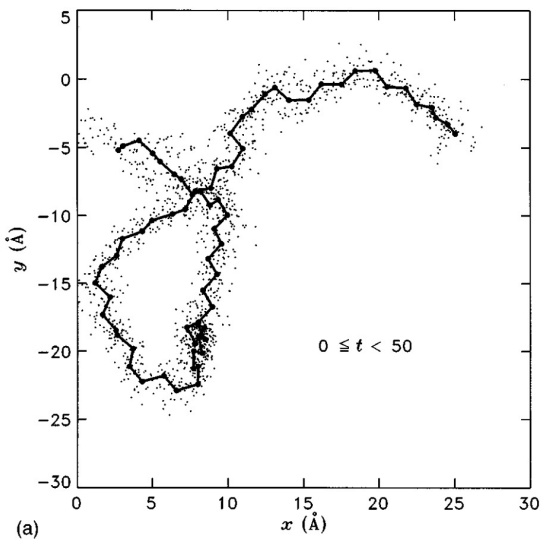


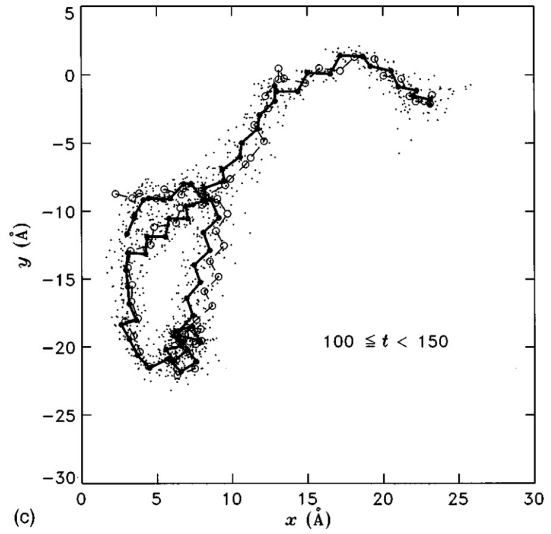


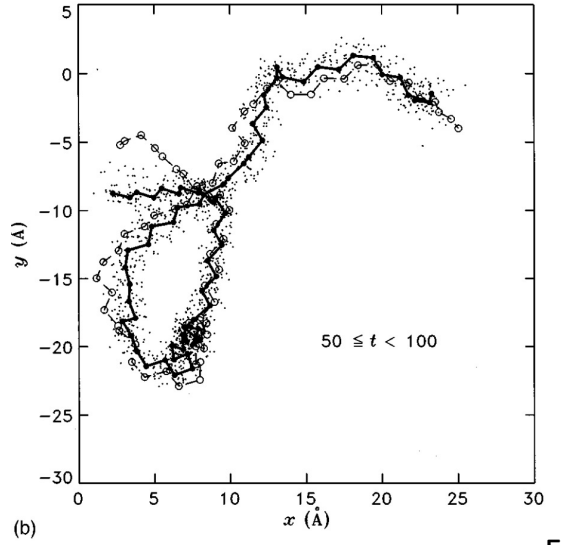


Forrest and Suter, JCP, 1995.

Time averaging of the fast dynamics is performed along with the slow motion of the whole chain

$$r_i(t_0+t)=R_i(t_0)+\Delta_i(t), \qquad 0\leqslant t<t_{\mathrm{av}}$$

$\Delta_i(t)$ = fluctuation of atom *i*

$R_i$ = mean position, where atoms fluctuate around and constant for duration of $t_{\mathrm{av}}$

# Coarse-grained potential

Level of average fluctuations is important!

Integration out of the fast vibrations leads to a softer effective pair-wise potential

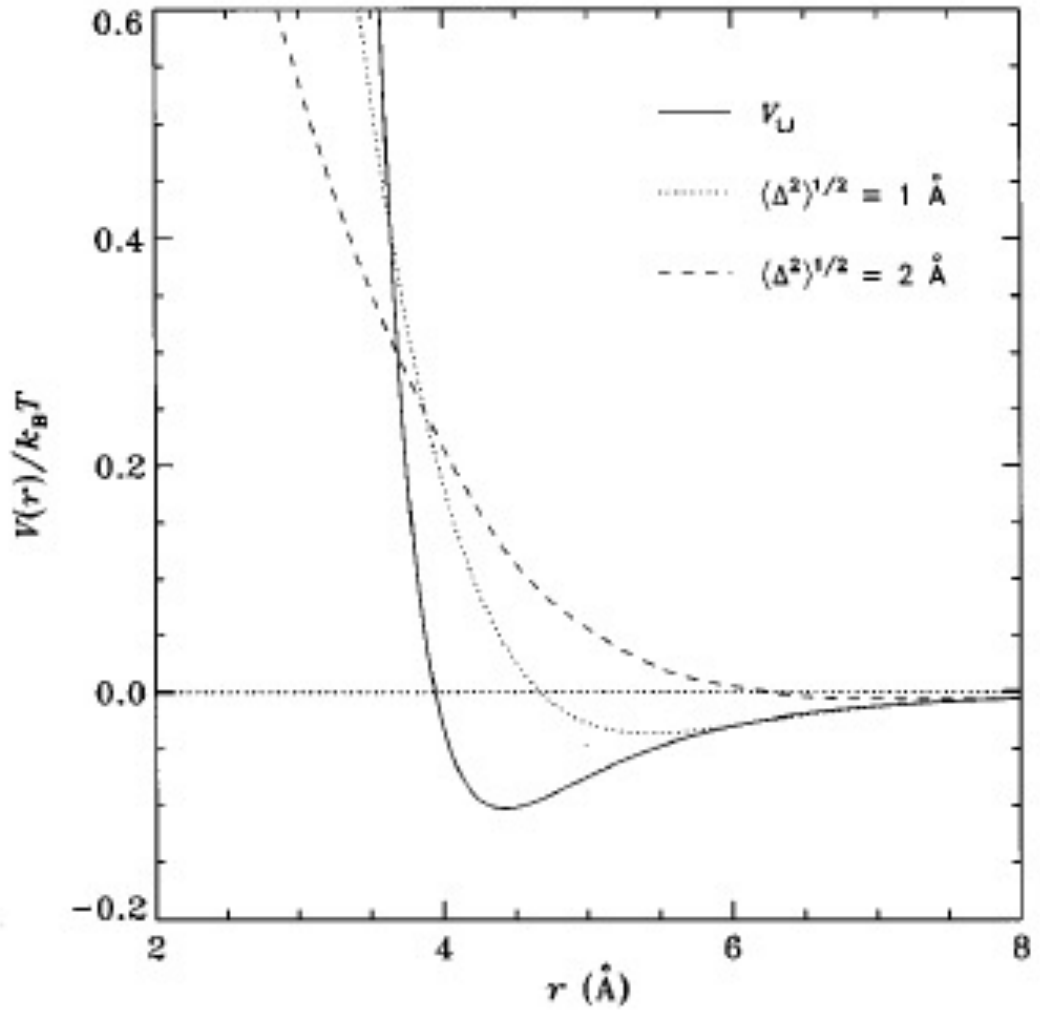


Forrest and Suter, JCP, 1995.

# Dissipative Particle Dynamics DPD

First developed by Hoogerbrugge and Koelman to simulate the 'hydrodynamic phenomena'

Particle-based method replacing Lattice Gas automata

Proper description of complex fluids with computational efficiency

Presented as a simple model contains dissipation that conserves momentum

EUROPHYSICS LETTERS 1 June 1992

*Europhys. Lett.*, **19** (3), pp. 155-160 (1992)

## Simulating Microscopic Hydrodynamic Phenomena with Dissipative Particle Dynamics.

P. J. HOOGERBRUGGE and J. M. V. A. KOELMAN

*Shell Research B.V. - P.O.Box 60, 2280 AB Rijswijk, The Netherlands*

(received 19 February 1992; accepted in final form 29 April 1992)

PACS. 02.70 – Computational techniques.
PACS. 51.10 – Kinetic and transport theory.

**Abstract.** – We present a novel method for simulating hydrodynamic phenomena. This particle-based method combines features from molecular dynamics and lattice-gas automata. It is shown theoretically as well as in simulations that a quantitative description of isothermal Navier-Stokes flow is obtained with relatively few particles. Computationally, the method is much faster than molecular dynamics, and the at same time it is much more flexible than lattice-gas automata schemes.

# DPD

Español and Warren later reformulized the total force term as

$$\dot{\boldsymbol{p}}_i = \sum_{j \neq i} \boldsymbol{F}_{ij}^{\mathrm{C}} + \sum_{j \neq i} \boldsymbol{F}_{ij}^{\mathrm{D}} + \sum_{j \neq i} \boldsymbol{F}_{ij}^{\mathrm{R}}$$

where,

$$\boldsymbol{F}_{ij}^{\mathrm{D}} = -\gamma \omega_{\mathrm{D}}(r_{ij})(\boldsymbol{e}_{ij} \cdot \boldsymbol{v}_{ij})\boldsymbol{e}_{ij}$$

$$\boldsymbol{F}_{ij}^{\mathrm{R}} = \sigma \omega_{\mathrm{R}}(r_{ij})\boldsymbol{e}_{ij}\zeta_{ij},$$

Stochastic white noise term

satisfying $\zeta_{ij} = \zeta_{ji}$ to conserve momentum

Holds fluctuation-dissipation theorem such that (similar to Brownian motion)

$$\sigma = (2k_{\mathrm{B}}T\gamma)^{1/2}$$

EUROPHYSICS LETTERS 1 May 1995

*Europhys. Lett.*, **30** (4), pp. 191-196 (1995)

**Statistical Mechanics of Dissipative Particle Dynamics.**

P. ESPAÑOL (*) (§) and P. WARREN (**)

(*) *Cavendish Laboratory, University of Cambridge Madingley Road, Cambridge CB3 OHE, UK*
(**) *Unilever Research Port Sunlight Laboratory Quarry Road East, Bebington, Wirral, L63 3JW, UK*

(received 22 December 1994; accepted in final form 30 March 1995)

PACS. 02.70−c – Computational techniques.
PACS. 51.10+y – Kinetic and transport theory of gases.

**Abstract.** – The stochastic differential equations corresponding to the updating algorithm of Dissipative Particle Dynamics (DPD), and the corresponding Fokker-Planck equation are derived. It is shown that a slight modification to the algorithm is required before the Gibbs distribution is recovered as the stationary solution to the Fokker-Planck equation. The temperature of the system is then directly related to the noise amplitude by means of a fluctuation-dissipation theorem. However, the correspondingly modified, discrete DPD algorithm is only found to obey these predictions if the length of the time step is sufficiently reduced. This indicates the importance of time discretisation in DPD.

# DPD (Dissipative Particle Dynamics)

**In summary**

**C**onservative, **R**andom and **D**issipative forces

**C** force characterizes the equilibrium structure

**R** and **D** forces are coupled and act as a thermostat

$$\mathbf{F}^{\mathrm{T}} = m\vec{a}$$
$$= \mathbf{F}^{\mathrm{C}} + \mathbf{F}^{\mathrm{R}} + \mathbf{F}^{\mathrm{D}}$$

$$\mathbf{r}_i(t+\Delta t) = \mathbf{r}_i(t) + \Delta t \mathbf{v}_i(t) + \tfrac{1}{2}(\Delta t)^2 \mathbf{f}_i(t),$$

$$\tilde{\mathbf{v}}_i(t+\Delta t) = \mathbf{v}_i(t) + \lambda \Delta t \mathbf{f}_i(t),$$

$$\mathbf{f}_i(t+\Delta t) = \mathbf{f}_i(\mathbf{r}(t+\Delta t), \tilde{\mathbf{v}}(t+\Delta t)),$$

$$\mathbf{v}_i(t+\Delta t) = \mathbf{v}_i(t) + \tfrac{1}{2}\Delta t(\mathbf{f}_i(t) + \mathbf{f}_i(t+\Delta t)).$$

For $\lambda = \frac{1}{2}$ Verlet algorithm is recovered.

# How to compute the parameters?

## Dissipative particle dynamics: Bridging the gap between atomistic and mesoscopic simulation

Robert D. Groot and Patrick B. Warren
*Unilever Research Port Sunlight Laboratory, Quarry Road East, Bebington, Wirral, L63 3JW, United Kingdom*

(Received 27 March 1997; accepted 16 June 1997)

We critically review dissipative particle dynamics (DPD) as a mesoscopic simulation method. We have established useful parameter ranges for simulations, and have made a link between these parameters and $\chi$-parameters in Flory-Huggins-type models. This is possible because the equation of state of the DPD fluid is essentially quadratic in density. This link opens the way to do large scale simulations, effectively describing millions of atoms, by firstly performing simulations of molecular fragments retaining all atomistic details to derive $\chi$-parameters, then secondly using these results as input to a DPD simulation to study the formation of micelles, networks, mesophases and so forth. As an example application, we have calculated the interfacial tension $\sigma$ between homopolymer melts as a function of $\chi$ and $N$ and have found a universal scaling collapse when $\sigma/\rho k_{\mathrm{B}}T\chi^{0.4}$ is plotted against $\chi N$ for $N>1$. We also discuss the use of DPD to simulate the dynamics of mesoscopic systems, and indicate a possible problem with the timescale separation between particle diffusion and momentum diffusion (viscosity). 
[S0021-9606(97)51335-3]

# Groot-Warren approach

Conservative force is computed from non-bonded DPD interaction parameter $a_{ij}$

$$\mathbf{F}_{ij}^{\mathrm{C}}=\begin{cases} a_{ij}(1-r_{ij})\hat{\mathbf{r}}_{ij} & (r_{ij}<1) \\ 0 & (r_{ij}\geqslant 1) \end{cases}$$

How to choose the 'repulsion parameter'?

Building a DPD EoS!

For a sufficiently large density for $\rho > 2$

$$p=\rho k_{\mathrm{B}}T+\alpha a\rho^{2}(\alpha=0.101\pm0.001)$$

Non-bonded DPD interaction strength

Vary the density and plot the excess pressure

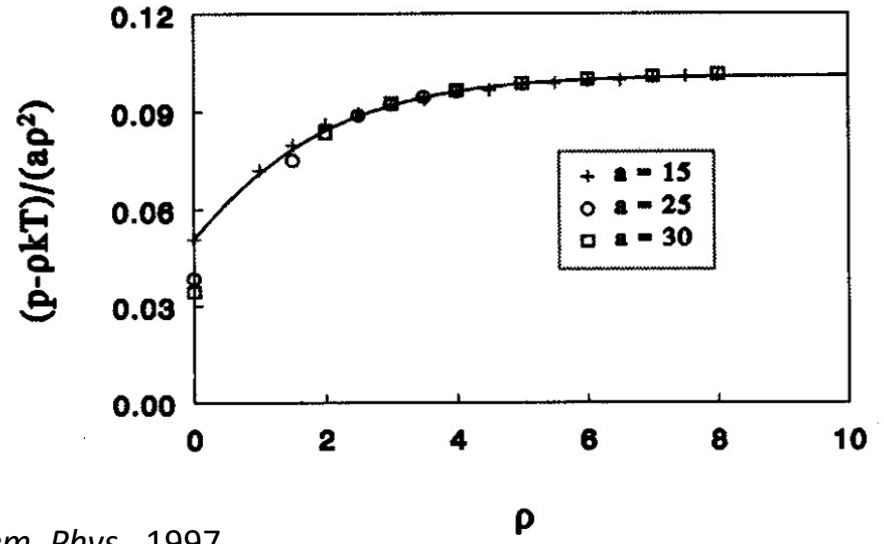


Groot and Warren, *J. Chem. Phys.*, 1997.

# Groot-Warren approach

Mapping onto Flory-Huggins theory of polymers

- Continuous version of the lattice model
- Internal energy is described as the perturbation from ideal mixing
- Free energy per lattice site

$$\frac{F}{k_{\mathrm{B}}T}=\frac{\phi_A}{N_A}\ln\,\phi_A+\frac{\phi_B}{N_B}\ln\,\phi_B+\chi\phi_A\phi_B$$

From $p=\rho k_{\mathrm{B}}T+\alpha a\rho^2(\alpha=0.101\pm0.001)$ for a two-component mixture

$$\frac{f_V}{k_{\mathrm{B}}T}=\frac{\rho_A}{N_A}\ln\,\rho_A+\frac{\rho_B}{N_B}\ln\,\rho_B-\frac{\rho_A}{N_A}-\frac{\rho_B}{N_B}+\frac{\alpha(a_{AA}\rho_A^2+2a_{AB}\rho_A\rho_B+a_{BB}\rho_B^2)}{k_{\mathrm{B}}T}$$

Groot and Warren, *J. Chem. Phys.*, 1997.

# Mapping onto Flory-Huggins theory

A $\chi$-parameter mapping $f_V/(\rho_A+\rho_B)=F$ (Flory-Huggins) yields

$$\chi=\frac{2\alpha(a_{AB}-a_{AA})(\rho_A+\rho_B)}{k_{\mathrm{B}}T}$$

We can have a reasonable estimation for the $a_{AA}$ from $\kappa^{-1}=\frac{1}{nk_{\mathrm{B}}T\kappa_T}=\frac{1}{k_{\mathrm{B}}T}\left(\frac{\partial p}{\partial n}\right)_T$

$$\kappa^{-1}=15.9835$$ Experimental data

$$\kappa^{-1}=1+2\alpha a\rho/k_{\mathrm{B}}T\approx 1+0.2a\rho/kT$$

$$\kappa_{\mathrm{water}}^{-1}\approx 16$$

$$a\rho/k_{\mathrm{B}}T\approx 75 \qquad a=25k_{\mathrm{B}}T$$

Groot and Warren, *J. Chem. Phys.*, 1997.

A linear relationship between $a$'s and $\chi$-parameter is identified

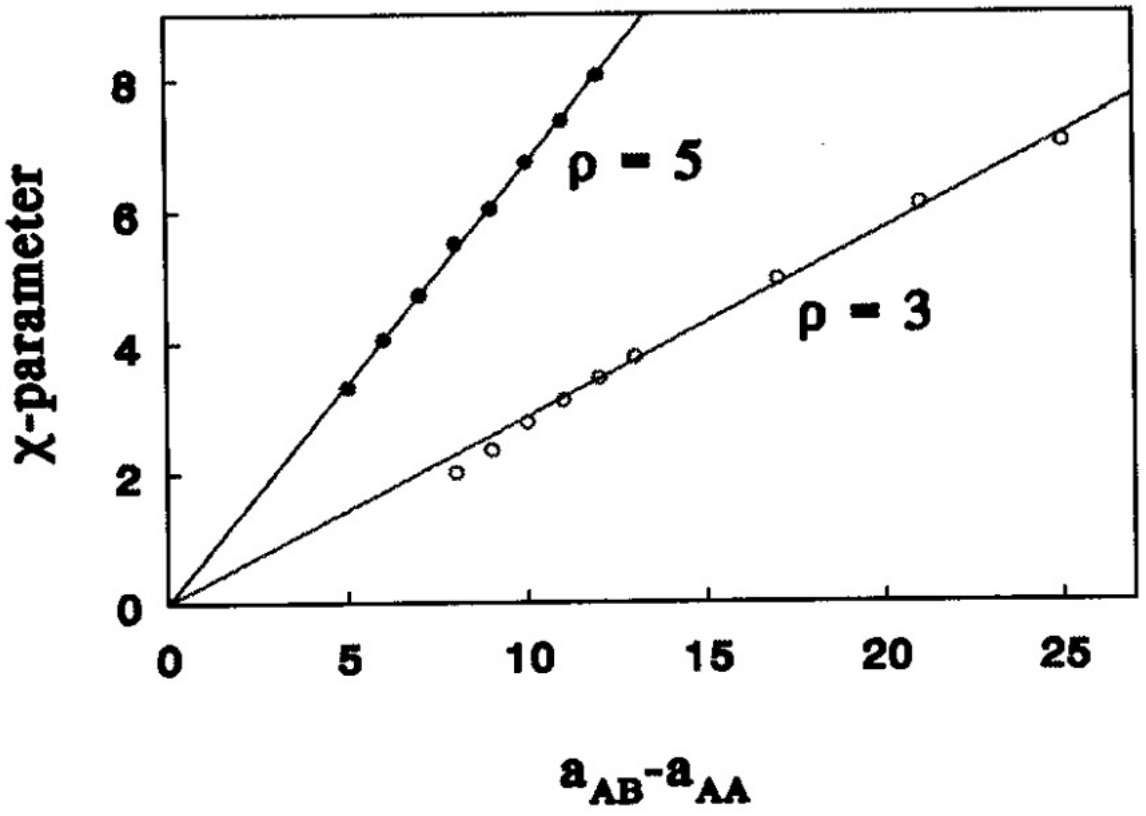


Groot and Warren, *J. Chem. Phys.*, 1997.

# DPD (Dissipative Particle Dynamics)

Non-bonded **soft** & **purely repulsive** pair-potential

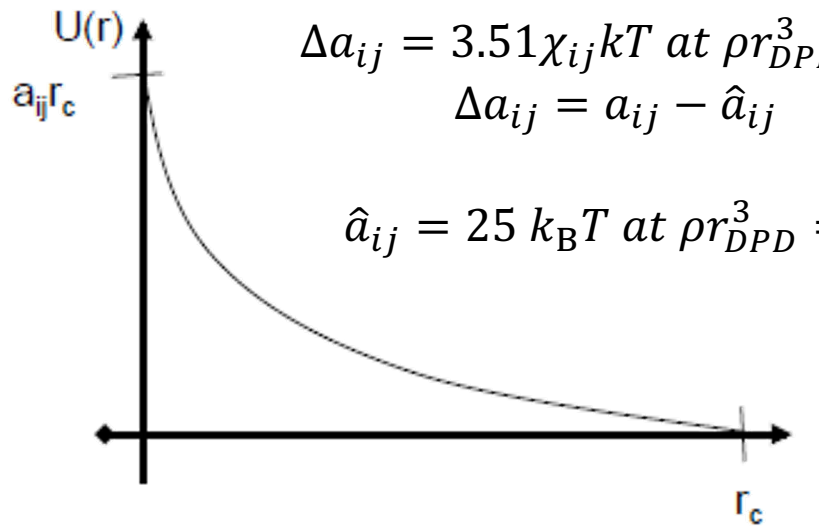


$$\Delta a_{ij} = 3.51\chi_{ij}kT \; at \; \rho r_{DPD}^3 = 3$$
$$\Delta a_{ij} = a_{ij} - \hat{a}_{ij}$$

$$\hat{a}_{ij} = 25\ k_B T \; at \; \rho r_{DPD}^3 = 3$$

$$a_{ij}(T) = \begin{cases} a_{ii} + 3.497 k_B T \chi_{ij}(T) (\rho = 3) \\ a_{ii} + 1.451 k_B T \chi_{ij}(T) (\rho = 5) \end{cases}$$

$$\chi = \frac{V_m}{RT}\left[(\delta_1 - \delta_2)^2\right]$$

*Relative attraction of beads based on preferential repulsions*

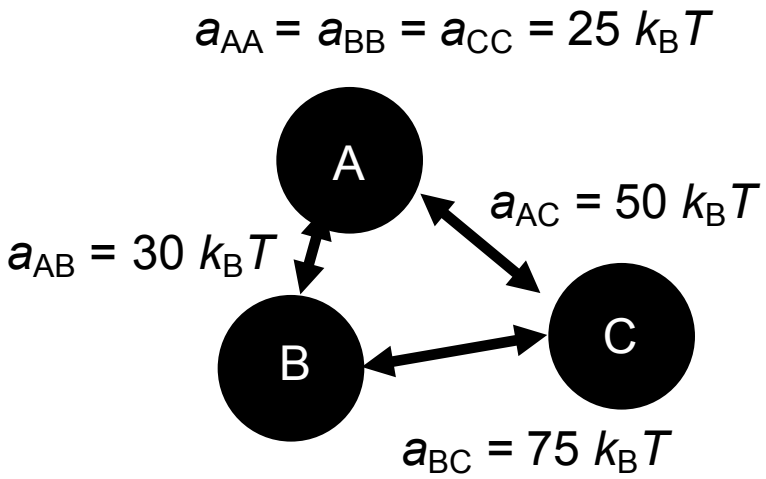


Groot and Warren, *J. Chem. Phys.*, 1997.

# DPD – Equal bead sizes

Assumption: Equal-size beads

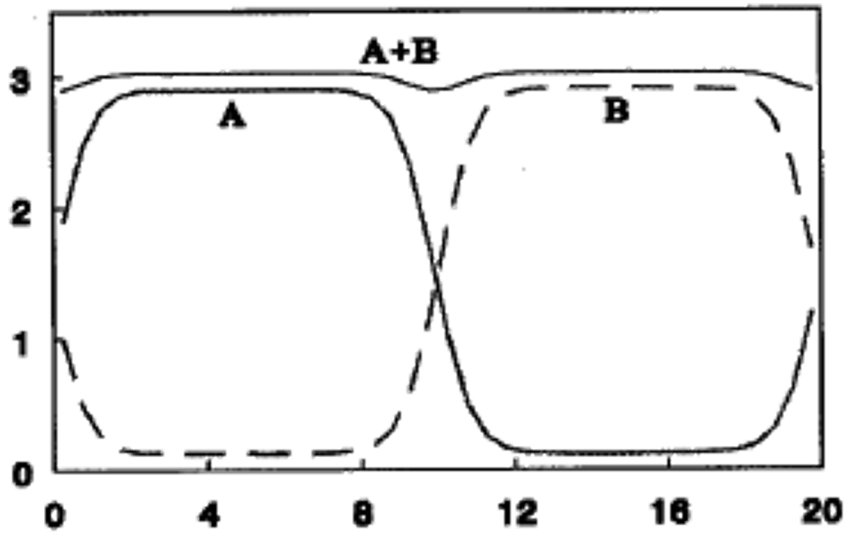


$$p_i = p_j$$

$$\rho_{i,\,\text{pure}} = \rho_{j,\,\text{pure}}$$

$$a_{ii} = a_{jj}$$

# DPD – Equal bead sizes

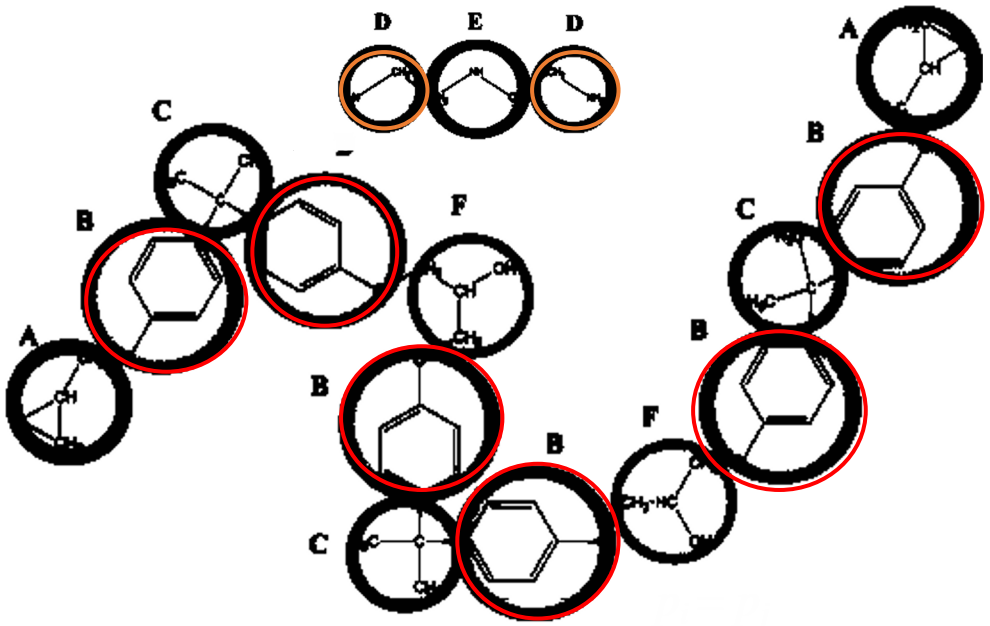


| $V_{bead,B}$ (Å$^3$) | $V_{bead,D}$ (Å$^3$) |
|---|---|
| 151 | 50 |

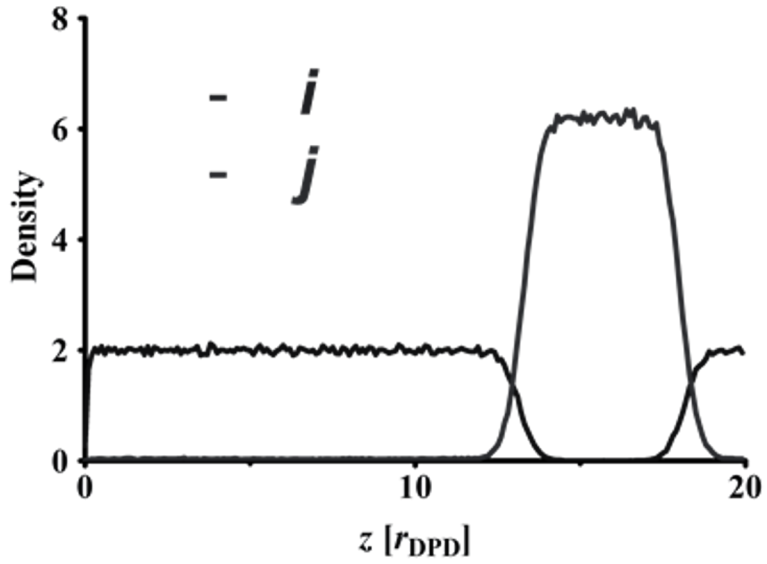


$$p_i = p_j$$

$$\rho_{i,\,\mathrm{pure}} \neq \rho_{j,\,\mathrm{pure}}$$

$$a_{ii} \neq a_{jj}$$

# DPD – Different bead sizes

DPD EoS

$$p = \rho kT + \alpha a \rho^2 r_{DPD}^3, \alpha = 0.101 \qquad \boxed{a_{ii} = \frac{p - \rho_{i,pure} kT}{\alpha \rho_{i,pure}^2 r_{DPD}^3}}$$

$$\rho_{i,pure}^2 a_{ii} \approx \rho_{j,pure}^2 a_{jj} \propto p \qquad \rho^{-1} = \bar{V} = \sum x_i \, \rho_{i,pure}^{-1} \approx \sqrt{\frac{\alpha r_{DPD}^3}{p}} \sum x_i \sqrt{a_{ii}}$$

$$p = \rho kT + \alpha \rho^2 r_{DPD}^3 A(x) \qquad A(x) = \sum x_i x_j \hat{a}_{ij}$$

$$A(x) = \sum x_i x_j \hat{a}_{ij} = \left( \sum x_i \sqrt{a_{ii}} \right)^2 + \sum x_i x_j \left( \hat{a}_{ij} - \sqrt{a_{ii} a_{jj}} \right)$$

$$= \frac{p}{\alpha r_{DPD}^3 \rho^2} + \sum x_i x_j \left( \hat{a}_{ij} - \sqrt{a_{ii} a_{jj}} \right)$$

$$\boxed{\hat{a}_{ij} = \sqrt{a_{ii} a_{jj}}}$$

Kacar, G. *et* al., *EPL*, 2013.

# Mapping on Flory Huggins parameter

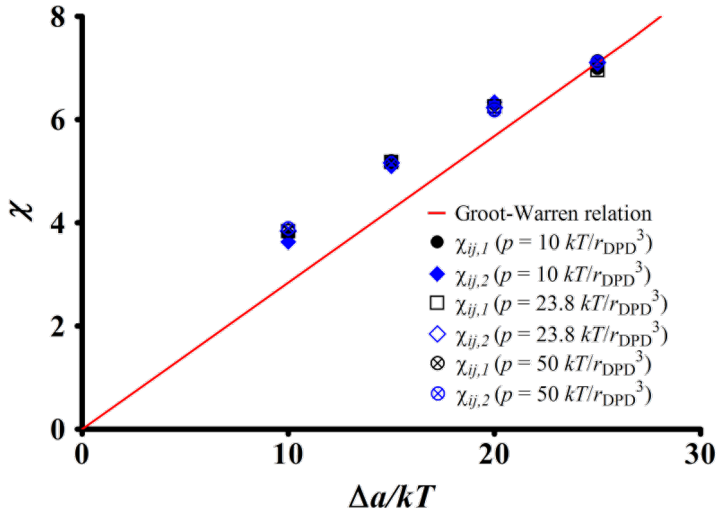


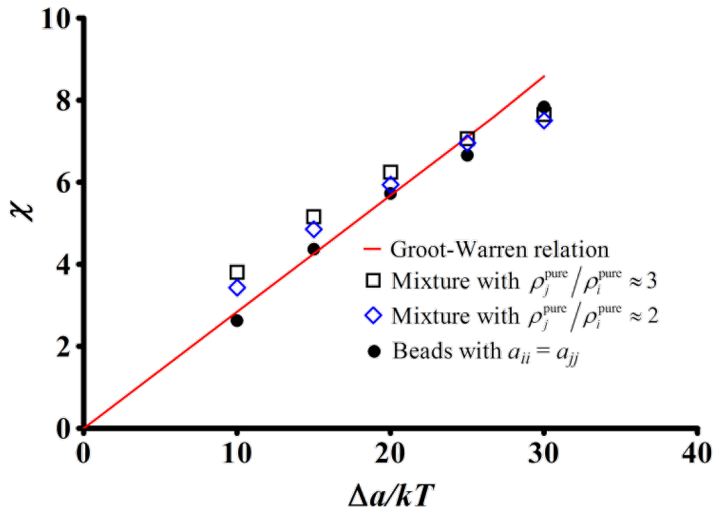


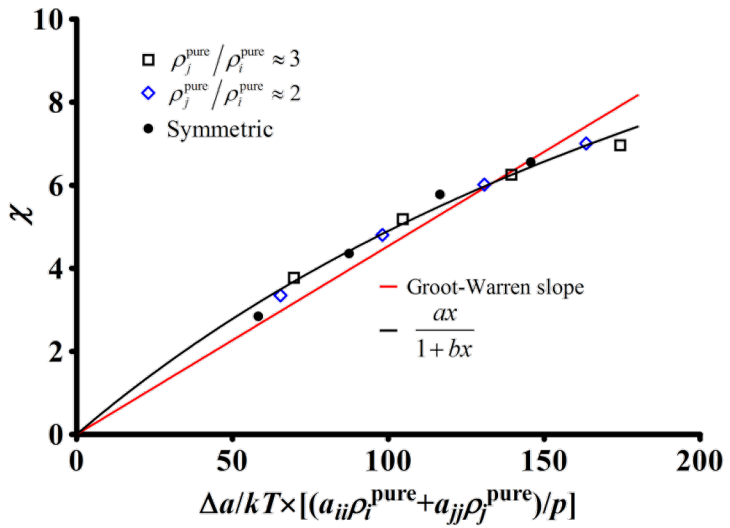


$$\phi_i = \frac{x_i\,\rho_{i,\text{pure}}^{-1}}{\sum_j x_j\,\rho_{j,\text{pure}}^{-1}}$$

$$\Delta G_{\text{mix}}/kT = \sum_i \phi_i \ln \phi_i + \sum_i \sum_{j>i} \chi_{ij}\phi_i\phi_j$$

$$\chi_{ij,1} = \frac{\ln\left[\phi_{j1}/\phi_{i1}\right]}{1-2\phi_{i1}}, \quad \chi_{ij,2} = \frac{\ln\left[\phi_{j2}/\phi_{i2}\right]}{1-2\phi_{i2}}$$

$$a_{ij} = \hat{a}_{ij} + \frac{p}{0.0454\left(a_{ii}\rho_i^{\text{pure}} + a_{jj}\rho_j^{\text{pure}}\right)}\chi_{ij}kT$$

Kacar, G. *et* al., *EPL*, 2013.

# Validation

Interface width ~ $\chi$-parameter

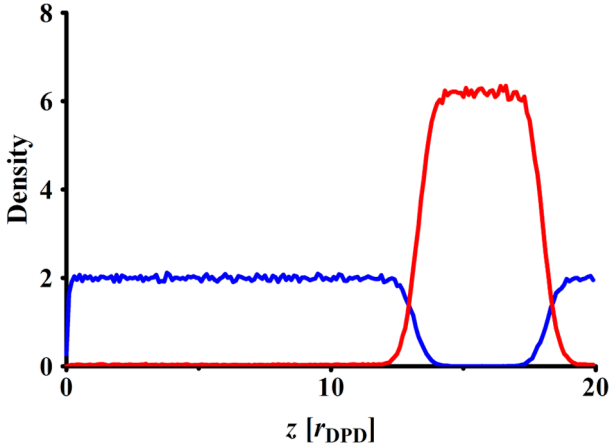


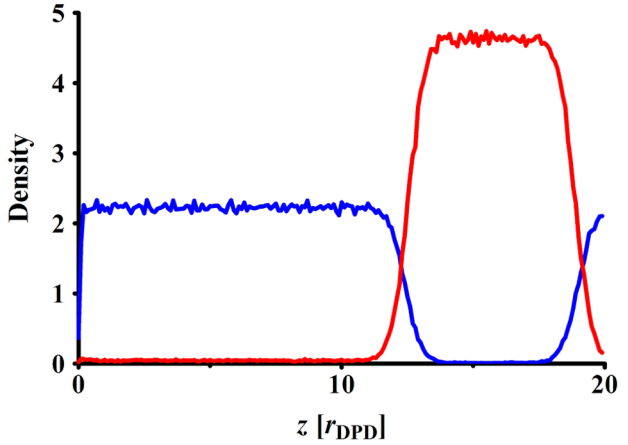


$$0.5\times\left[(a-b)+(b-a)\tanh\left((z-z_0)/w\right)\right]$$

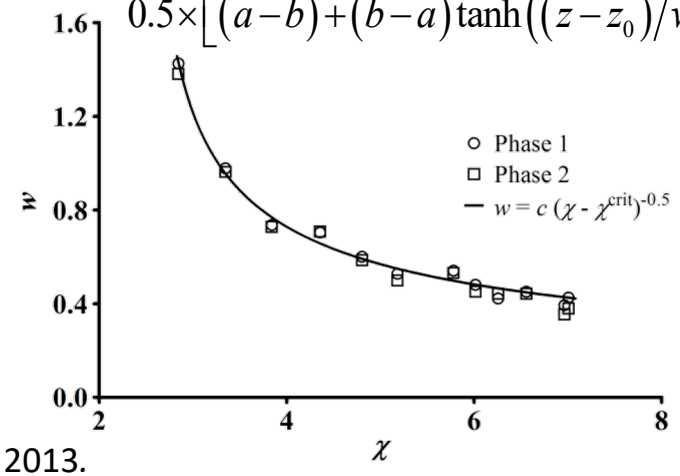


$\chi^{crit} = 2.44$ ($2.10 \pm 0.04$ in Groot-Warren)

Kacar, G. *et* al., *EPL*, 2013.

# DPD – Different bead sizes

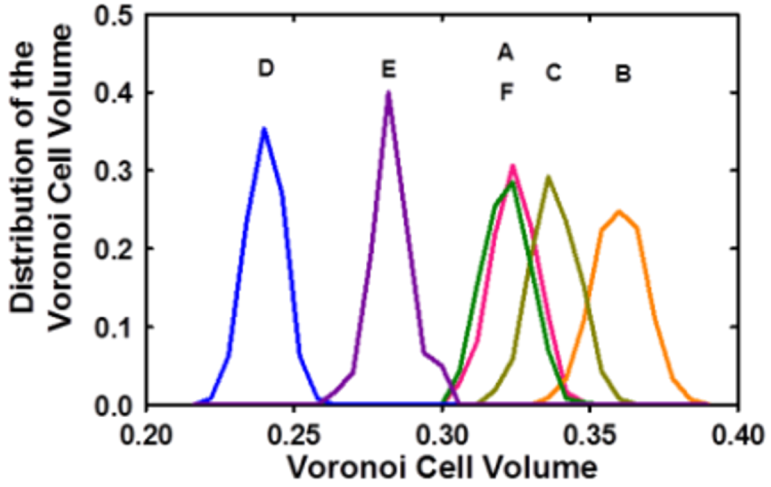


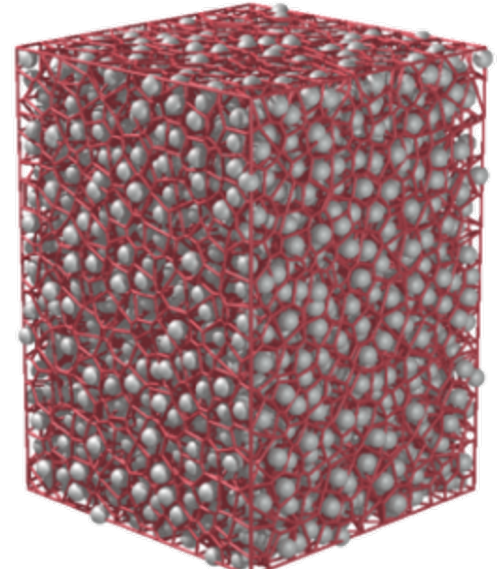

| Bead type | A | B | C | F | D | E |
|---|---|---|---|---|---|---|
| Pure liquid bead volume ($r_{DPD}^3$) | 0.281 | 0.413 | 0.316 | 0.276 | 0.136 | 0.205 |
| Volume of free beads ($r_{DPD}^3$) | 0.313 (0.007) | 0.364 (0.007) | 0.327 (0.007) | 0.311 (0.007) | 0.257 (0.006) | 0.282 (0.006) |

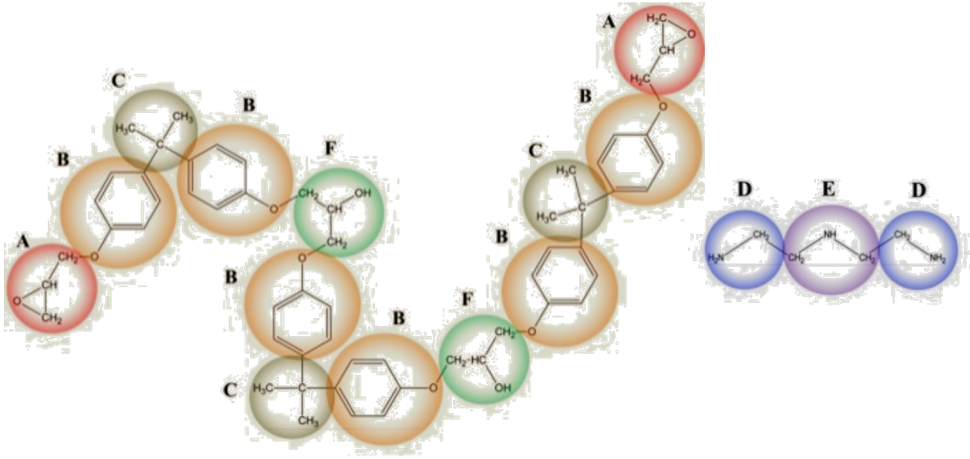



Kacar, G. *et* al., *EPL*, 2013.

Kacar, G. *et* al., *Soft Matter* 2013.

# Mesoscopic *interface* structure from DPD

Modeling polymer-surface interactions with DPD

- Coupling of atomistic and DPD scales
- Quantify amount of beads adsorbed with surface excess $\Gamma$

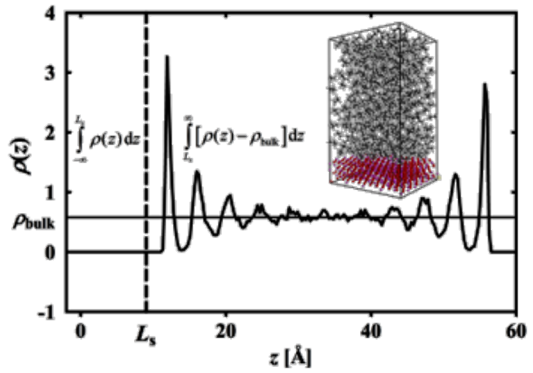


$$\Gamma(\mathrm{MD}) = \Gamma(\mathrm{DPD})$$

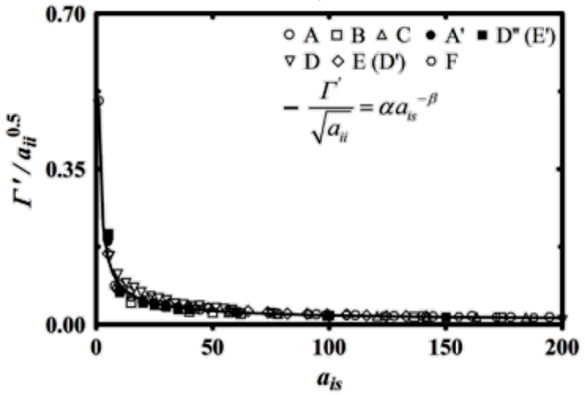


Different bead sizes are important to map MD to DPD

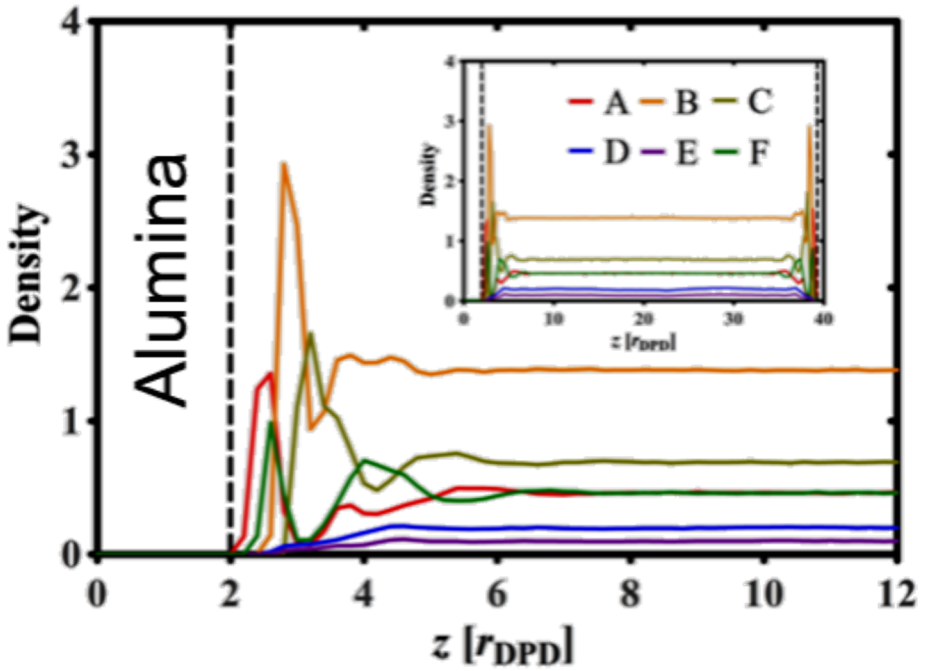


Kacar, G. *et* al., *J. Phys. Chem C*, 2013.

# Hydrogen bond interactions in DPD

Some low $M_W$ alcohol-water mixtures
Negative excess volume

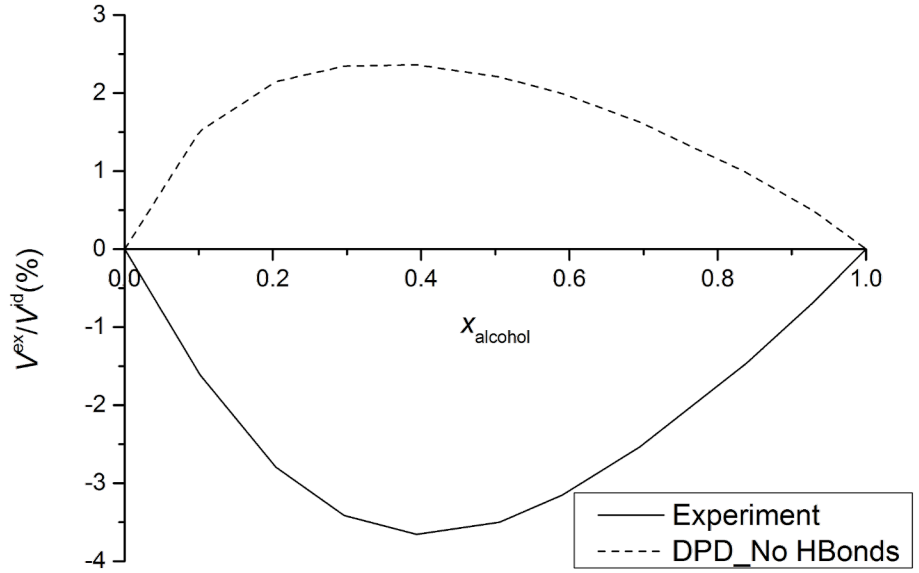


$$V^E = \frac{x_A M_A + x_B M_B}{\rho_L} - \underbrace{x_A V_{m,A} - x_B V_{m,B}}_{\text{Ideal contribution}}$$

# Modeling hydrophilic polymers with DPD

Self-replenishing hydrophilic surfaces

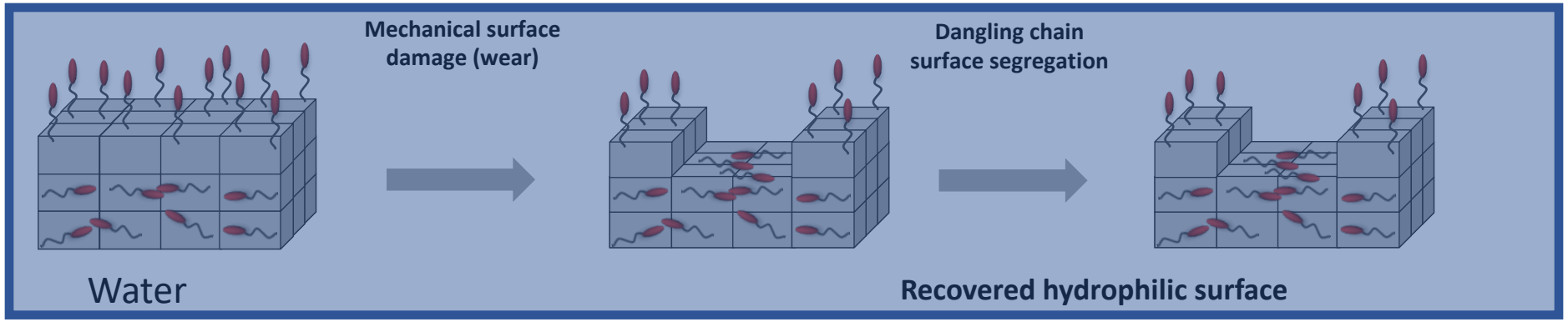


Dikić *et al. Adv. Mater.,* 2012.

Functional polymeric surfaces

Water mimics physiological conditions

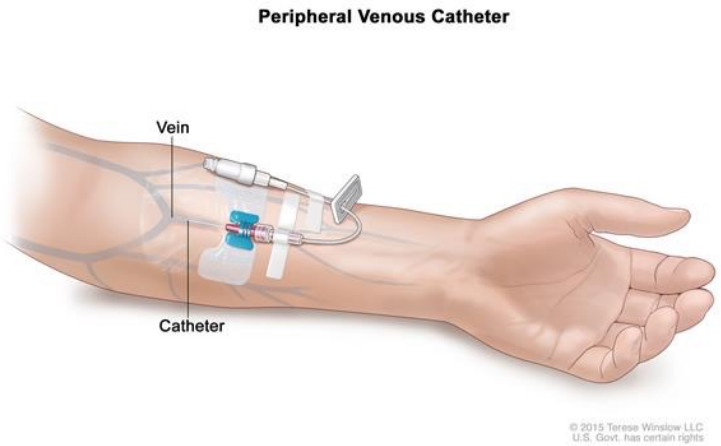

# Hydrogen bonding in DPD

Hydrogen bond interactions with Morse Potential

$$\vec{f}^{T} = \vec{f}^{C} + \vec{f}^{R} + \vec{f}^{D} + \vec{f}^{\text{Morse}}$$

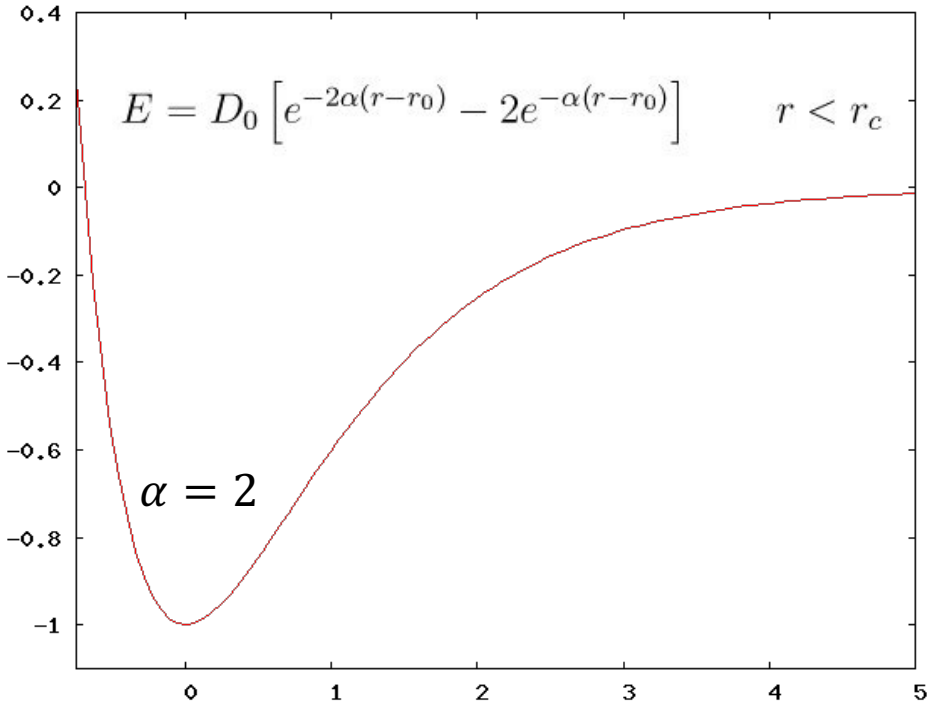


Two parameters required

- H-bond distance $r_0$
- Depth of the energy well $D_0$

To test

- Methanol– Water
- Ethanol – Water
- 1-Propanol – Water

Neimark *et* al. J. Phys. Chem. Lett. 3, 21, 3081-3087, 2012.

# Hydrogen bonding in DPD

Parameters of the Morse Potential from MD simulations

$r_0$: Mapping of the Radial Distribution Functions (RDF's)

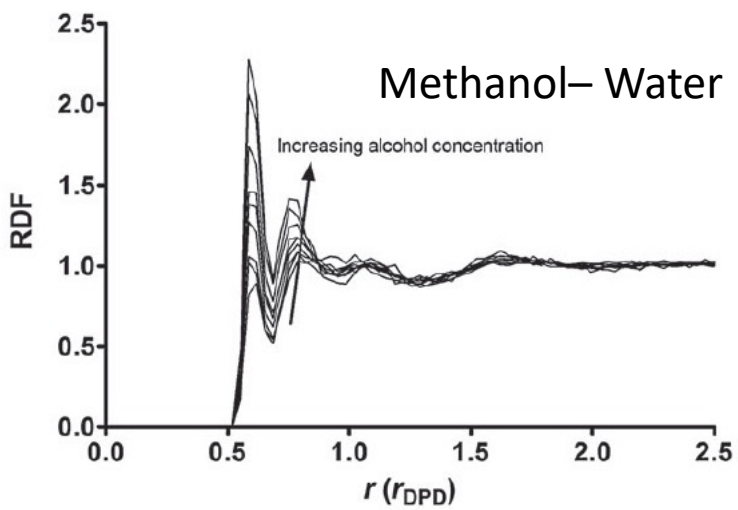


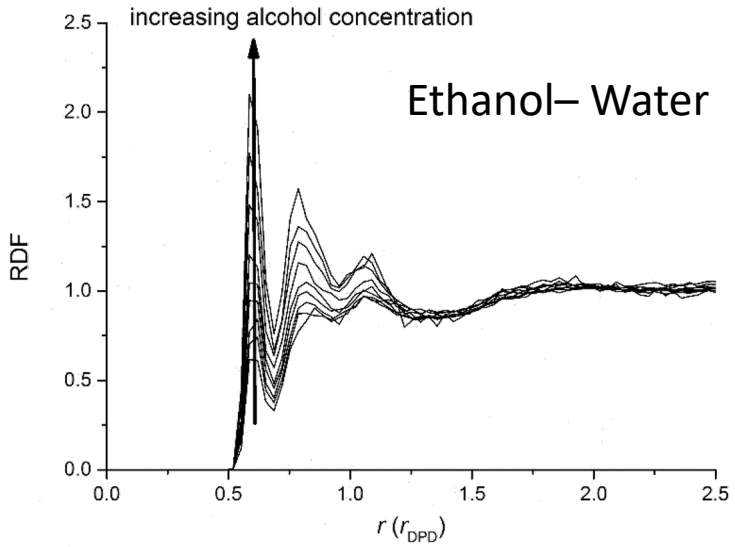


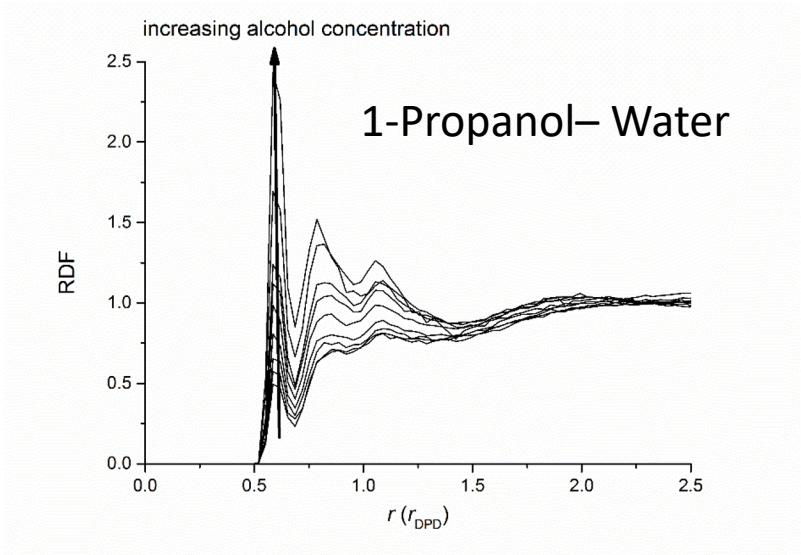

# Hydrogen bonding in DPD

$D_0$: Mapping of the mixing energies* $D_0(x) \equiv E_{\mathrm{H-bond}}(x) = E_{\mathrm{Pot,Mix}}(x) - E_{\mathrm{Pot,A}} - E_{\mathrm{Pot,W}}$

| | Methanol-Water | | Ethanol-Water | | 1-Propanol-Water | |
|---|---|---|---|---|---|---|
| $x_{\mathrm{alcohol}}$ | $D_0$ $[k_BT]$ | $r_0$ $[r_{\mathrm{DPD}}]$ | $D_0$ $[k_BT]$ | $r_0$ $[r_{\mathrm{DPD}}]$ | $D_0$ $[k_BT]$ | $r_0$ $[r_{\mathrm{DPD}}]$ |
| 0.10 | 5.06 | 0.78 | 8.22 | 0.78 | 7.21 | 0.60 |
| 0.20 | 6.33 | 0.78 | 9.14 | 0.78 | 8.28 | 0.69 |
| 0.30 | 7.46 | 0.78 | 9.97 | 0.78 | 9.23 | 0.73 |
| 0.39 | 8.68 | 0.78 | 10.85 | 0.78 | 10.25 | 0.75 |
| 0.51 | 10.07 | 0.78 | 11.86 | 0.78 | 11.42 | 0.77 |
| 0.59 | 11.12 | 0.78 | 12.62 | 0.78 | 12.3 | 0.77 |
| 0.69 | 12.41 | 0.78 | 13.56 | 0.78 | 13.38 | 0.78 |
| 0.84 | 14.20 | 0.78 | 14.86 | 0.78 | 14.88 | 0.78 |
| 0.93 | 15.31 | 0.78 | 15.66 | 0.78 | 15.82 | 0.78 |

*van der Spoel, et. al *J. Chem. Phys.* **2003**.

Conservative DPD interactions

| Type of Bead | $\rho_{m,i}$ [g/cm$^3$] | $M_W$ [g/mol] | $\rho_{i,\mathrm{pure}} = \rho_{m,i}/M_W$ [Å$^{-3}$] | $\delta$ [(J/cm$^3$)$^{0.5}$] | $a_{ii}$ $[k_BT]$ | $a_{i\text{-water}}$ $[k_BT]$ |
|---|---|---|---|---|---|---|
| Methanol (M) | 0.787 | 32.04 | 0.0148 | 29.61 | 177.44 | 73.27 |
| Ethanol (E) | 0.784 | 46.07 | 0.0103 | 26.49 | 409.71 | 107.58 |
| 1-Propanol (P) | 0.799 | 60.09 | 0.0080 | 24.53 | 729.59 | 143.03 |
| Water (W) | 1.000 | 18.02 | 0.0334 | 47.00 | 25.00 | 25.00 |

# Hydrogen bonding in DPD

Experimental comparison of simulation results

Negative volume excess low $M_W$ alcohol-water mixtures

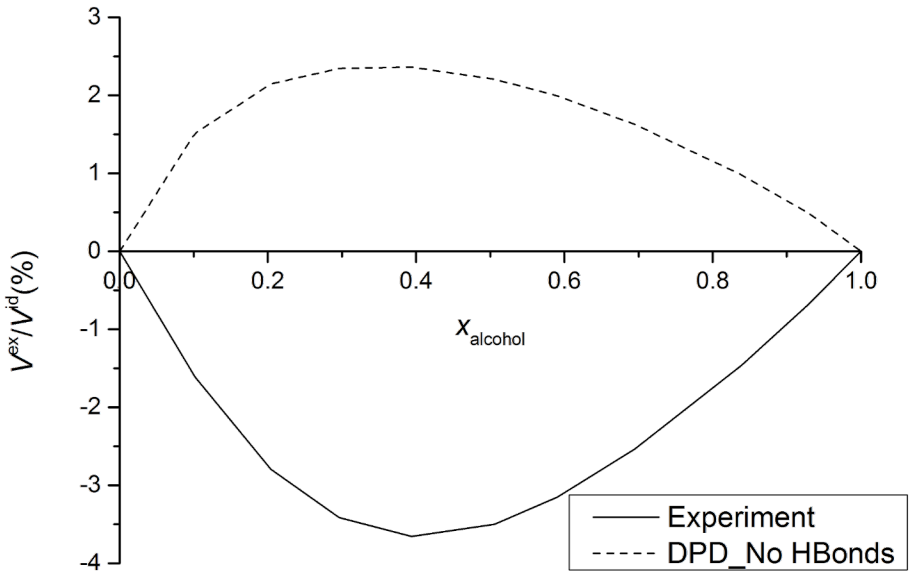


$$V^E = \frac{x_A M_A + x_B M_B}{\rho_L} - \underbrace{x_A V_{m,A} - x_B V_{m,B}}_{\text{Ideal contribution}}$$

# Hydrogen bonding in DPD

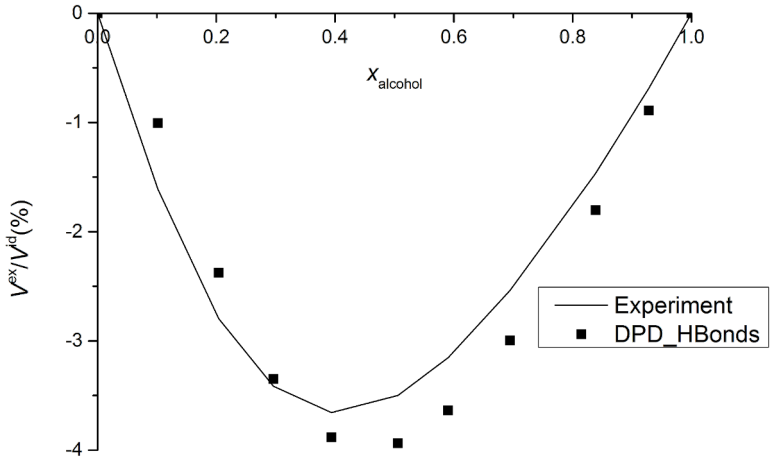


Methanol-Water

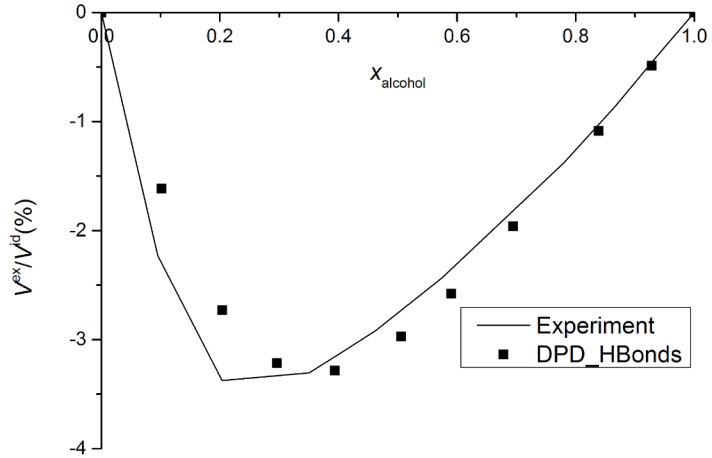


Ethanol-Water

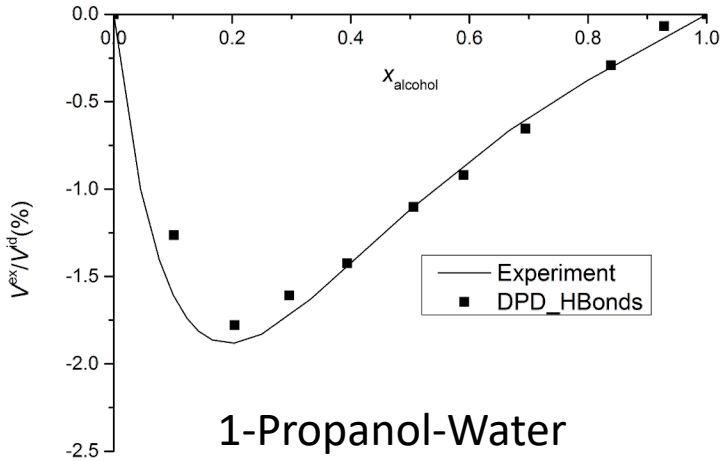


1-Propanol-Water

# Hydrogen bonding in DPD

Experimental evidence on surface enrichment of alcohols at air interface*

**Raina et al., J. Phys. Chem. A 2001, 105, 10204-10207.*

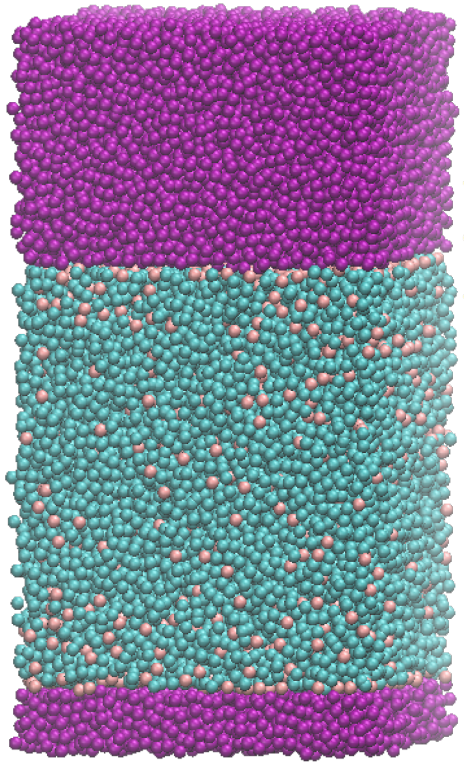

**Methanol-Water**

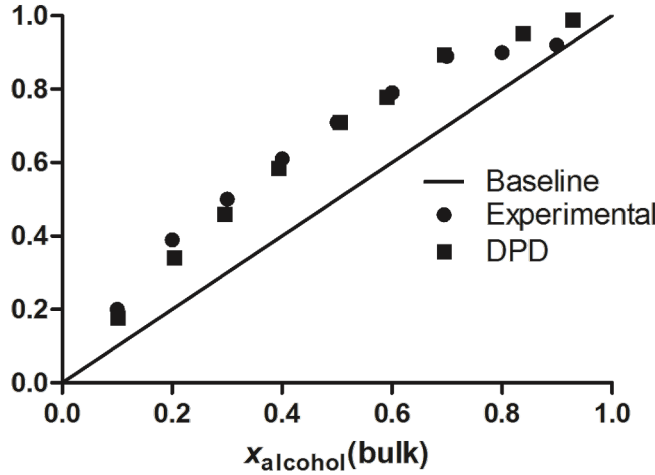


**Ethanol-Water**

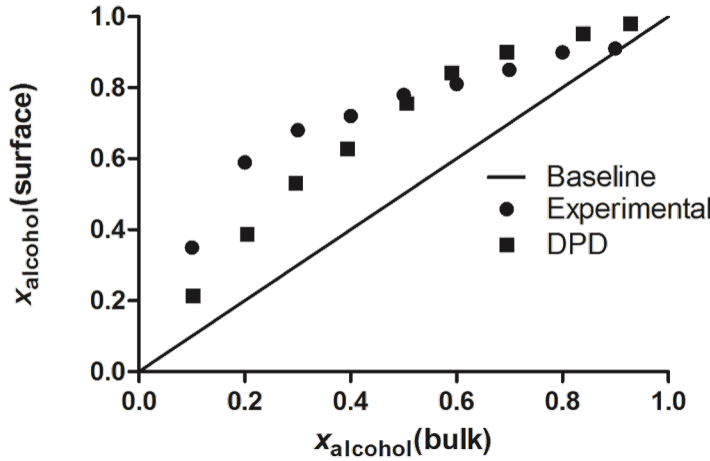


**1-Propanol-Water**

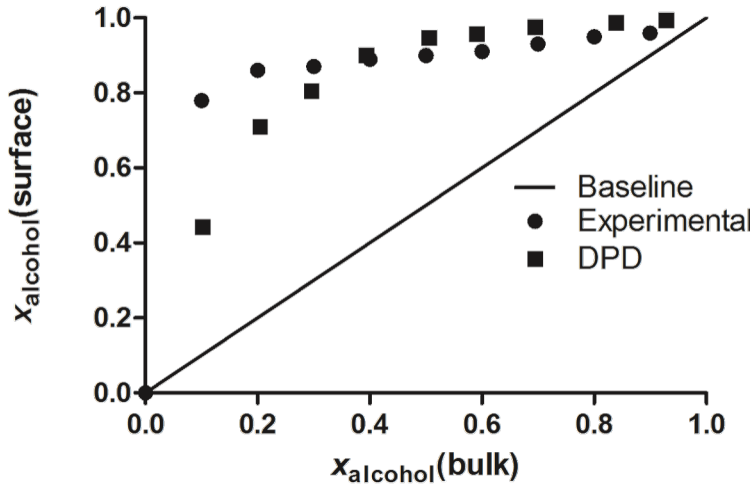


Kacar, G. *et* al., *PCCP*, 2016.

# Hydrogen bonding in DPD

PEG 400 + Water interactions

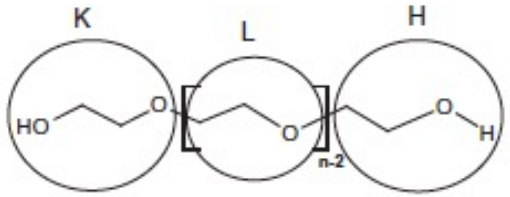


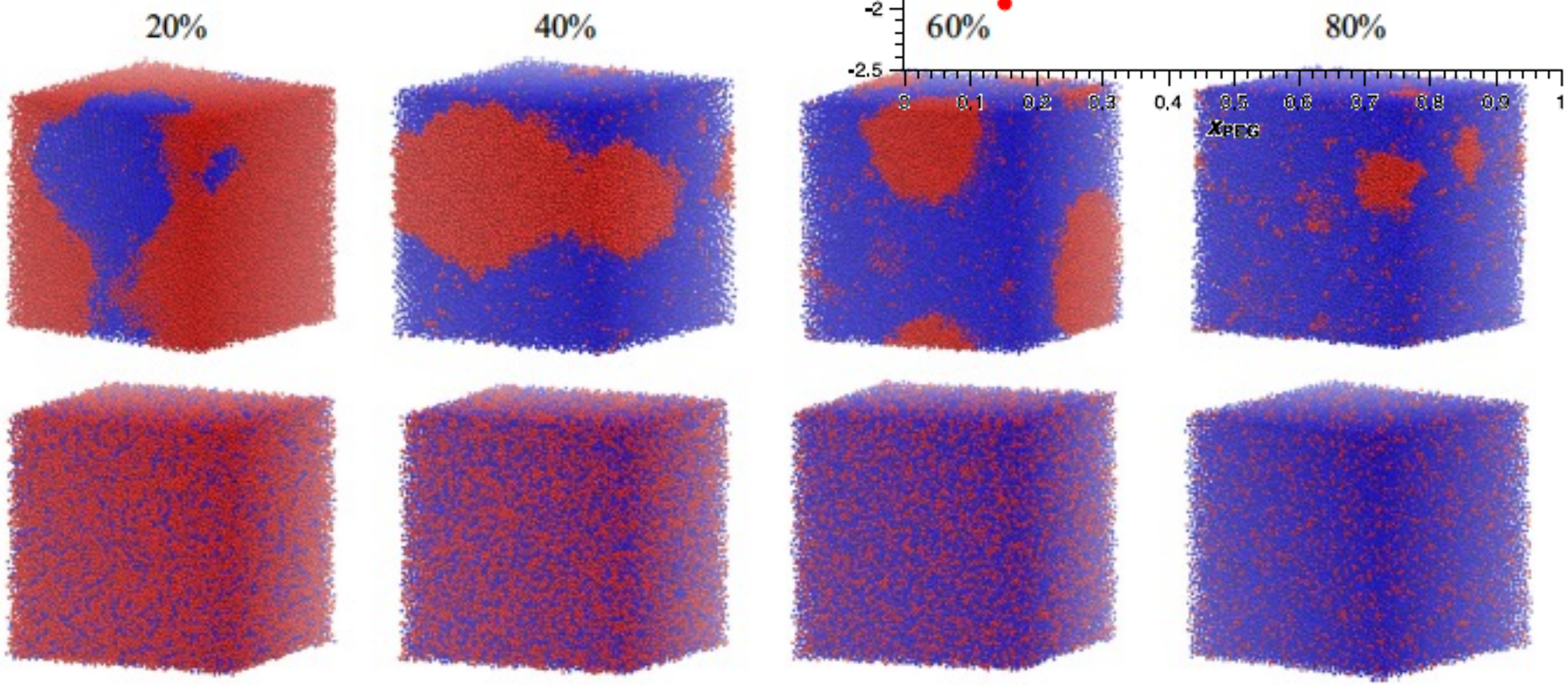


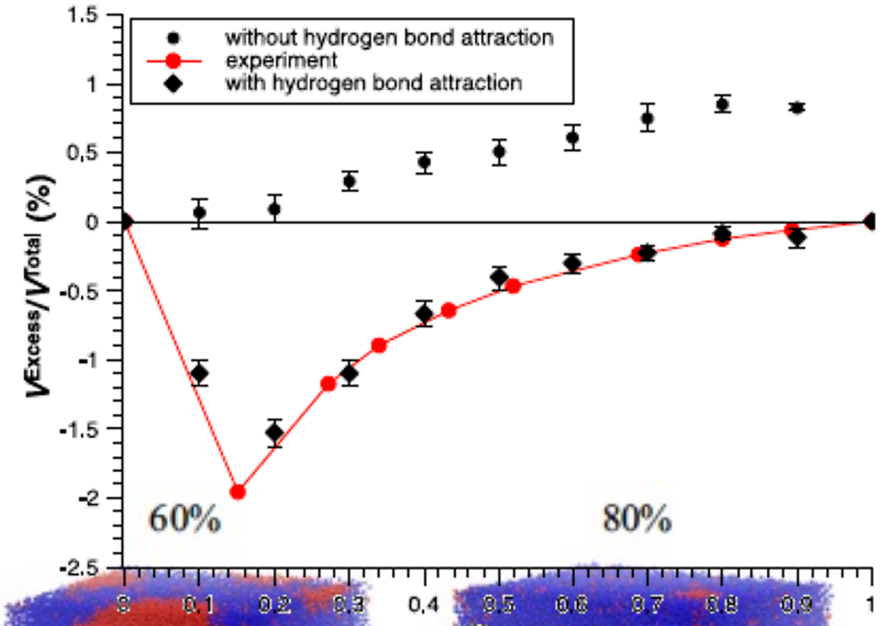


Kacar, G. Chem. Phys. Lett., 2017.

# Single PEG chain conformations

PEG chains are known to exhibit helical structures

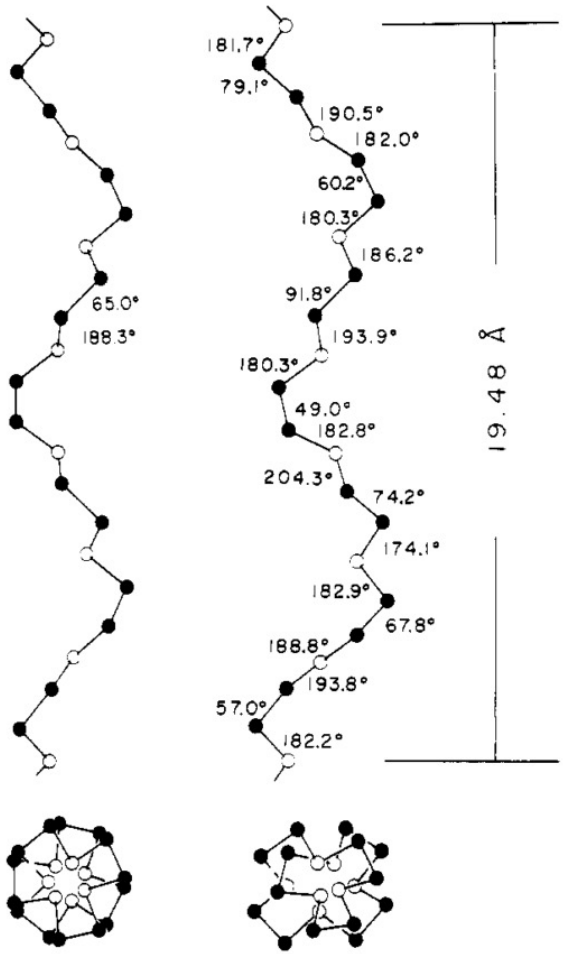


2 turns per 7 –($CH_2$–$CH_2$–O)– units

Number of helical chains quantified from DPD simulations

Distance between *i*-(*i*+3) and *i*-(*i*+6) contacts

Takahashi and Tadokoro, Macromolecules, 1973, 6, 672-675.

# Single PEG chain conformations

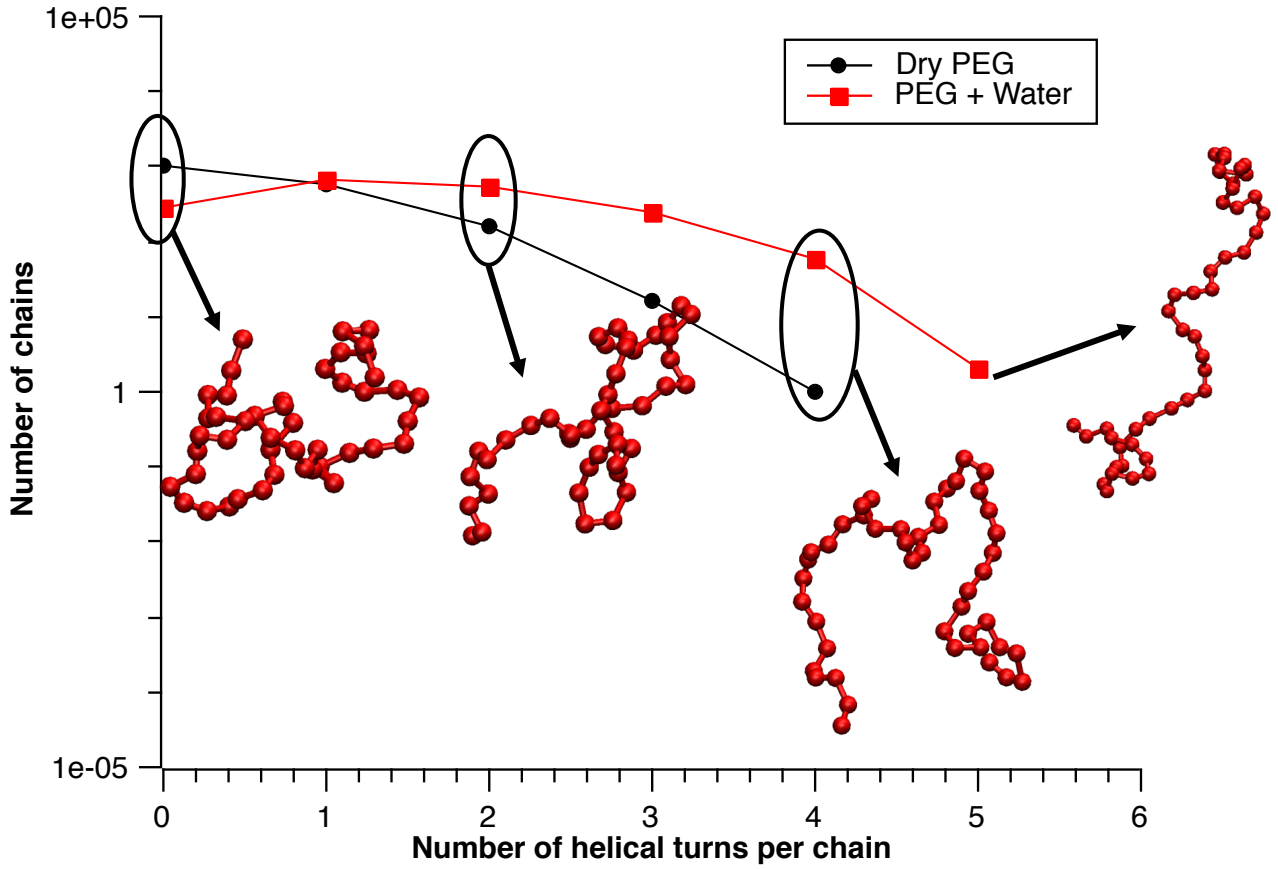


Water significantly increases PEG chain helicity

Kacar, G., PCCP, 2018.

# A more generic approach

## A statistical mechanics-based approach to parameterize ‘hydrogen bond strength’

PHYSICAL REVIEW E **85**, 061503 (2012)

**Analytical model for three-dimensional Mercedes-Benz water molecules**

T. Urbic

*Faculty of Chemistry and Chemical Technology, University of Ljubljana, Askerceva 5, 1000 Lubljana, Slovenia*

(Received 7 May 2012; revised manuscript received 13 June 2012; published 25 June 2012)

We developed a statistical model which describes the thermal and volumetric properties of water-like molecules. A molecule is presented as a three-dimensional sphere with four hydrogen-bonding arms. Each water molecule interacts with its neighboring waters through a van der Waals interaction and an orientation-dependent hydrogen-bonding interaction. This model, which is largely analytical, is a variant of a model developed before for a two-dimensional Mercedes-Benz model of water. We explored properties such as molar volume, density, heat capacity, thermal expansion coefficient, and isothermal compressibility as a function of temperature and pressure. We found that the volumetric and thermal properties follow the same trends with temperature as in real water and are in good general agreement with Monte Carlo simulations, including the density anomaly, the minimum in the isothermal compressibility, and the decreased number of hydrogen bonds upon increasing the temperature.

DOI: 10.1103/PhysRevE.85.061503 PACS number(s): 61.20.Gy

# Computing $\epsilon_{HB}$

Chemical potential $\mu = -\frac{k_B T}{N} \ln Q$

$$Q = Q_1^{N/3} \quad \text{where} \quad Q_1 = \left(\Delta_{HB} + \Delta_{LJ} + \Delta_o\right)^n$$

$$\Delta_{HB} = 4\pi^2 c(T) v_{ef}^{HB} \exp\left(\frac{\epsilon_{HB} + \epsilon_{LJ} - P\, v_{HB}/2}{k_B T}\right) \sqrt{\frac{4\pi k_B T}{k_s}}\, \mathrm{erf}\left(\sqrt{\frac{k_s}{4 k_B T}}\right)$$

$$\Delta_{LJ} = 2\pi^2 c(T) v_{ef}^{LJ} \exp\left(\frac{\epsilon_{LJ} - P\, v_{LJ}/2}{k_B T}\right)$$

$$\Delta_0 = 2\pi^2 c(T) \frac{k_B T}{p} \exp\left(\frac{-P v_o}{2 k_B T}\right)$$

$$\mu(\exp) = -237.14 \frac{kJ}{mol} \rightarrow \boldsymbol{\epsilon_{HB} = 14.6\, k_B T}$$

T. Urbic, Phys Rev E 85 (2012).

# DPD modeling of simple hydrogen bonding liquids

Water, ethanol, methanol, 1-propanol

Hydrophobic and hydrophilic parts form different CG beads

CG beads are connected *via* covalent bonds

Only h-bonds between hydrophilic beads are defined

Properties estimated

- RDFs
- 3-body angular distributions
- Transport properties
- Thermodynamic properties
- Temperature-dependent properties

# RDFs of pure liquids

RDFs of pure liquids $g_{ij}(r) = \frac{\langle \Delta N_{ij}(r \to r + \Delta r) \rangle V}{4\pi r^2 \Delta r N_i N_j}$

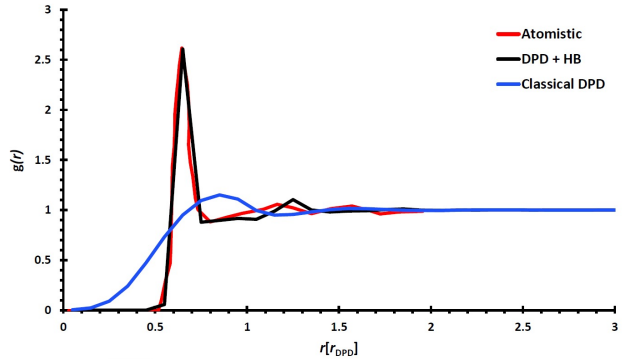


Water

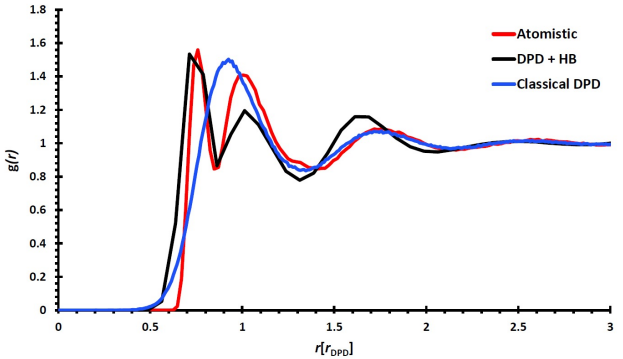


Methanol

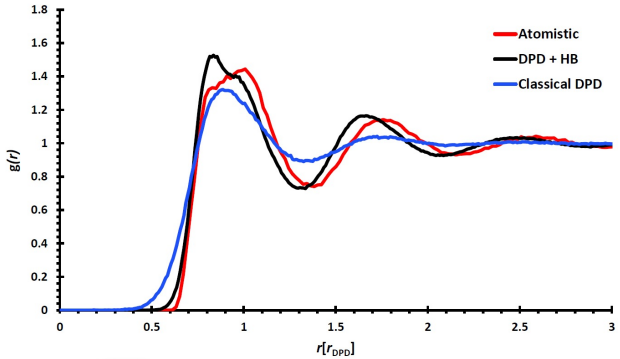


Ethanol

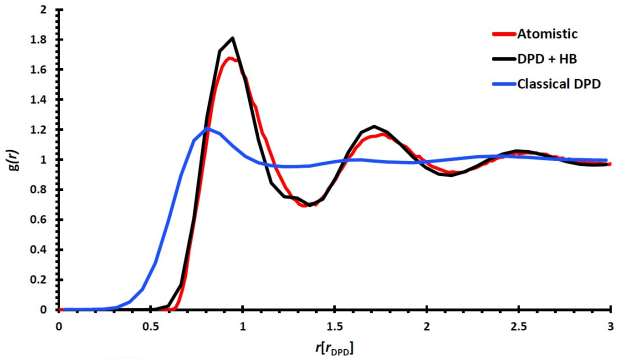


1-propanol

# 3-body angular distributions

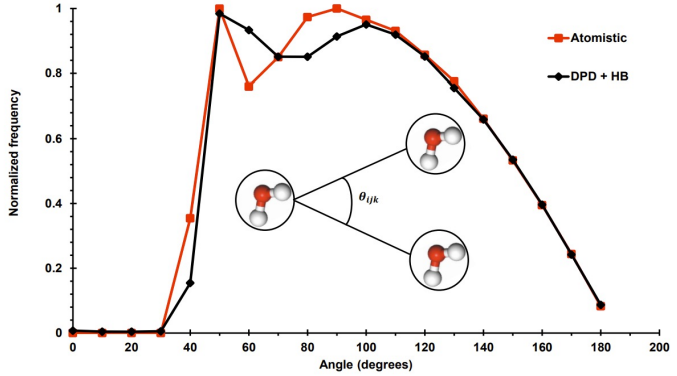


Water

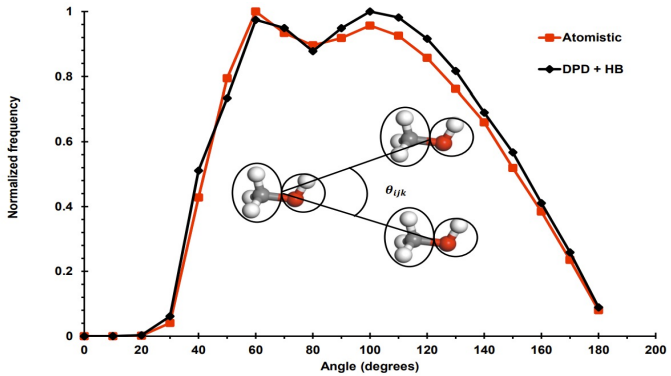


Methanol

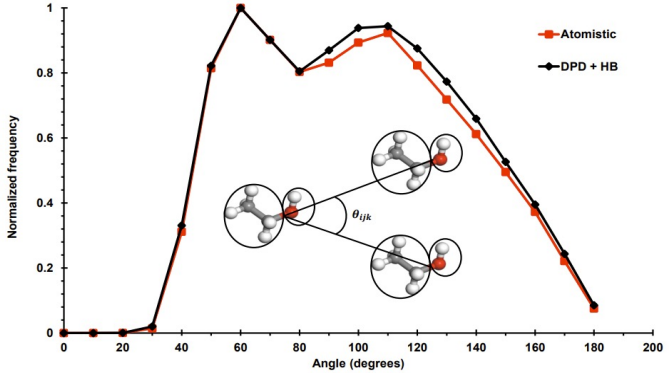


Ethanol

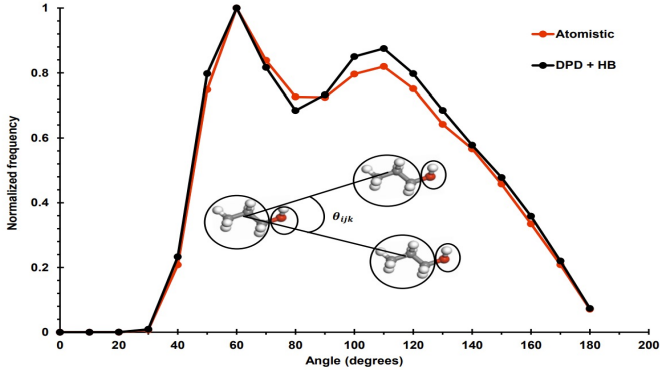


1-propanol

Hydrophilic-Hydropholic

Hydrophobic-Hydrophobic

Methanol

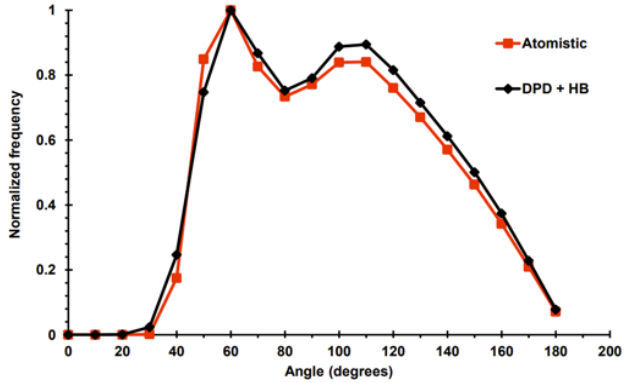


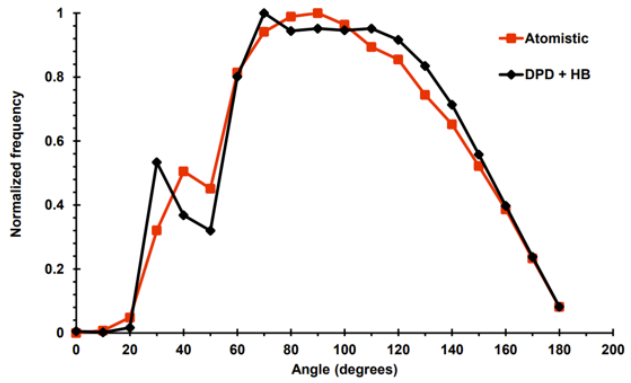


Ethanol

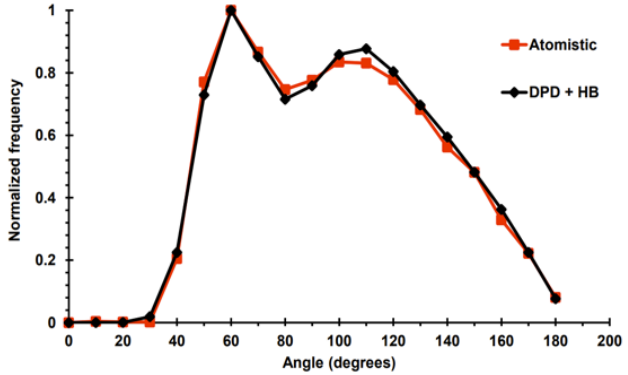


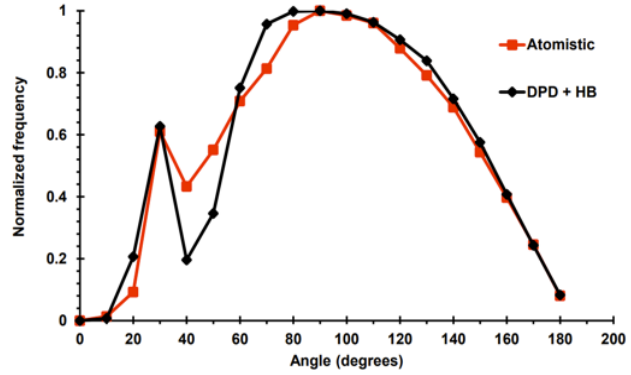


1-propanol

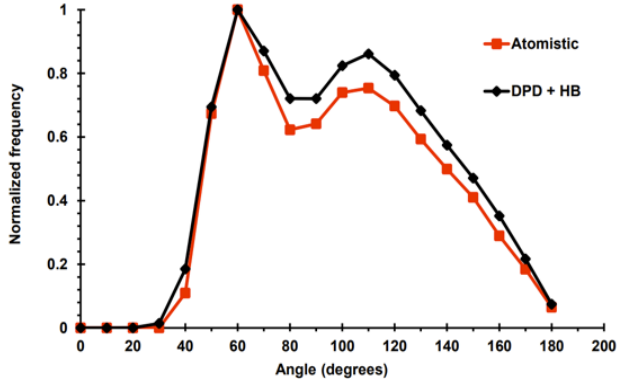


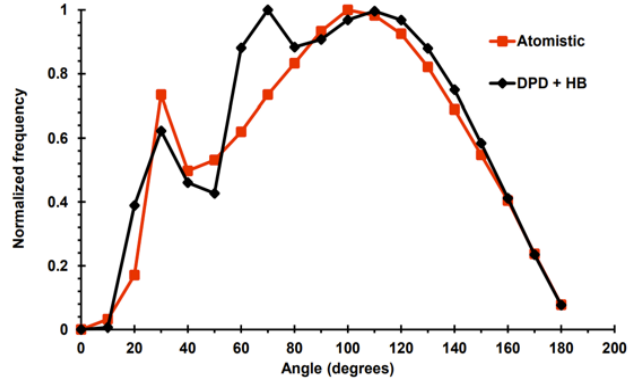

# Transport properties: Viscosity

## Green-Kubo formalism

## Shear viscosity

$$\eta = \frac{V}{k_B T}\int_0^\infty \mathrm{d}t\langle P_{\mathrm{cross}}(0)P_{\mathrm{cross}}(t)\rangle \text{ where } \quad P_{\mathrm{cross}} = (P_{xy} + P_{yz} + P_{xz})/3$$

Mapping diffusion equations from DPD to experimental values

$$\tau = \frac{N_m D_{DPD} r_{DPD}^2}{D_{exp}} \qquad \eta_{real} = \eta_{DPD}\tau k_B T / r_{DPD}^3$$

| | $D_{DPD}$ $[r_{DPD}^2/t_{DPD}]$ | $D_{exp}$ $\times 10^{-9}$ $[m^2/s]$ | $\tau$ [ps] | $\eta_{DPD}$ $[k_B T/r_{DPD}^3 \cdot s]$ | $\eta_{real}$ $\times 10^{-3}$ [Pa.s] | $\eta_{exp}$ $\times 10^{-3}$ [Pa.s] |
|---|---|---|---|---|---|---|
| **Water** | $7.27\times10^{-2}$ | 2.42 | 6.02 | 3.20 | 0.88 | 0.89 |
| **Methanol** | $2.32\times10^{-2}$ | 2.27 | 2.06 | 5.65 | 0.53 | 0.54 |
| **Ethanol** | $1.80\times10^{-2}$ | 1.01 | 4.61 | 6.68 | 0.97 | 1.00 |
| **1-propanol** | $6.17\times10^{-3}$ | 0.59 | 3.19 | 15.45 | 1.21 | 1.95 |

# Thermodynamic properties: Isothermal compressibility

$$\kappa_T = \frac{1}{k_B T} \frac{\langle V^2 \rangle - \langle V \rangle^2}{\langle V \rangle} \quad \text{and} \quad \kappa^{-1} = \frac{1}{\rho k_B T \kappa_T}$$

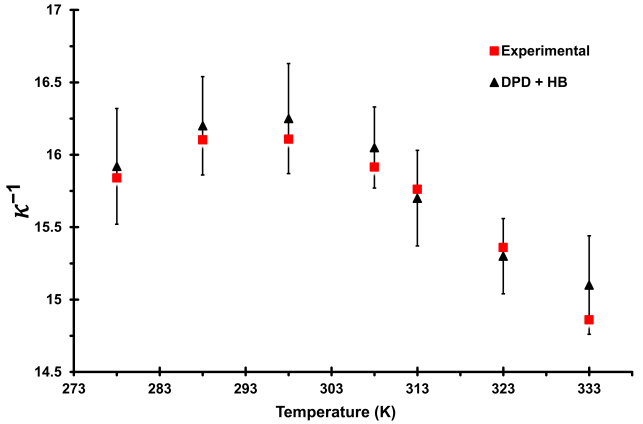


Water

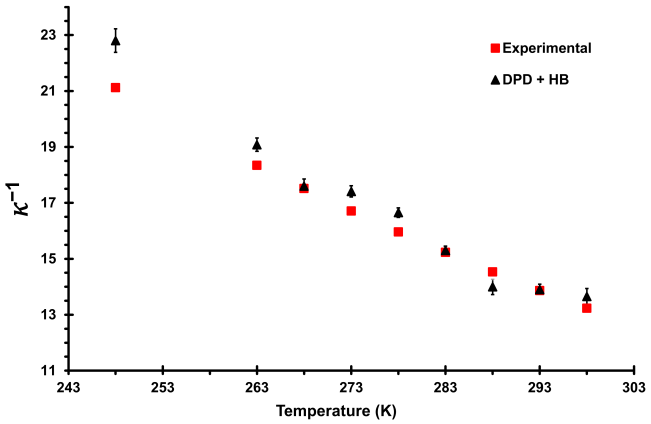


Methanol

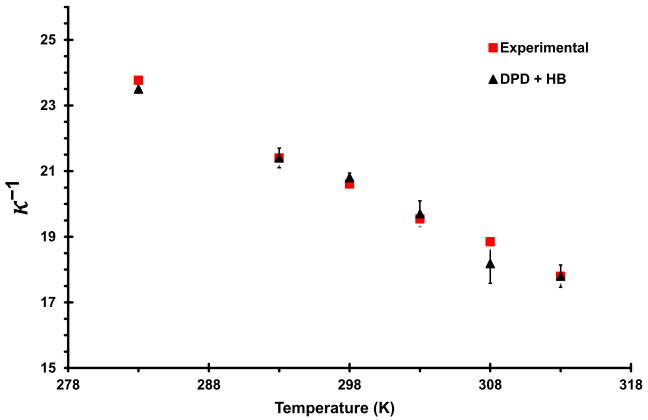


Ethanol

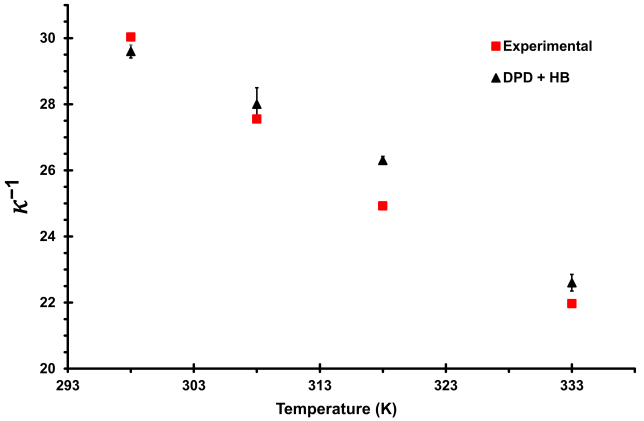


1-propanol



Camoglu, Urbic, de With, Kacar, J. Mol. Liq., 2022.

# Mixtures

## Mixtures of simple liquids: Case of Methanol

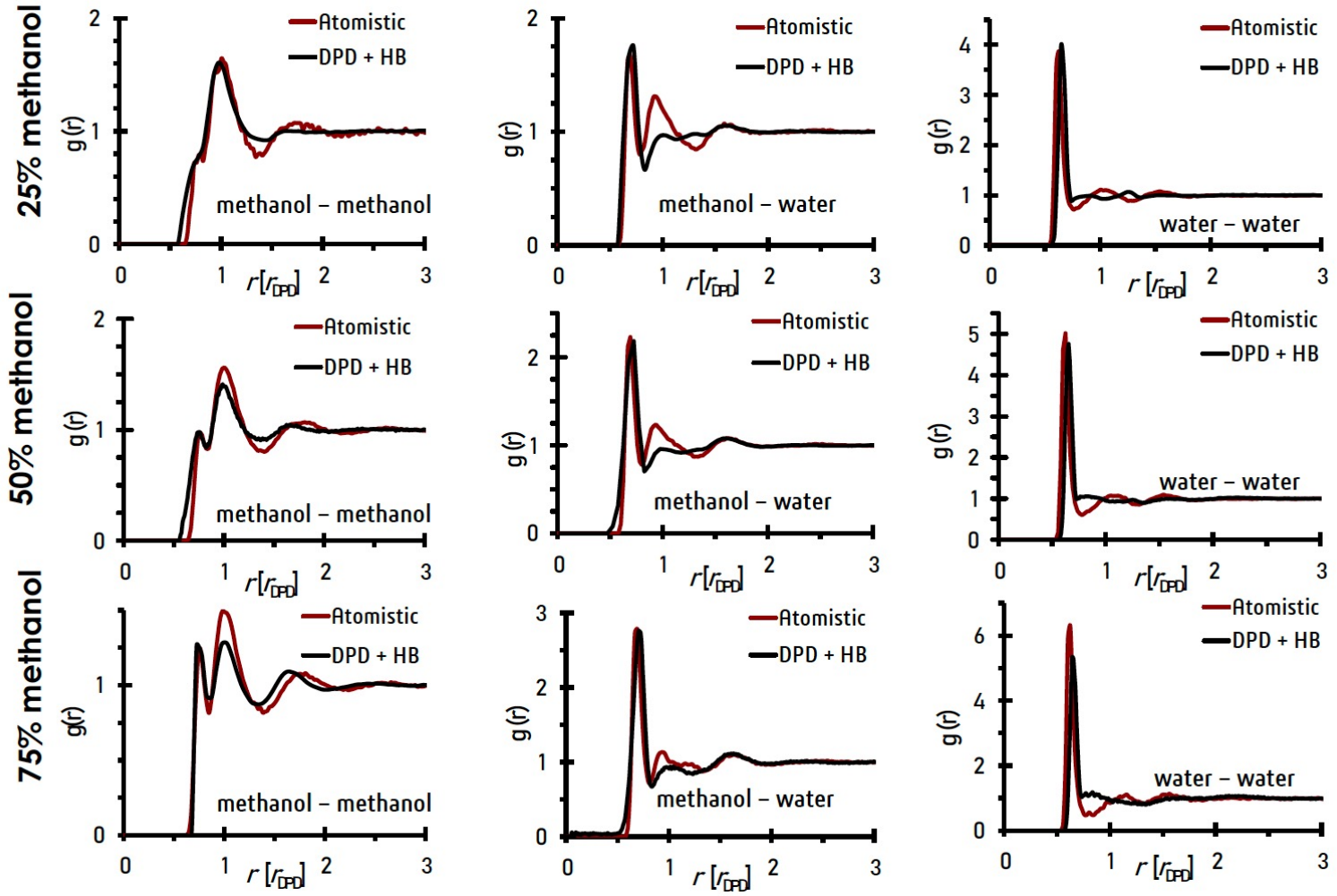

# Simulated soft matter by DPD

## Surface segregation of PU coatings

Adaptive surface behavior

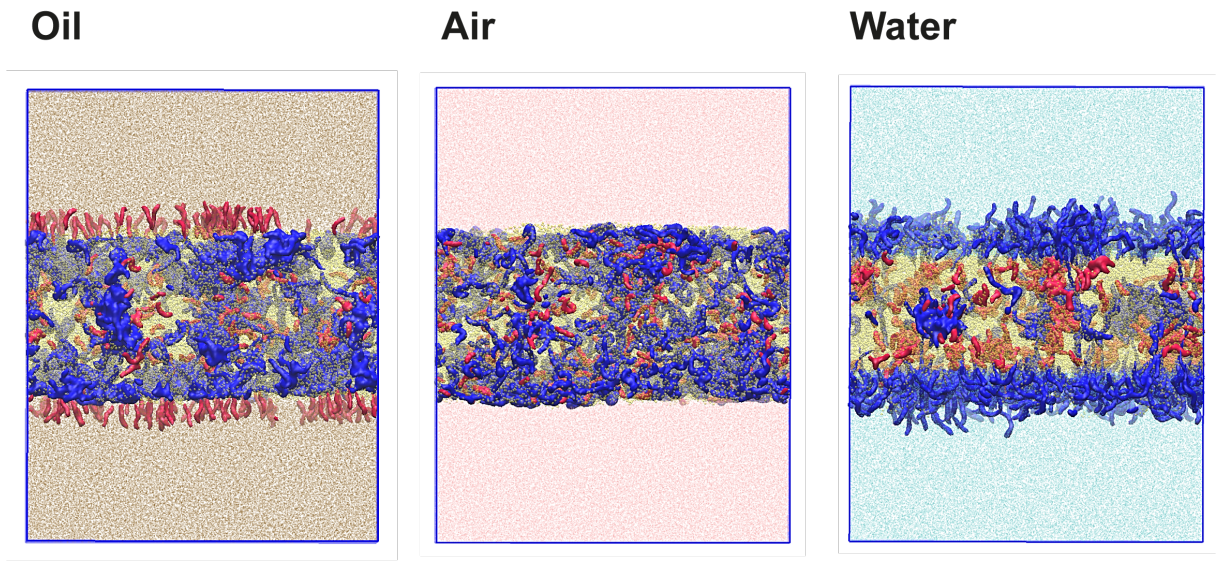


mPEG (hydrophilic) and oDEC (hydrophobic) dangling chains

# Surface segregation of PU coatings

## Adaptive surface behavior

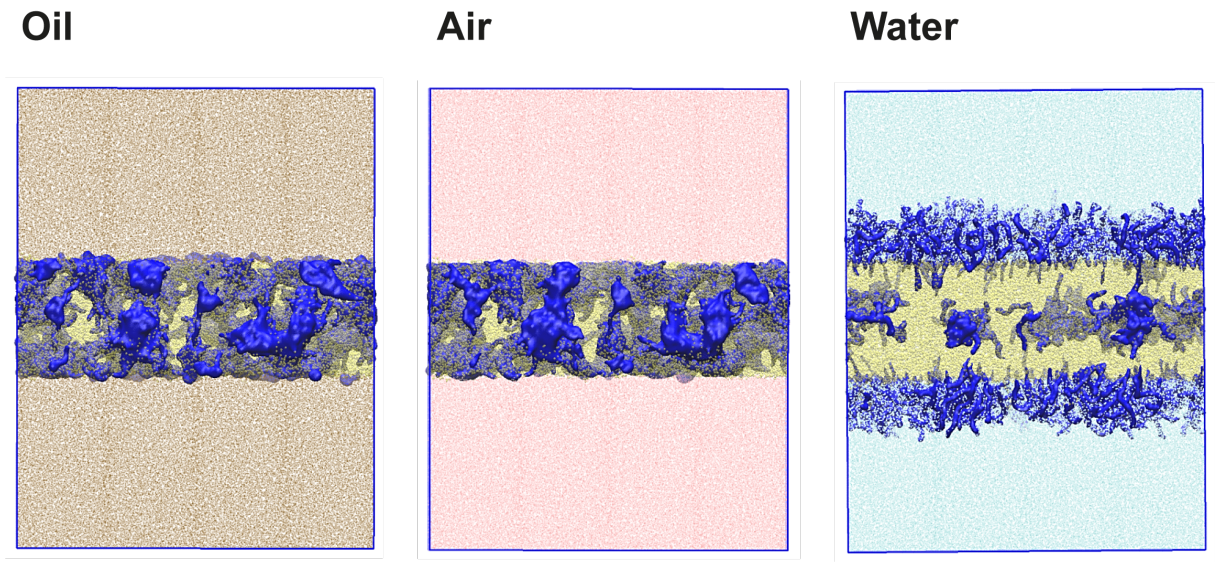


mPEG (hydrophilic) dangling chains

Kizilkaya, et al. Prog. Org. Coat., 2023.

# Polymeric drug delivery systems

PEG-PPO-PEG micelles

Ibuprofen

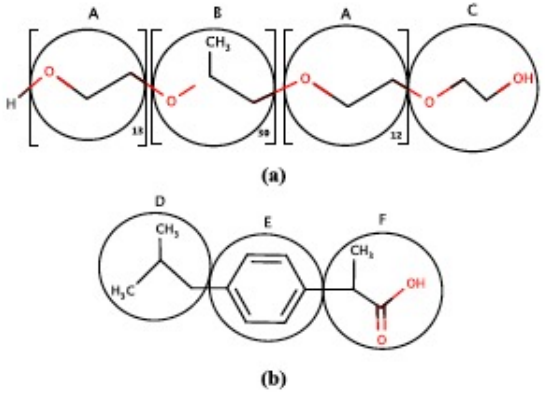


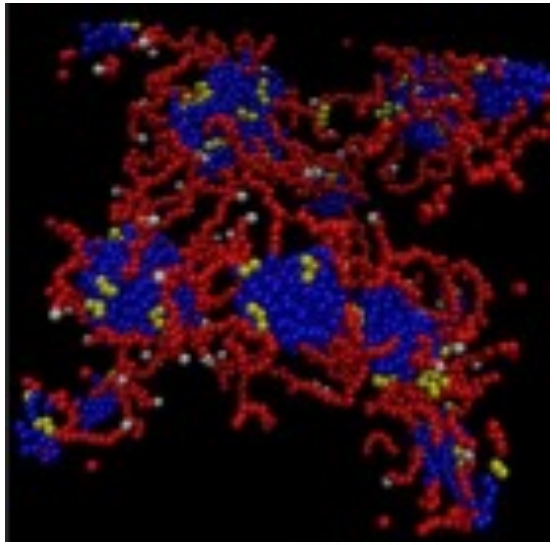

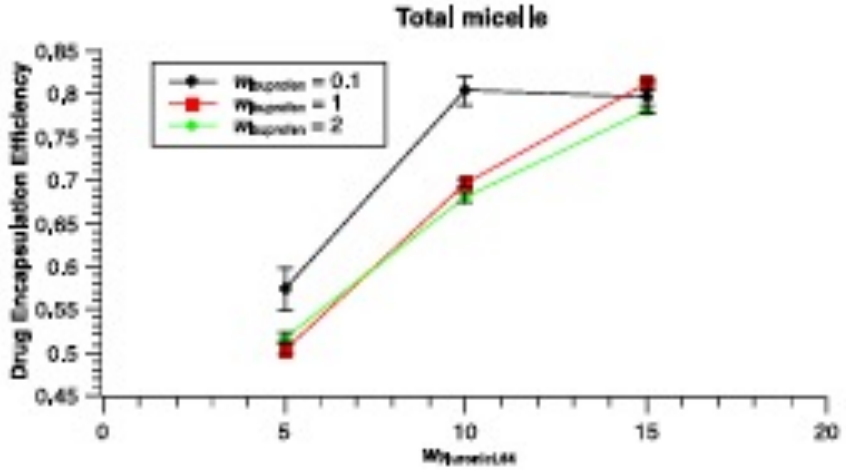


Kacar, Coll. Polym. Sci, 2019.

# Polymeric drug delivery systems

## PEG-PLA-PEG micelles

Dissipative Particle Dynamics simulations

Morphology

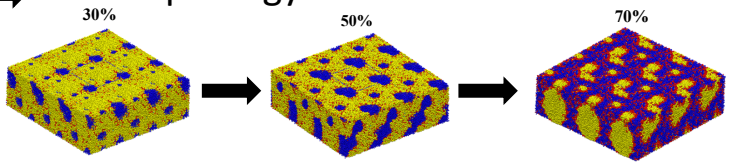


Micelle structure

$N_{agg}$, $N_m$, $V_m$, $\kappa^2$

+

Release kinetics

$C(t)/C_\infty = kt_{DPD}^n$

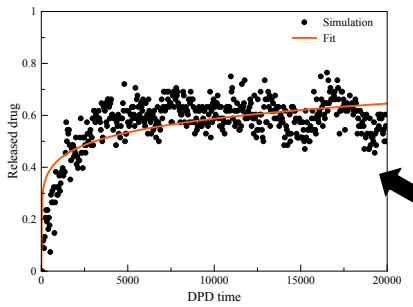


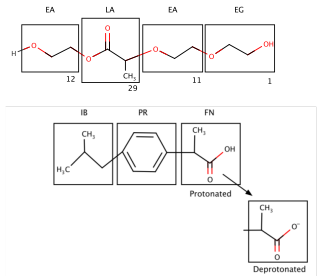


Drug encapsulation

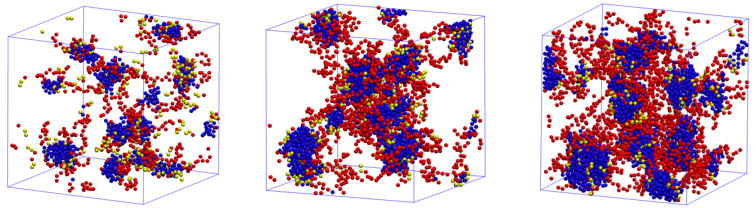


Drug release

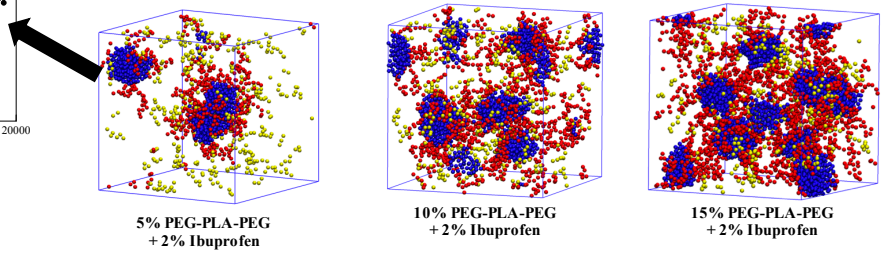


Kuru, Dalgakiran, Kacar, Coll. Surf. A, 2021.

# Polymeric drug delivery systems

## PEG-PLGA-PEG micelles

Dissipative Particle Dynamics simulations

$$a_{ij} = \hat{a}_{ij} + \frac{p}{0.0454(a_{ii}\rho_{i,pure} + a_{jj}\rho_{j,pure})}\chi_{ij}k_BT$$

$$a_{ii} = \frac{p - \rho_{i,pure}k_BT}{\alpha\rho_{i,pure}^2 r_{DPD}^3}$$

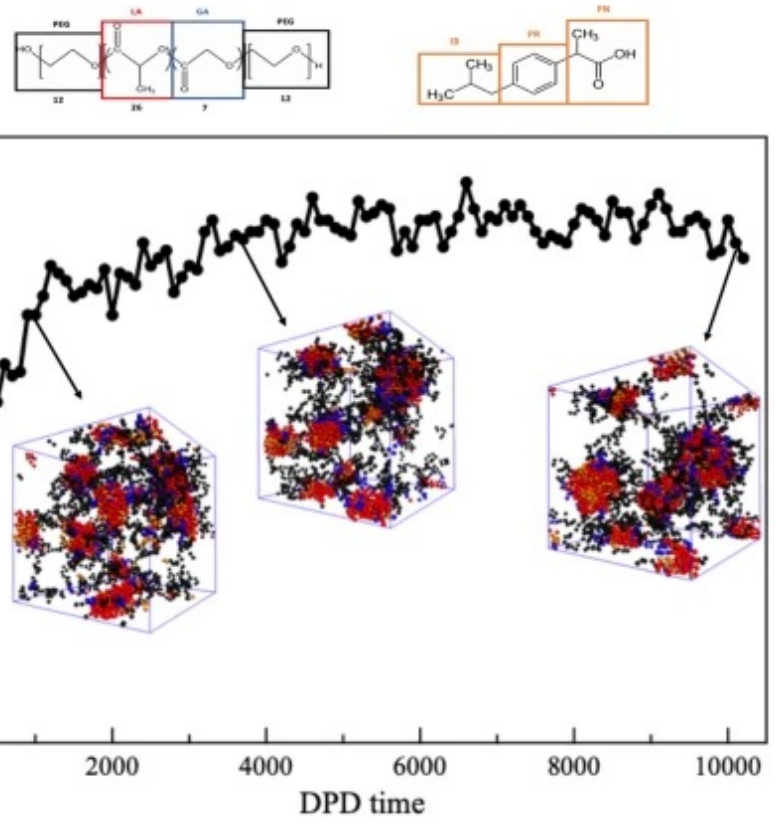


Yildiz, Kacar, MRS Advances, 2021.

# Lipid-based carriers

Coenzyme Q10 encapsulation in lecithin liposomes

mRNA carriers

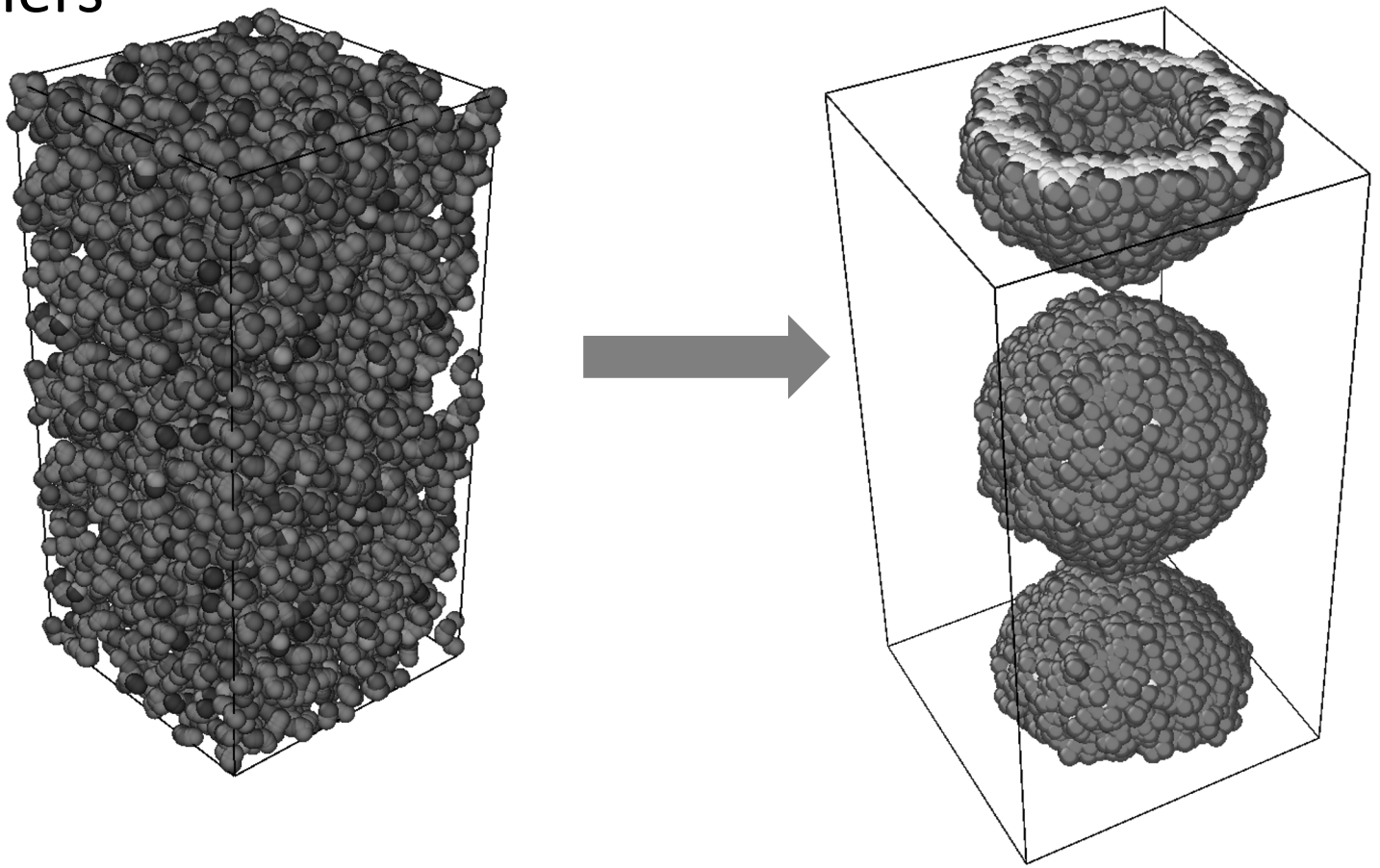

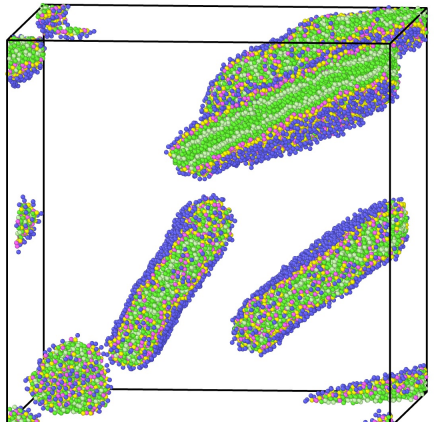

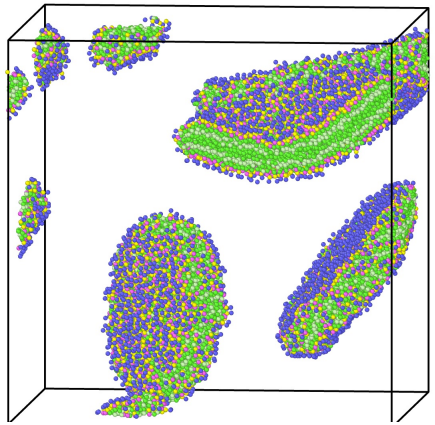

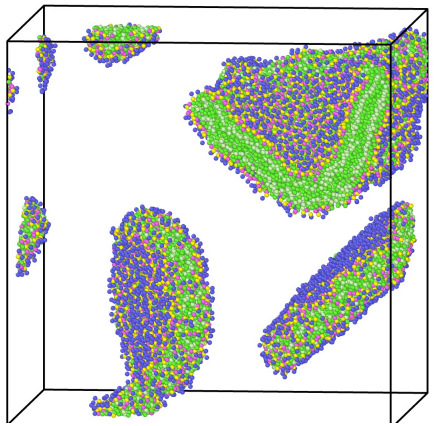

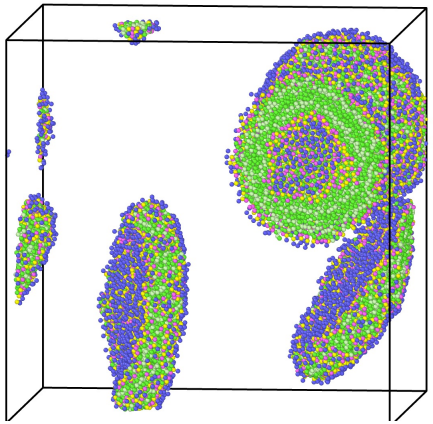

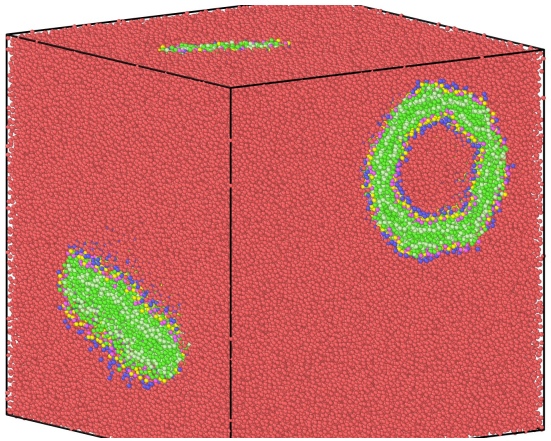

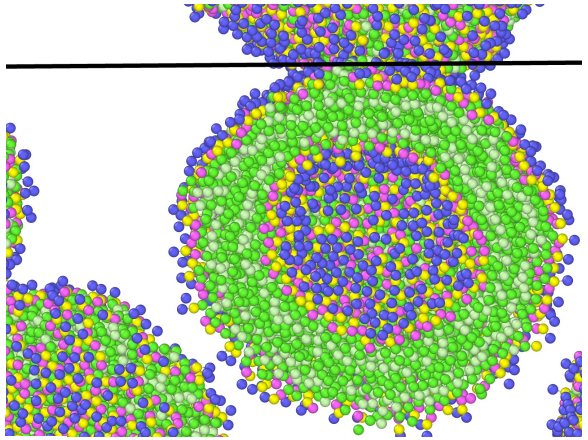

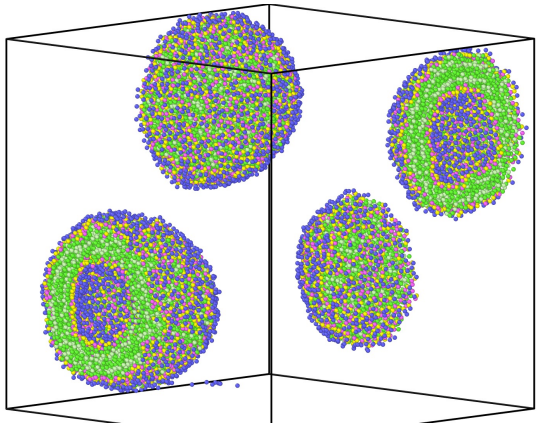

# Other DPD examples

Polymer micelle self-assembly

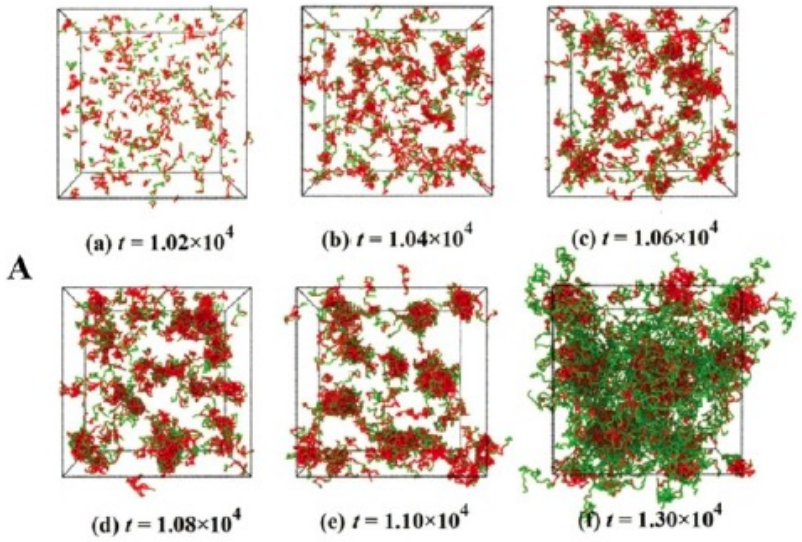


Kong, S. M.; *v.d.* Phys. Chem. Chem. Phys., 2018.

Drug encapsulation and XRD

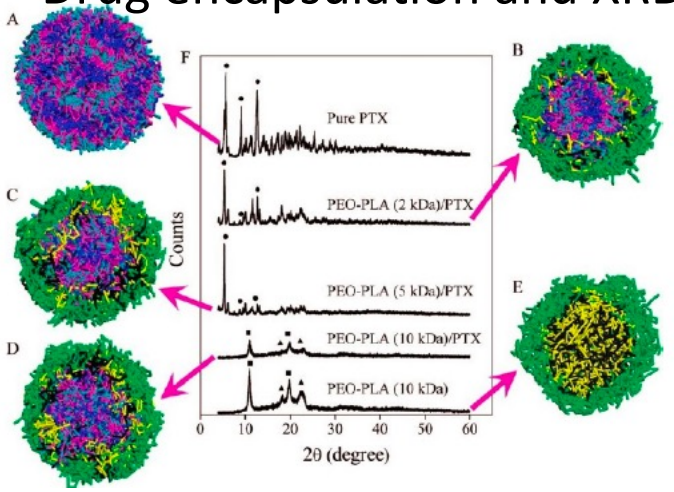


Guo, X. D.; Zhang, L. J.; Qian, Y. Ind. Eng. Chem. Res., 2012.

Micellization behavior

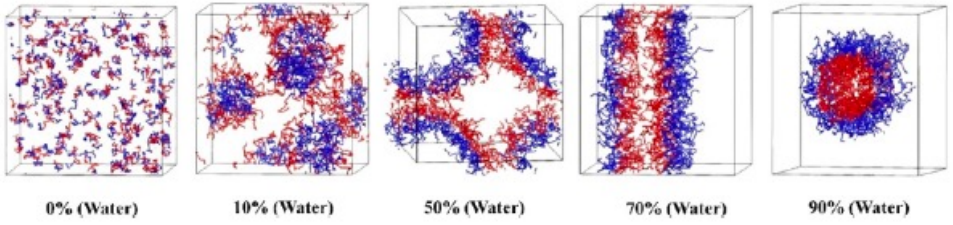


Huo, J. H.; Chen, Z.; Zhou, J. Langmuir, 2019.

pH reponsive polymer – drug loading/release

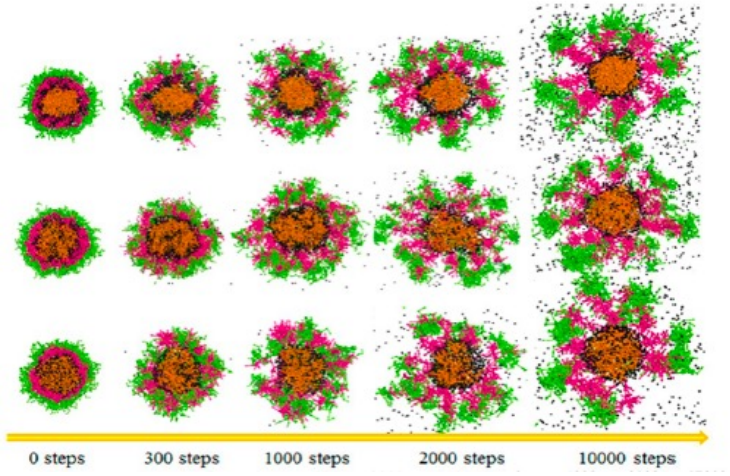


Nie, S. Y.; *v.d.* ACS Appl. Mater. Interfaces, 2014.

# Other DPD examples

## siRNA – polymer – Au NP

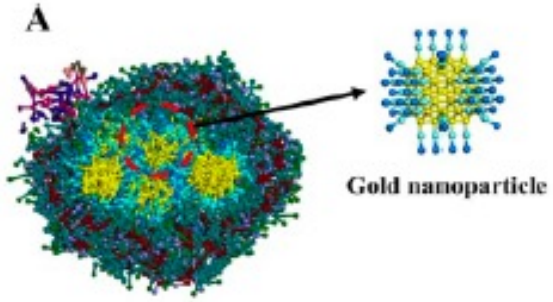


Xie, X. N. *v.d.* AIChE J., 2018.

## DPD – TEM comparison

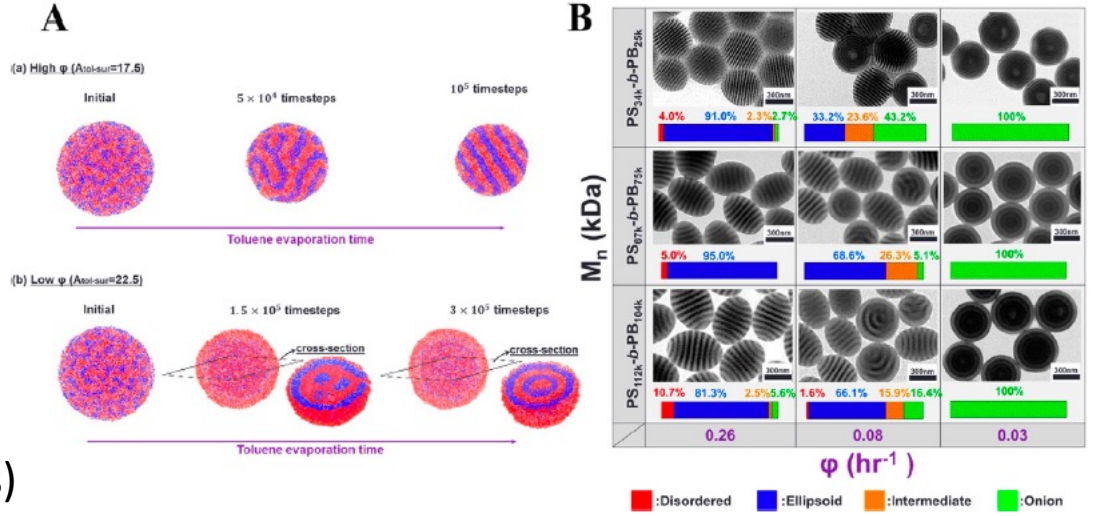


Shin, J. M.; Kim, Y.; Yun, H.; Yi, G. R.; Kim, B. J., ACS Nano, 2017.

## RME (Receptor mediated endocytosis)

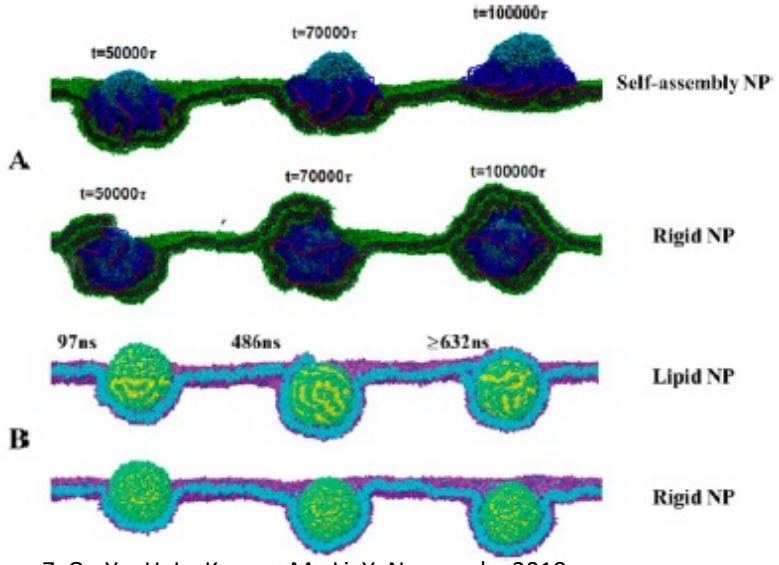


Shen, Z. Q.; Ye, H. L.; Kroger, M.; Li, Y. Nanoscale, 2018.
Bai, X.; Xu, M.; Liu, S. J.; Hu, G. Q. ACS Appl. Mater. Interfaces, 2018.

## Cancer cell detection

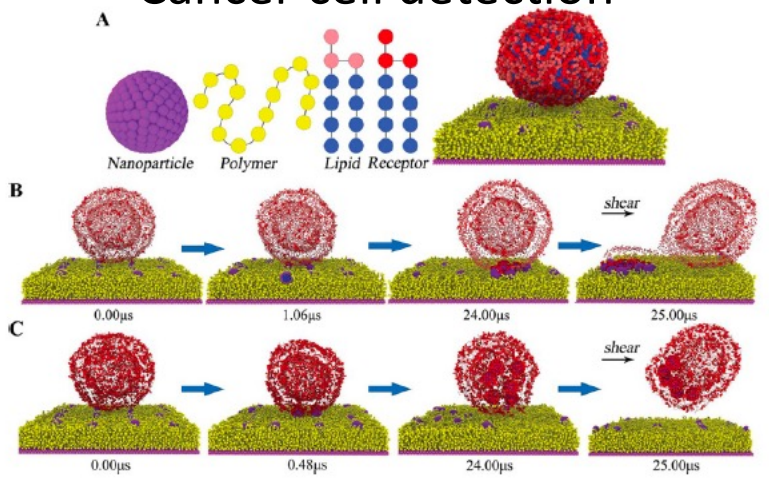


Huang, L. Y.; Yu, Y. S.; Lu, X.; Ding, H. M.; Ma, Y. Q. Nanoscale, 2019.

# Hands-on session

## 1. Phase separation of monomers

Monitor phase separation process

Observe repulsion strength dependency on phase separation

- 1:1 A:B mixture

## 2. Micelle formation

Monitoring micelle formation process

Effect of concentration

- $A_x$-$B_x$ type diblock copolymers in solvent

## 3. Cross-linking

Modeling chemical reactions in DPD

A-B-B-A oligomer + star-shaped cross-linker

Dynamics of cross-link formation

# Properties

## Radial Distribution Function

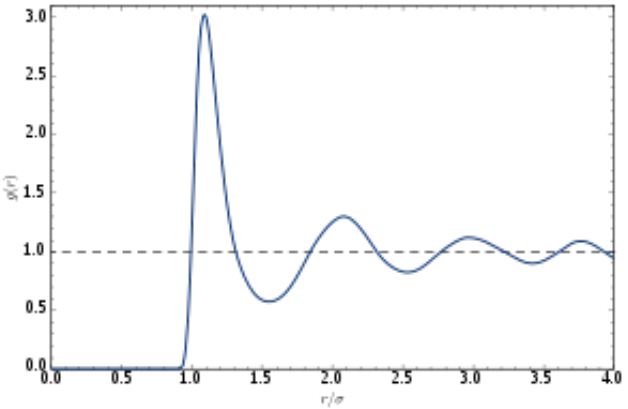


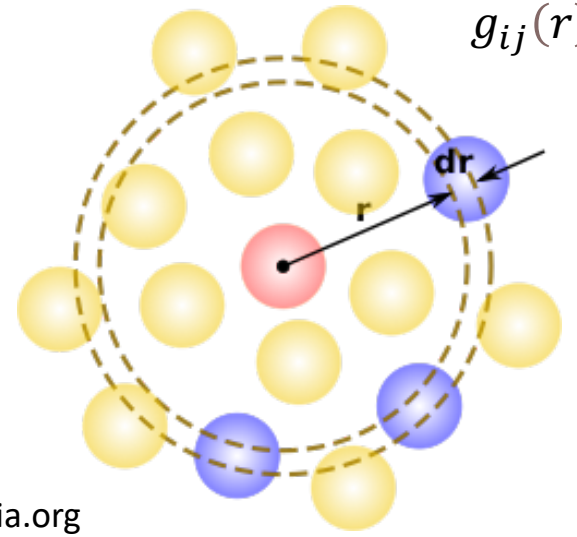


$$g_{ij}(r) = \frac{\langle \Delta N_{ij}(r \to r + \Delta r) \rangle V}{4\pi r^2 \Delta r N_i N_j}$$

## Isothermal compressibility

$$\kappa_T = \frac{1}{k_B T} \frac{\langle V^2 \rangle - \langle V \rangle^2}{\langle V \rangle} \quad \text{and} \quad \kappa^{-1} = \frac{1}{\rho k_B T \kappa_T}$$

## Mean Squared Displacement

$$\text{MSD} = \frac{1}{N} \sum_{i=1}^{N} \left| r^i(t) - r^i(0) \right|^2$$

## Cross-link conversion

$$X = \frac{N_{\text{new formed}}}{N_{\text{Total}}}$$

## Density profile

$$\rho = \frac{N_{\text{beads}}}{V_{\text{Slab}}}$$

wikipedia.org

# Time for fun!